



PLATTE RIVER RECOVERY IMPLEMENTATION PROGRAM

Data Synthesis Compilation

Sediment Augmentation



Prepared by staff of the Executive Director's Office for the Governance Committee of the Platte River Recovery Implementation Program

August 2023



PREFACE

This document was prepared by the Executive Director’s Office (EDO) of the Platte River Recovery Implementation Program (“Program” or “PRRIP”). The information and analyses presented herein are focused on informing the use of Program land, water, and fiscal resources to achieve the Program’s long-term goal of improving and maintaining the associated habitats for the target species (interior least tern, piping plover, whooping crane, and pallid sturgeon). While the sediment regime and effect of sediment augmentation apply for the entire suite of target species, these actions have the highest potential to effect the channel planform as it relates to whooping crane habitat; as such, the Program has focused efforts on informing the relationship between sediment augmentation and the whooping crane management objective: contribute to the survival of whooping cranes by increasing habitat suitability and thus use of the Associated Habitat Reach (AHR) along the central Platte River in Nebraska. The Program has invested fourteen years in implementation of an adaptive management program (AMP) to reduce uncertainties about proposed management strategies and learn about river and species responses to management actions. During that time, the Program has implemented management actions, collected a large body of physical and species response data, and developed modeling and analysis tools to aid in the interpretation and synthesis of data.

Implementation of the Program’s AMP has proceeded with the understanding that management uncertainties, expressed as hypotheses and summarized as Big Questions, encompass complex physical and ecological responses to limited treatments that occur within a larger ecosystem that cannot be controlled by the Program. The lack of experimental control and complexity of response precludes the sort of controlled experimental setting necessary to cleanly follow the strong inference path of testing alternative hypotheses by devising crucial experiments (Platt, 1964). Instead, adaptive management in the Platte River ecosystem must rely on a combination of monitoring of physical and biological response to management treatments, predictive modeling, and retrospective analyses (Walters, 1997).

One of the Program’s primary management uncertainties is the need for long-term sediment (sand) augmentation. Due to significant variation and uncertainty in the sediment balance throughout the central Platte River, the Program focused its efforts at the upper end of the Associated Habitat Reach (AHR) to offset the largest and most well-known historical sediment deficit in the central Platte River due to clearwater hydropower return flows. Stakeholders have long been concerned that incision and narrowing due to mining of sediment from the bed of the channel downstream of the return will migrate downstream and impact habitat suitability for the Program’s target species. Efforts to quantify the magnitude of the sediment deficit and develop augmentation methods began soon after Program initiation in 2007. By 2016, Program stakeholders reached consensus that the best next step in evaluating sediment augmentation would be implementation of a full-scale sediment augmentation experiment immediately downstream of the hydropower return. The full-scale augmentation experiment was initiated in 2017 with augmentation occurring annually from 2017 through 2021. In 2022, the Executive Director’s Office began analysis of the effectiveness of sediment augmentation, producing multiple lines of evidence across a range of spatial and temporal scales.



1 The results of our analyses are organized into a four-chapter synthesis report. The
2 Executive Summary provides a condensed and consolidated summary of the findings presented
3 in the following chapters. Chapter 1 provides history and context including a summarization of
4 modeling and research conducted during the First Increment of the Program. Chapter 2 is
5 comprised of retrospective analyses of spatial and temporal patterns of incision prior to initiation
6 of the sediment augmentation experiment. Chapter 3 focuses on two-dimensional longitudinal
7 channel response to sediment augmentation. Chapter 4 is comprised of an analysis of volumetric
8 change in the period prior to and during the sediment augmentation experiment.

9 10 **References**

- 11
12 Platt, J. R. 1964. Strong inference. *Science*, 146(3642), 347-353.
13
14 Walters, C. 1997. Challenges in adaptive management of riparian and coastal
15 ecosystems. *Conservation ecology*, 1(2), 1.
16



CONTENTS

1		
2		
3	LIST OF ACRONYMS.....	7
4	EXECUTIVE SUMMARY.....	8
5	E.1 Why did we conduct a sediment augmentation management experiment?	8
6	E.2 What have we learned about historical degradation in the J2 Return Channel prior to	
7	augmentation?	9
8	E.3 What have we learned about the J2 Return Channel during the sediment augmentation	
9	management experiment?	9
10	E.4 What have we learned about sediment balance downstream of Overton during the	
11	sediment augmentation management experiment?	10
12	E.5 What is our overall assessment of the performance of the sediment augmentation	
13	management experiment?	10
14	CHAPTER 1 Sediment augmentation: History and Context	12
15	1.1 Abstract	12
16	1.2 Introduction	12
17	1.3 Pre-Program monitoring, modeling, and research 1978-2006	13
18	1.4 Sediment augmentation research during the First Increment (2007-2016).....	17
19	1.5 Full-scale sediment augmentation management experiment (2017-2021)	21
20	1.5.1 Sediment augmentation area	21
21	1.5.2 Timing	21
22	1.5.3 Design considerations	22
23	1.5.4 Sediment augmentation summaries	22
24	1.6 First increment extension – Big Question #3	24
25	References	26
26	CHAPTER 2 Evaluation of trends in incision prior to full-scale sediment augmentation.....	28
27	2.1 Abstract	28
28	2.2 Introduction	28
29	2.2.1 Study area.....	29
30	2.2.2 Overview of analyses.....	30
31	2.3 Geomorphic Grade Line and relative elevation model	31
32	2.3.1 Methods.....	31



1	2.3.2	Results.....	31
2	2.4	Analysis of spatial and temporal trends in incision 1989-2016 relative to predictions .	35
3	2.4.1	Methods.....	35
4	2.4.2	Results.....	37
5	2.5	Specific gage analysis	40
6	2.5.1	Methods.....	40
7	2.5.2	Results.....	41
8	2.6	Channel sinuosity upstream of the Overton Bridge	52
9	2.6.1	Methods.....	52
10	2.6.2	Results.....	52
11	2.7	Discussion	53
12	2.8	References	55
13	CHAPTER 3	Evaluation of longitudinal change after sediment augmentation in the Central	
14		Platte River, NE, USA	56
15	3.1	Abstract	56
16	3.2	Introduction	56
17	3.3	Relative elevation model.....	57
18	3.3.1	Methods.....	57
19	3.3.2	Results.....	57
20	3.4	Longitudinal profile of channel thalweg 2016–2021	63
21	3.4.1	Methods.....	63
22	3.4.2	Results.....	64
23	3.5	Longitudinal profile of mean channel elevation 2016–2021	72
24	3.5.1	Methods.....	72
25	3.5.2	Results.....	73
26	3.6	Wetted Width.....	76
27	3.6.1	Methods.....	76
28	3.6.2	Results.....	77
29	3.7	Sinuosity of the J2 Return Channel.....	80
30	3.7.1	Methods.....	80
31	3.7.2	Results.....	80



1	3.8	Focused analysis of incision in the vicinity of Station 70,000	81
2	3.9	Discussion	87
3	3.10	References	90
4	CHAPTER 4	Volume change analysis	92
5	4.1	Abstract	92
6	4.2	Introduction	92
7	4.3	Methods	93
8	4.3.1	Data sources	93
9	4.3.2	Volume change (LiDAR raster differencing).....	98
10	4.3.3	Flow normalization of volume change	100
11	4.3.4	Uncertainty in LiDAR differencing	100
12	4.4	Results	102
13	4.4.1	Pre- and post-augmentation volume change results.....	102
14	4.4.2	Flow-normalized volume change results	106
15	4.4.3	Effectiveness of sediment augmentation	107
16	4.4.4	Year-by-Year Volume Change During Augmentation.....	109
17	4.5	Discussion	113
18	4.6	References	115
19			
20			
21			



1

LIST OF ACRONYMS

1D	One dimensional
2D	Two dimensional
ADCP	Acoustic doppler current profilers
AHR	Associated Habitat Reach
AMP	Adaptive management plan
CNPPID	Central Nebraska Public Power and Irrigation District
CWR	Cottonwood Ranch
DEM	Digital elevation model
EDO	Executive Directors Office
EIS	Environmental impact statement
GAM	Generalized additive model
GAMM	Generalized additive mixed model
GC	Governance Committee
GGL	Geomorphic Grade Line
ISAC	Independent Scientific Advisory Committee
J2 Return	Johnson No. 2 Hydropower Return
KCD	Kearney Canal Diversion
LiDAR	Light Detection and Ranging
MUCW	Maximum unobstructed channel width
NE	Nebraska
PRRIP	Platte River Recovery Implementation Program, or Program
QSI	Quantum Spatial Inc.
REM	Relative elevation model
SED-VEG	Platte River Sediment Transport and Riparian Vegetation Model
USBR	United States Bureau of Reclamation
USGS	United States Geological Survey
Ft	Foot
Cfs	Cubic feet per second
yd ³	Cubic yard

2

3

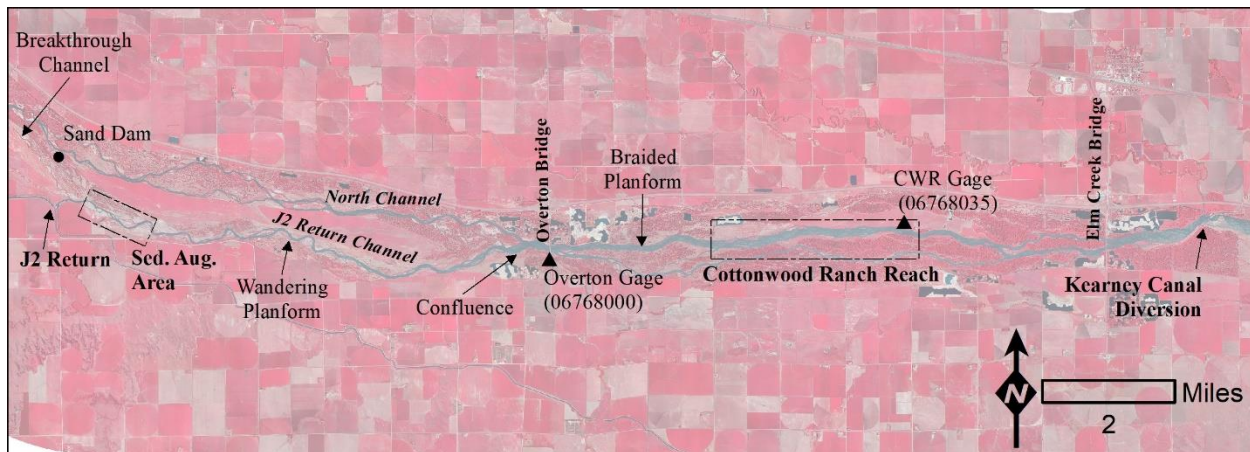


EXECUTIVE SUMMARY

E.1 Why did we conduct a sediment augmentation management experiment?

Extension Science Plan Big Question 3 asks if sediment augmentation is necessary to create and/or maintain suitable whooping crane habitat in the future. More specifically, clearwater hydropower return flows entering the south channel of the Platte between Lexington and Overton (the J2 Return Channel) have resulted in incision and narrowing in that reach. We hypothesized that annual sand augmentation of 60,000 to 80,000 tons (40,000 to 53,000 yd³)¹ may be necessary to supply sediment in sufficient quantities to stabilize channel incision and prevent it from progressing downstream past the Overton Bridge and negatively impacting whooping crane habitat suitability.² Alternative hypotheses include the need for more or less sediment and/or alternate augmentation locations, as well as the hypothesis that incision is progressing slowly enough that it does not pose a threat to downstream habitat.

To answer this question, the Program initiated a full-scale sediment augmentation management experiment in 2017 that involves mechanically augmenting 40,000–60,000 yd³ of sand into the channel immediately downstream of the J2 Return each year. A combination of transect surveys and LiDAR data has been analyzed to evaluate channel response to the increase in sediment supply. Preliminary findings, along with a map of the augmentation evaluation reach and features, follow.



Overview map of sediment augmentation evaluation reach and features.

¹ Earlier work computed sediment deficit and transport in units of tons, while current work is computed in cubic yards. In 2016, Twin Rivers Testing and Environmental determined an average sediment density and proposed 1.5 yd³ would be equal to 1 T. This conversion rate was used to approximate volumes from sediment masses where necessary.

² The narrow, incised reach of the J2 Return Channel does not meet minimum habitat suitability requirements for whooping crane roosting habitat. If impacts progress downstream past the Overton Bridge, habitat suitability at the Cottonwood Ranch habitat complex will be negatively impacted.



E.2 What have we learned about historical degradation in the J2 Return Channel prior to augmentation?

The J2 Return began clearwater hydropower returns in 1942. Since then, J2 Return Channel has incised and its slope has decreased, diverging markedly from historical elevations (Figures 2.5-2.6; relative elevation model). Limited transect survey data prior to LiDAR gives an indication of the progression of this change. In 1989, transect data indicated that the thalweg below the return had incised 14 feet (0.3 ft/yr) below the floodplain, followed by an additional six feet of incision by 2002 (0.5 ft/yr). After this point, however, incision seems to have slowed with no measurable lowering between 2002 and 2016. This period of slowing incision coincided with a steady increase in sinuosity (i.e. more lateral channel movement). We interpret the shift from vertical incision to lateral migration to be caused by the channel dropping below the slope threshold to maintain a straight braided channel, causing it to transition to a wandering planform. Lateral erosion now comprises >50% of total erosion in the channel, supplying downstream reaches with sediment from bank material rather than bed material.

Overall, we assess that a wave of vertical incision propagated down through the study area after J2 Return began operations. In the early 2000s, the primary mechanism of channel degradation shifted from incision to lateral migration, with the highest intensity of migration occurring in upper half of the J2 Return Channel.

E.3 What have we learned about the J2 Return Channel during the sediment augmentation management experiment?

Mechanical augmentation operations began in 2017 and full-scale augmentation of 40,000–60,000 yd³ occurred annually from 2018–2021.³ Calculation of year-to-year volume change in the augmentation area indicates most augmented material was mobilized downstream out of the augmentation area annually. Annual comparisons of volume change downstream of the augmentation area found that lateral erosion did not decrease consistently during the augmentation period and averaged approximately 55,000 yd³ per year. Bed erosion did decrease by 20,000–40,000 yd³ (45%–60%) from the pre-augmentation period. This roughly equals the annual increase in sediment transported out of the sediment augmentation area (36,000 yd³) during augmentation operations.

The decrease in bed erosion occurred in the first three miles downstream of the augmentation area. Bed elevations in that segment were stable to slightly aggradational. However, incision was observed farther down the J2 Return Channel. In 2019, a 6,000 ft reach of pronounced bed erosion (thalweg incision averaged 1.3 ft) occurred mid-way down the reach likely due to April and July flood flows conveyed from the North Channel to the J2 Return Channel upstream of

³ Full-scale augmentation also occurred in 2022 but remote sensing data was not available in time to include in this analysis.



Jeffrey Island (breakthrough channel). The incised area has been stable since 2020 and may be recovering slightly.⁴

Overall, we assess that the annual augmentation volume was sufficient to offset approximately half the bed erosion in the J2 Return Channel Reach but had no effect on lateral erosion.

E.4 What have we learned about sediment balance downstream of Overton during the sediment augmentation management experiment?

A specific gage analysis for low to moderate flows at the Overton Bridge indicates channel degradation at the bridge prior to 2013 followed by slight channel aggradation since. At the Cottonwood Ranch (CWR) stream gage located at the downstream end of the CWR habitat complex, the channel was slightly aggradational during the period of 2005–2015 and has been stable since.⁵ Thalweg and volume change analyses indicate a dynamic channel with a high degree of spatial and temporal variability during the augmentation period. Spatially, the reach from the Overton Bridge to CWR was stable to slightly aggradational, the CWR reach was slightly degradational, and the reach from CWR to the Kearney Canal Diversion (KCD) was aggradational during augmentation years. Temporally, the channel bed was net aggradational or relatively stable in three out of five years, but degradational from 2017–2019. When compared to the pre-augmentation period and normalized for discharge, we observed no major difference in bed erosion during the pre- and post-augmentation periods downstream of Overton Bridge. The one substantial difference we did observe was significant lateral erosion that occurred because of the prolonged peak flow event in 2015 which increased mean channel width by more than 200 ft. Channel widths have remained stable since.

Overall, we assess that effects of sediment augmentation were not detectable downstream of Overton Bridge. The reach continues to be dynamic and highly variable but generally stable and the increase in channel width that occurred during the pre-augmentation period has been maintained.⁶

E.5 What is our overall assessment of the performance of the sediment augmentation management experiment?

Augmentation operations reduced annual bed erosion in the J2 Return Channel by approximately 20,000–40,000 yd³ (45%–60%) which is consistent with the 35,000 yd³ increase in sediment transported out of the augmentation area following augmentation operations. Nonetheless, we observe continued incision and planform change midway down the J2 Return Channel (Station 70,000). In the absence of augmentation, we would expect bed erosion in the J2 Return Channel to return to pre-augmentation levels and for incision and planform change to accelerate near Station 70,000. We are unable to predict short term changes in the rate of incision because:

⁴ A breakthrough channel upstream of the J2 Return is a complicating factor in J2 Return Channel evaluations. This channel contributed a substantial amount of water and sediment prior to 2020. It has since been completely disconnected.

⁵ NPPD and then PRRIP channel widening occurred upstream of this gage annually until ~2012.

⁶ Whooping crane habitat suitability in the CWR reach is being maintained at the highest level in 60-70 years.



- 1) The absence of detailed thalweg elevation data during the pre-augmentation period (no topobathymetric LiDAR) prevented a detailed analysis of thalweg incision rates immediately prior to augmentation.
- 2) The confounding effect of a breakthrough channel across Jeffrey Island that contributed flow and sediment to the J2 Return Channel prior to 2020. That channel has now been completely blocked to protect utility infrastructure.

Long-term channel evolution with and without augmentation is also uncertain. Pre-augmentation analyses indicate that since 2002, incision has decreased and lateral erosion has increased. Will meander bends in the wandering portion of the J2 Return Channel continue to migrate and supply sufficient lateral erosion to forestall downstream incision, or will the reach stabilize and downstream incision increase? Will the elimination of flood flows (and associated sediment) through the breakthrough channel reduce the potential for episodic incision events or will the elimination of the external sediment supply accelerate baseline incision?

Regardless of these uncertainties we can say with confidence that there is a substantial sediment deficit in the J2 Return Channel that has, and continues to, impact channel form. At present the most serious planform impact (transition from braided to wandering) has not progressed downstream of Overton Bridge but may at some unknown point in the future. As such, mechanical augmentation at the upper end of the J2 Return Channel theoretically reduces future risk to downstream habitat but near- and long-term benefits are difficult to quantify and weigh against the annual cost of augmenting sediment. Alternatives that allow for sediment replenishment without annual mechanical augmentation may offer a longer-term solution, though their effectiveness, when compared to recent mechanical augmentation efforts, is unknown.



CHAPTER 1 Sediment augmentation: History and Context

1.1 Abstract

Prior to implementation of a full-scale sediment augmentation experiment in 2017, the Platte River Recovery Implementation Program (PRRIP) and others have undertaken multiple monitoring, modeling and small-scale augmentation experiments to describe, quantify, and predict channel response to clearwater releases from the Johnson No. 2 Hydropower Return (J2 Return) near Lexington, NE. Since construction in the 1940s, the J2 Return has released sediment-free water into the south channel of the Platte River resulting in significant channel incision and planform change. This chapter summarizes findings from five decades of investigations leading up to full-scale augmentation. It also describes implementation of full-scale augmentation operations, with a focus on the location and volume of sediment augmentation.

1.2 Introduction

The Platte River Recovery Implementation Program (Program or PRRIP) is responsible for implementing certain aspects of the recovery plans for three threatened and endangered species including the highly endangered whooping crane (*Grus americana*). More specifically, the Program has a management objective to improve survival of whooping cranes during migration through increased use of the Associated Habitat Reach (AHR) of the Platte River in central Nebraska (PRRIP 2006a). This ninety-mile reach extends from Lexington, NE downstream to Chapman, NE and includes the Platte River channel and off-channel habitats within three and a half miles of the river (Figure 1.1).

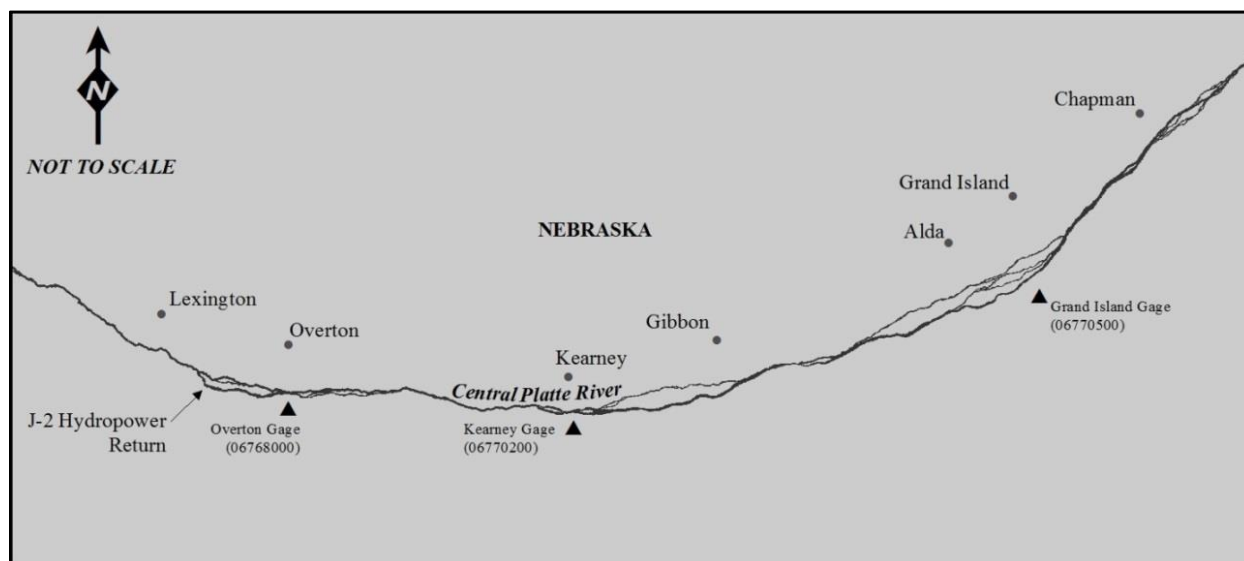


Figure 1.1. Associated Habitat Reach (AHR) of the central Platte River in Nebraska extending from Lexington downstream to Chapman.

The Program has invested fourteen years implementing an adaptive management program to test strategies for increasing suitability of whooping crane habitat in the AHR. One area of focus has



1 been the impact of a sediment deficit at the upstream end of the AHR on channel morphology.
2 More specifically, channel incision and narrowing has occurred downstream of a clearwater
3 hydropower return and Program stakeholders are concerned those impacts could progress
4 downstream through time, impeding our ability to maintain the wide, unvegetated, braided river
5 morphology that is suitable for whooping crane roosting. Concerns about incision emerged in the
6 1980s, approximately 40 years after the Johnson No. 2 Hydropower Return (J2 Return) began
7 operations. Several investigations were conducted in the late 1990s and early 2000s to evaluate
8 the magnitude of the deficit and develop the concept of sediment augmentation into a
9 management action to be implemented during the First Increment of the Program (2007-2019).

10 During the First Increment of the Program, Adaptive Management Plan (AMP; PRRIP 2007)
11 activities included additional monitoring, modeling, and evaluation of the feasibility and
12 performance of various strategies to augment sediment. By 2016, Program decision makers
13 advised by the Independent Science Advisory Committee (ISAC) concluded the best way to
14 evaluate the performance of sediment augmentation was to initiate a full-scale sediment
15 augmentation management experiment designed to offset the total sediment deficit downstream
16 of the J2 Return. Implementation began in 2017 and annual augmentation continued through
17 2022.⁷ Subsequent chapters of this document present analyses and interpretation of data collected
18 prior to and during the sediment augmentation experiment. The objective of this introductory
19 chapter is to provide an overview of the body of research and monitoring that led to
20 implementation of full-scale augmentation. This begins with work leading up to Program
21 initiation in 2007, including efforts to quantify the magnitude of the sediment deficit in the AHR
22 and devise a sediment augmentation concept to be implemented under the AMP. We then
23 transition to a description of adaptive management implementation efforts during the First
24 Increment leading up to the full-scale augmentation experiment. The chapter concludes with an
25 overview of full-scale augmentation including the location, timing, and magnitude of
26 augmentation operations.

27 ***1.3 Pre-Program monitoring, modeling, and research 1978-2006***

28 The first known discussion of sediment as a potential driver in morphologic change in the central
29 Platte River occurs in Williams (1978). In that Geological Survey (USGS) Circular (781),
30 Williams describes changes in width, braiding, sinuosity and bed aggradation/degradation in the
31 North Platte and Platte Rivers in Nebraska over historical timeframes. Much of the publication
32 focuses on large reductions in channel width that occurred in the decades following the initiation
33 of reservoir construction in the North Platte River basin in the early 1900s. Williams focuses
34 much of the publication on correlations between declining discharge and width metrics.
35 However, he also included a specific gage analysis, noting that observed fluctuations in bed
36 elevations at stream gage locations reflected complex regulation of both water and sediment
37 delivery to the river.

38 In 1981, the USGS published a series of open-file reports describing sediment transport, channel
39 morphology and other physical characteristics of various segments of the Platte River. Kircher
40 (1981a) collected bedload and suspended sediment samples from segments of the South Platte,
41 North Platte, and central Platte Rivers and used them to develop estimates of sediment transport

⁷ This analysis focuses on the period of 2017-2021 due to the lag time in remote sensing data processing.



1 and effective discharge for each segment (Kircher 1981b). Karlinger et al. (1981) explored the
2 relationship between discharge, sediment, and channel width in the Central Platte, providing
3 theoretical predictions of channel width adjustment to changes in sediment and flow. Finally,
4 Crowley (1981) produced a detailed investigation of bedforms downstream of Grand Island, NE,
5 characterizing the geometry and movement of macroforms as well as their relationship to
6 channel narrowing.

7 In the late 1980s, O'Brien & Currier (1987) produced a report that explored changes in the
8 morphology and vegetation in the Big Bend Reach of the Central Platte River.⁸ The authors
9 attempted to quantify magnitude of incision through comparison of historical quadrangle maps,
10 concluding the channel had degraded three to ten feet from the late 1890s to the 1960s. Finally,
11 the authors referenced several published works on empirical threshold relationships in alluvial
12 channels (regime theory) and expressed concern that the reductions in flow and sediment supply
13 in the Big Bend Reach could cause the channel to shift from a braided to meandering
14 morphology. The authors concluded by recommending a complete analysis of sediment supply
15 and transport capacity of the Central Platte.

16 In the early 1990s, basin stakeholders began the negotiations that ultimately led to the
17 authorization of the Program in 2007. As part of those negotiations, a number of different
18 investigations were initiated by the Platte River Environmental Impact Statement (EIS) Office
19 and were published in the early 2000s. The first was a comprehensive evaluation of the physical
20 history of the Central Platte River conducted by Simons and Associates (2000) which focused on
21 drivers of vegetation expansion into the channel in the 20th century. The authors noted that the
22 bed of the Central Platte has coarsened over time and limited bed degradation has been observed.
23 They ultimately concluded that sediment transport played a secondary role in channel narrowing,
24 and that the channel bed was generally in a condition of dynamic equilibrium. Despite relegating
25 sediment supply to a secondary factor in channel narrowing, the authors did (for the first time)
26 introduce the concept of augmenting sediment to reduce bed degradation where it occurs. They
27 recommended further analysis of potential relationships between augmentation, sediment
28 transport, and riparian vegetation with a combined sediment transport and vegetation model
29 developed by the United States Bureau of Reclamation (USBR).

30 Randle and Samad (2003) produced the first detailed evaluation of historical changes in sediment
31 transport, reporting trends for the period of 1895-1999. Near the end of that report, the authors
32 note that the main source of sediment between the J2 Return Channel and Overton was the bed
33 and banks of the channel. They also noted that the thalweg was approximately 20 feet below the
34 top of the right bank and had eroded six feet vertically between 1989 and 2002. These incision
35 estimates were developed as part of a separate aggradation/degradation analysis by EIS Team
36 published in 2006 (Holburn et. al. 2006). That work analyzed repeat channel cross section
37 surveys to identify spatial and temporal trends in channel aggradation and degradation. The
38 authors found a clear trend of degradation in a 25-mile reach from the J2 Return to Odessa. The
39 most pronounced degradation occurred at the upstream end and gradually diminished until the

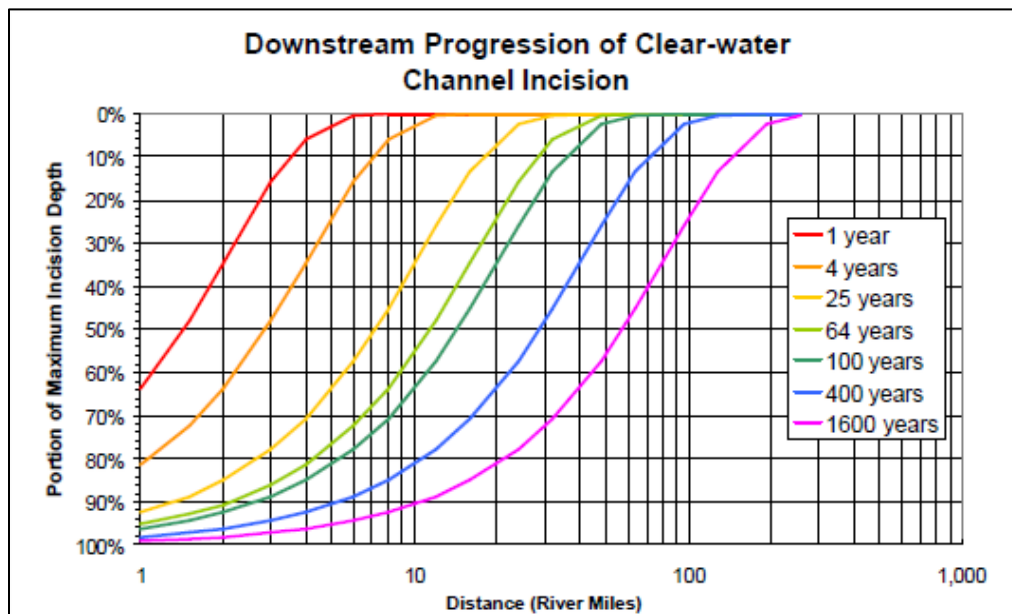
⁸ The Big Bend Reach roughly encompasses the 90-mile Associated Habitat Reach of the central Platte from Lexington, NE to Chapman, NE.



1 difference in average annual change in cross-sectional area declined below 10 ft² which was
2 assessed to be stable.

3 The major publication presenting the EIS Team's analysis and proposed restoration strategy was
4 published in 2004. As with prior comprehensive assessments, Platte River Channel: History and
5 Restoration (Murphy et al. 2004) discusses sediment along with other potential drivers of
6 planform change. The authors discuss the theoretical progression of incision below the J2 Return,
7 describing the process of winnowing of fine material from the riverbed, causing bed material in
8 the reach that is incising to become significantly coarser through time. This process gradually
9 results in armoring that limits the depth of channel incision at that location (assuming enough
10 coarse material is available). Critically, the authors assessed that the process of incision would
11 progress downstream until it was arrested by a combination of armoring and a decrease in local
12 river slope.

13 Murphy et al. (2004) cited Graf (1998) and de Vries et.al. (1973) to predict how quickly channel
14 incision would expand both vertically and downstream from the J2 Return under the theoretical
15 assumption of steady flow and a channel bed of uniform sand. The figure of predicted incision
16 through time is reproduced below as Figure 1.2. The figure predicts the progression of incision
17 through the AHR and the authors note it could take centuries for the channel to reach
18 equilibrium.



19
20 **Figure 1.2.** Reproduction of Figure 4.16 from Murphy et al (2004). Figure shows estimated
21 progression of incision over time below the J2 Return.

22 As with prior EIS Team reports, the authors concluded that increased sediment supply is
23 necessary to offset the deficit due to clearwater returns and to bring sediment supply into balance
24 with cumulative sediment transport capacity of the river. The proposed solution was sand
25 augmentation via mechanical pushing of island and bank material into the channel. This would
26 have the effect of 1) increasing sediment supply and reducing median grain size of the riverbed,



1 increasing bed mobility, and 2) widening the channel in augmentation reaches. Murphy et al.
2 provided the hypothetical example of mechanically pushing 500 tons per day, or 100,000⁹ yd³
3 per year, requiring 20 acres of islands be leveled over the course of a year.

4 The EIS Team's final estimates of sediment deficit in the AHR and proposed volume of sediment
5 augmentation were developed using an integrated hydraulic, sediment transport, and vegetation
6 model called the Platte River Sediment Transport and Riparian Vegetation Model or SED-VEG
7 model (Murphy et al. 2006). Model results indicated 85,000 to 175,000 tons (57,000 to 120,000
8 yd³) of sediment were eroded annually from the bed and banks of J2 Return Channel, another
9 50,000 to 100,000 tons (35,000 to 70,000 yd³) eroded annually from the bed and banks between
10 the confluence with the North Channel and the Overton Bridge, and 180,000 tons (120,000 yd³)
11 eroded annually from the bed and banks of the river between Overton and Wood River 56 miles
12 downstream.

13 Within the Program's AMP is the culmination of the EIS Team research described above. The
14 AMP prescribes sediment augmentation as a management action to be tested under an adaptive
15 management framework during the First Increment of the Program (2007-2019). Priority
16 hypothesis Sediment 1 (reproduced as Figure 1.3) provides an overview of the magnitude and
17 hypothesized benefits of sediment augmentation. Specifically, annual mechanical augmentation
18 of 185,000 tons (125,000 yd³) of sediment near Overton under existing flow regime and 225,000
19 tons (150,000 yd³) of sediment under the proposed flow regime¹⁰ achieves sediment balance,
20 eliminating the sediment deficit due to clearwater hydropower returns. Subsequent hypotheses
21 (Sediment 2-4) predict increases in braiding and channel width due to augmentation.

⁹ Murphy et al. used a different volume to mass conversion factor.

¹⁰ Proposed flow regime refers to implementation of the Program's Water Action Plan designed to reduce deficits to United States Fish and Wildlife Service (USFWS) target flows by 130,000 – 150,000 acre-feet annually.

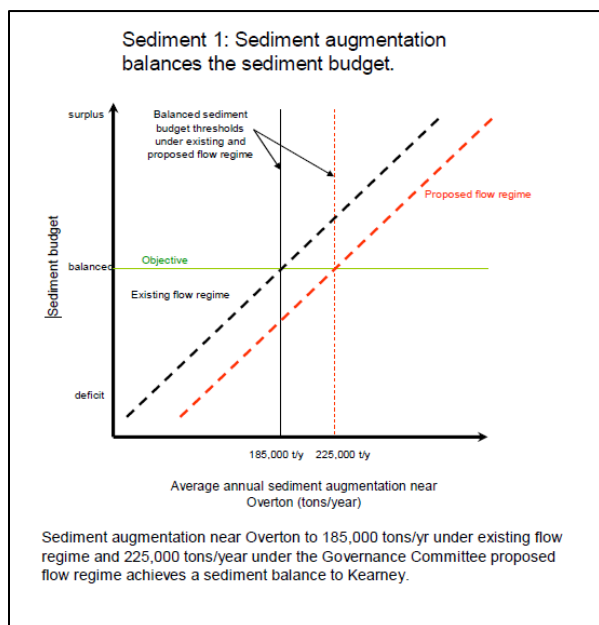


Figure 1.3 Priority hypothesis Sediment 1 reproduced from the Program Adaptive Management Plan (PRRIP 2006).

1.4 Sediment augmentation research during the First Increment (2007-2016)

Following Program authorization in 2007, a team of consultants was retained to evaluate the feasibility of implementing sediment augmentation (The Flatwater Group 2010). The scope of work included development of an updated sediment transport model for the AHR¹¹ and evaluation of alternative methods and locations to implement the experiment. A baseline mobile bed sediment transport model was developed using the U.S. Army Corps of Engineers HEC-RAS program (HEC-RAS, 2008). It was then modified to represent and evaluate a range of sediment augmentation alternatives. Figure 1.4 is a recreation of baseline (no augmentation) sediment transport modeling results from the study. The modeled annual sediment deficit for the 12.5-year simulation period was 152,000 tons (100,000 yd³).

¹¹ The SED-VEG model was abandoned after Program authorization due to concerns about accuracy of model results and the custom/proprietary nature of the code which made it difficult to use.



Table 4-1 Total Sediment Deficit and Surplus Volumes in Each Reach					
Subreach	Upstream Limit	Downstream Limit	Specific Location	Aggradational/ Degradational	Deficit (-)/ Surplus (+) (t/y)
1	Lexington Bridge	Overton Bridge	North Channel	Slightly to moderately aggradational	+66,400
2	J-2 Return	Overton Bridge	South Channel	Degradational	-96,700
3	Overton Bridge	Elm Creek Bridge	Cottonwood Ranch Reach	Degradational	-108,500
4	Elm Creek Bridge	Kearney Canal diversion structure	Immediately Upstream of Kearney Diversion	Slightly to moderately aggradational	+32,700
5	Kearney Canal diversion structure	Odessa Bridge	Immediately Downstream of Kearney Diversion	Degradational	-46,100
Total Reach					-152,200¹
<i>Note:</i>					
¹ For the purpose of the Study, the sediment deficit for the entire Project reach has been rounded to 152,000 t/y.					

Figure 1.4 Reproduction of Table 4-1 from The Flatwater Group (2010) providing baseline HEC-RAS sediment transport model results for the reach from Lexington, NE downstream to Odessa, NE.

Augmentation material gradations, sediment sources, methods of introducing sediment into the channel and augmentation locations were evaluated in the feasibility study. The report recommended two augmentation alternatives be implemented as part of a pilot-scale management experiment. The first alternative was similar to augmentation as proposed in the AMP. Bulldozers would push sediment from banks and islands (median grain size of 1.2 mm) into the channel, spreading the material across the width of channel to be mobilized by flow. This method had the benefit of widening the channel while augmenting sediment. The second alternative involved hydraulic mining of sediment from an existing gravel mine adjacent to the channel and screening it to produce a median grain size of 0.5mm. The screened sand and water slurry would then be pumped/piped directly into the channel. This alternative was similar to typical gravel mining operations with the expectation that unusable fines are discharged back into the mine.

Both augmentation alternatives were designed, permitted, and implemented in 2012–2013. Analysis of the alternatives concluded a year later (The Flatwater Group 2014). During the experiment, approximately 82,000 tons (55,000 yd³) of hydraulically mined sand (D50 0.5 mm) were pumped into the lower end of the J2 Return Channel upstream of the confluence with the North Channel. Over 100,000 tons (70,000 yd³) of overbank material (D50 of 1.2 mm) were bulldozed into the main channel downstream of the Overton Bridge at the upper end of the Cottonwood Ranch Habitat Complex. Monitoring was conducted during the experiment and used to assess the feasibility of augmentation methods as well as update sediment transport modeling and augmentation volume targets.



Implementation of mining/pumping and bulldozer augmentation revealed pros and cons for each augmentation method. Sand pumping maximized the volume of source material per surface area disturbed (material can be hydraulically mined to a depth of at least 40 ft) and allowed control of the gradation of the augmentation material. On the other hand, sand pumping had a much higher unit cost, low spatial flexibility due to the point source nature of the method, and it was difficult to match the augmentation rate to the channel transport capacity during low flows. Augmentation by bulldozer had a much lower unit cost and provided more flexibility in both location and placement of sediment, maximizing mobilization. Cons included low material volume per surface area disturbed and inability to control the sediment gradation.

The project team concluded that an annual average of 60,000 tons (40,000 yd³) of annual augmentation (D50 of 1.2 mm) could be sustained in the lower portion of the J2 Return Channel without excess sediment accumulation. However, actual transport would range from 11,000 tons (7,000 yd³) in dry years to 135,000 tons (90,000 yd³) in wet years and rates would increase or decrease depending on material gradation. The volume of augmentation that could be sustained without excess sediment accumulation was lower than the model-derived annual sediment deficit between Overton and Elm Creek, which averaged 109,000 tons (73,000 yd³) and ranged from 25,000 tons to 220,000 tons (17,000 to 150,000 yd³).

The feasibility study team also modeled over-augmentation in the J2 Return Channel. Pumping 150,000 tons (100,000 yd³) of sediment (D50 ~ 0.5 mm) annually into the J2 Return Channel was estimated to reduce the downstream deficit to approximately 43,000 tons (30,000 yd³) on average. Using larger material from riverbanks (D50 ~ 1.2 mm), the deficit was reduced to 73,000 tons (50,000 yd³) on average.

The Program paused sediment augmentation following completion of the pilot-scale management experiment while two other sediment-related efforts were concluded. The first was an update of sediment transport modeling to estimate the sediment deficit caused specifically by J2 Return flows (Tetra Tech 2015). This was accomplished by comparing sediment transport model results with and without J2 Return flows. The model indicated a relatively strong correlation between the volume of J2 releases and the sediment deficit downstream of the Overton Bridge. The reach was generally near balance during years when J2 releases were less than about 300,000 acre-feet, and the deficit increased to approximately 100,000 tons (70,000 yd³) in years when J2 releases were in the range of 1,000,000 acre-feet. Eliminating J2 releases from the model reduced the average annual deficit downstream of Overton from 92,000 tons to 61,000 tons (60,000 to 40,000 yd³), a reduction of 31,000 tons (20,000 yd³) per year. Most of the remaining incision in the model occurred in the Cottonwood Ranch reach.

The second effort was the conclusion of an eight-year field-based monitoring program to assess system-scale changes in geomorphology and vegetation in the AHR (Tetra Tech 2017). Monitoring included repeat transect surveys of the channel, bed and bank material sampling, sediment transport measurements, and vegetation monitoring. Analyses of that data led to the conclusion that the annual sediment deficit in the Overton to Kearney reach was most likely in the range of 50,000 tons to 75,000 tons (30,000 to 50,000 yd³). However, estimates of the deficit from cross section surveys and sediment transport estimates were highly variable with large confidence intervals, leading to low confidence in conclusions.



1 The ISAC provided feedback in 2014 and 2015 (ISAC 2014 and ISAC 2015) recommending that
2 the Program implement large-scale augmentation in the reach immediately downstream of the J2
3 Return and intensively monitor channel response using multiple lines of evidence. The
4 committee specifically mentioned application of geomorphic change detection techniques with
5 Topobathymetric Light Detection and Ranging (LiDAR) data, analysis of trends in cross-sections
6 and other geomorphic metrics through time, evaluation of the magnitude of change in the
7 longitudinal profile, and specific gage analyses.

8 The Program's policy-making Governance Committee (GC) concurred with this advice and
9 authorized the Executive Directors Office to design and implement a full-scale sediment
10 augmentation experiment. That experiment commenced in 2017 with partial scale augmentation
11 in that year¹² and full-scale augmentation in 2018-2021. The next section of Chapter 1 provides
12 an overview of sediment augmentation implementation over the course of the management
13 experiment.

14

¹² More than the full-scale augmentation volume was moved during 2017, but the majority of that material was used to eliminate a meander bend and restore farmland that had been eroded. A berm was constructed to prevent the channel from continuing to migrate south towards a road and farmstead.



1.5 Full-scale sediment augmentation management experiment (2017-2021)

1.5.1 Sediment augmentation area

The Sediment augmentation sites are located in the J2 Return Channel, beginning approximately 0.75 miles downstream of the J2 Return and extending one mile east. This one-mile section includes three augmentation sites (Figure 1.5) that Central Nebraska Public Power and Irrigation District (CNPPID) has designated as available source sites for augmentation. These sites are bounded by the black, red, and yellow polygons in Figure 1.5. Since 2017, only two have been used for source material. Pending evaluation of results, augmentation may continue in a downstream direction with one more major grading site targeted in this upstream reach (Site 3 in Figure 1.5) before moving downstream to the Plum Creek Complex, approximately 4 miles further downstream.

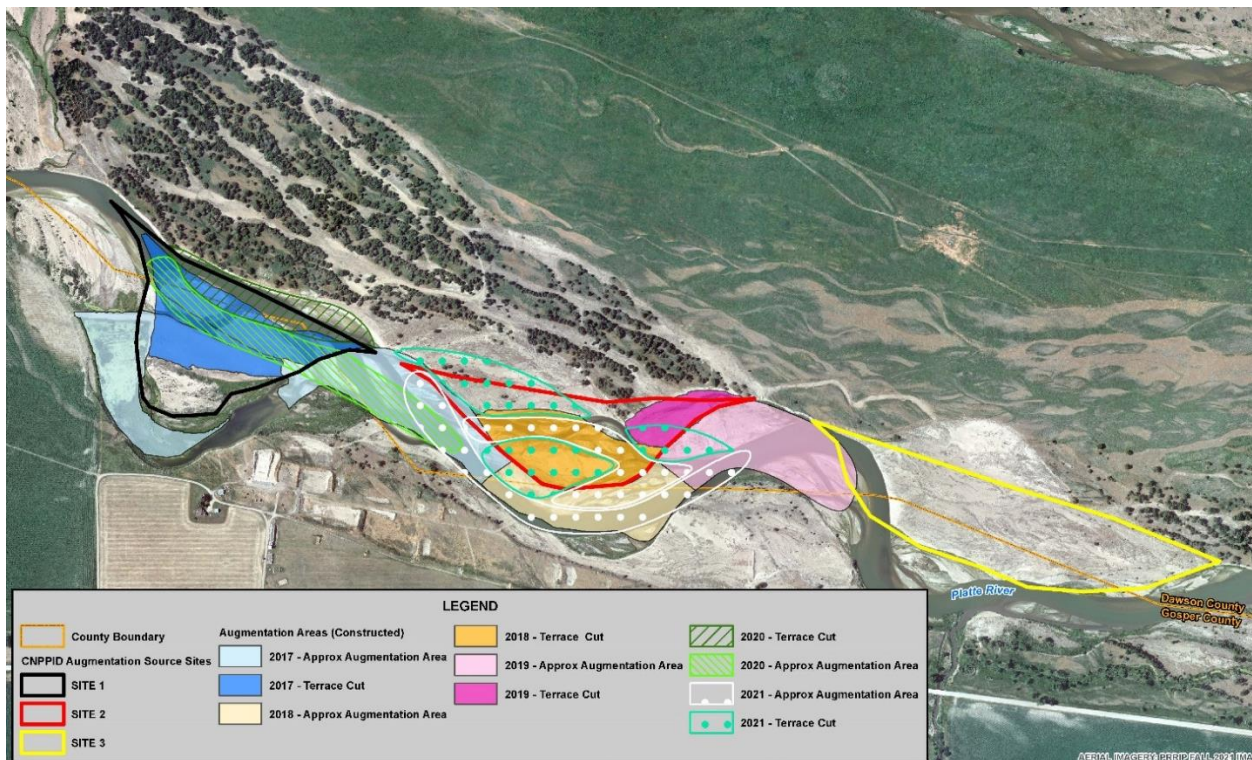


Figure 1.5 CNPPID Source Locations & 2017-2022 Augmentation Project Boundaries.

1.5.2 Timing

Sediment augmentation is implemented in the late summer/early fall each year to coincide with conducive flows out of the J2 Return. Summer low flows allow sediment to be staged, whereas long, high flow releases beginning in mid-September transport material away from the site. Due to CNPPID's hydropower production schedule, these high flow releases are interrupted by intermittent low flows. During these low flows, contractors can operate heavy equipment such as bulldozers and scrapers within the channel and stage more sediment for transport.



1.5.3 Design considerations

Alluvial material augmented to the riverbed is intended for transport downstream to mitigate sediment deficits. A full-scale sediment augmentation target was set between 60,000 to 80,000 tons (40,000–55,000 yd³) per year over a design-life of 18 years of augmentation beginning along the high banks below the J2 Return (Figure 1.5).

To begin the design process, the existing stage range elevations within the chosen area must be calculated. These elevations are calculated by running hydraulic models at peak and low flows (1650 cfs and 300 cfs, respectively) typical for CNPPID hydrocycling during late summer/early fall. These values are used to guide excavation (cut) and augmentation area elevation targets.

To encourage natural erosion of high terraces on the north bank, an elevation near the average of the stage range is chosen as the final grade for the excavation area (terrace cut areas in Figure 1.5 from which the sediment is excavated). This allows occasional inundation during high flow events, during which some bank material will be removed. To prevent nominal stage increase within the reach, the augmentation area of the project is designed at an elevation near or below the lowest end of the stage range.

Given those elevation targets, the design volume of the project must be determined. System-scale monitoring data collected from 2009 to 2014 demonstrated that trends in aggradation-degradation are highly dependent on hydrology (Tetra Tech 2014). Knowing this, it is important to consider the hydrologic condition for the given design year. If it appears that there is a dry trend, CNPPID may operate in a conservation mode, releasing less flow into the J2 Return Channel. Under these conditions, design volume tends to be lower to match expected lower flows for sediment distribution. If it is a wet year, flow releases may be higher, allowing for the distribution of more material pushed into the channel.

Knowing elevation and volume targets, the last piece of the design equation is choosing an excavation area. Loading LiDAR data from the previous year into AutoCAD Civil3D (Autodesk, San Francisco, CA) provides an existing grade against which the design surfaces can be compared. By creating an approximate design surface set to the final grade elevation, volume differencing calculations can be run. Due to the variability of elevation along the existing grade surface, an iterative approach is necessary to adjust the excavation area until the “Cut” volume is approximately equal to the target value.

Given the possibility that flows may be too low for sediment transport during construction, it is important that there is enough area within the channel for the augmented material to be placed at the lowest stage elevation. An approximate design surface is created within the channel at the lowest stage elevation. This surface is compared to the existing grade and its area adjusted until “Fill” volume is approximately equal to “Cut” volume.

1.5.4 Sediment augmentation summaries

The design approach for 2017 and 2018 targeted 60,000 tons (40,000 yd³) of immediate augmentation (Table 1.1), while encouraging the channel to continue to erode material out of the high terrace (north bank) on Jeffrey Island (PRRIP 2018). In fall of 2017, the upstream-most meander in the channel was cut off by excavating a pilot channel through an abandoned terrace and constructing a berm to shift the river to the north and mobilize sediment. 23,000 yd³ were



augmented to the main channel and 13,500 yd³ of sediment were placed into the abandoned meander.

In fall of 2018, efforts moved downstream with the same target of 40,000 yd³ and a more passive approach. By cutting down the next downstream bar, we were able to keep the sediment source on the adjacent high terraces on the left bank and encourage some deposition from upstream sources. The passive approach from 2018 was maintained in 2019, again with a target of 40,000 yd³. This excavation was completed just downstream of the 2018 site. Construction can be seen in Figure 1.6. The 2020 design moved upstream, overlapping some of the original 2017 site. Due to Normal-to-Wet hydrologic conditions and high terraces on the site, the augmentation target was higher at 50,000 yd³. The fall 2021 design also had a higher volume at 53,000 yd³. This was due to the spread-out nature of the design, with 3 separate excavation sites being augmented into the channel. Augmentation in 2022 was designed in the same area as 2017 and 2020 since the high terraces of the area provided ample material for augmentation. With flows lower in 2022, the design volume was reduced to 45,000 yd³.

Table 1.1 Sediment augmentation as-built volumes 2017-2022.

Year	Augmented (tons)	Sediment Augmentation Volume (yd ³)	Volume Leaving Sed Aug Area (yd ³)*
2017	34,500	23,000	34,500
2018	64,305	42,900	73,100
2019	63,500	42,300	116,500
2020	86,475	57,700	42,200
2021	76,982	51,300	60,600
2022	65,789	43,900	

*Volume change in augmentation area measured by differencing LiDAR elevations



Figure 1.6 Construction of 2019 Sediment Augmentation Project (42,300 yd³).

1.6 First increment extension – Big Question #3

In 2015, Program stakeholders concluded that it was not possible to meet all Program Milestones prior to the end of the First Increment in 2019. This led to a negotiated 13-year extension of the Program referred to as First Increment Extension or just Extension. The first science priority in the Extension was an overhaul of the AMP to reflect current learning priorities, called the First Increment Extension Science Plan (PRRIP 2022). Extension Big Question #3 (Figure 1.7) and related management hypotheses focus on the sediment deficit below the J2 Return, progression of impacts due to the deficit, and potential consequences for whooping crane habitat downstream of Overton. The following chapters of this data synthesis present multiple lines of evidence to address this Big Question. Chapter 2 is a retrospective analysis of the magnitude and progression of incision through time, Chapter 3 evaluates longitudinal response to sediment augmentation, and Chapter 4 expands that evaluation into three-dimensions, exploring both vertical and lateral channel evolution in the periods before and after initiation of the full-scale augmentation management experiment.

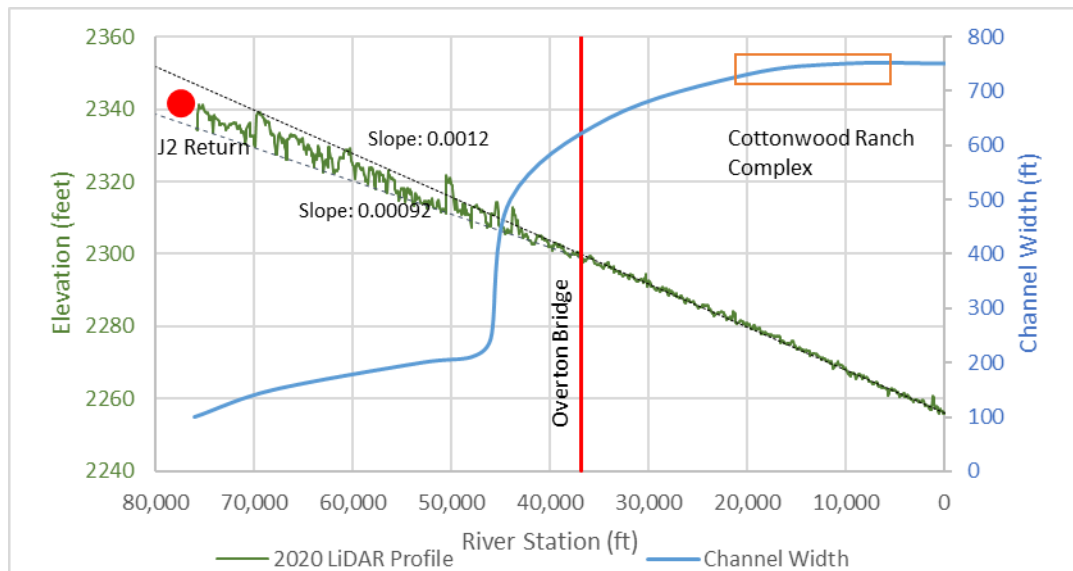


Extension Big Question #3: Is sediment augmentation necessary to create and/or maintain suitable whooping crane habitat?

**Channels with ≥ 650 ft maximum width unobstructed by dense vegetation (MUCW) are highly suitable for whooping crane roosting.*

Management Hypothesis: Sediment augmentation is necessary to halt narrowing and incision in the south channel downstream of the J-2 Return.

X-Y Graph



Full scale sediment augmentation (60,000–80,000 tons annually in the south channel below J2 Return) is necessary to offset the sediment deficit and halt narrowing and incision that has caused the upper portion of the south channel to transition to a narrow meandering planform, which is much less suitable for WC roosting. If incision is not halted, the affected reach will continue to expand downstream past the Overton Bridge, reducing habitat suitability at the Cottonwood Ranch complex.

Alternative Hypotheses:

- More or less sediment must be augmented to offset the south channel deficit.
- Augmentation at alternative locations will halt narrowing and incision.
- Full scale augmentation is not feasible over the long term – not enough supply.
- Incision and narrowing progresses downstream so slowly that augmentation is not necessary.
- Mechanical channel widening will halt narrowing and incision at habitat complexes.

Figure 1.7 Extension Big Question #3. South channel refers to the J2 Return Channel.



References

- Crowley, K.D. (1981). Large-scale bedforms in the Platte River downstream from Grand Island, Nebraska; structure, process, and relationship to channel narrowing (No. 81-1059). US Geological Survey,.
- de Vries, M. (1973). "River-bed Variations— Aggradation and Degradation," Delft Hydraulic Laboratory Publication No. 107, Delft, Netherlands.
- Graf, W. (1998). Fluvial Hydraulics, Flow and Transport Processes in Channels of Simple Geometry, John Wiley & Sons, New York, New York, 681 pp.
- HEC-RAS. (2008). Hydraulic Reference Manual. U.S. Army Corps of Engineers, Hydrologic Engineering Center.
- Holburn, E.R., Fotherby, L.M, Randle, and D.E. Carlson. (2006). Trends of Aggradation and Degradation along the Central Platte River: 1985 to 2005. United States Bureau of Reclamation.
- ISAC. (2014). Responses to Questions Posed by the Platte River Recovery Implementation Program (PRRIP) in October 2014, prepared for the Platte River Recovery Implementation Program, 18 p.
- ISAC. (2015). Responses to Questions Posed by the Platte River Recovery Implementation Program (PRRIP) in July 2015, prepared for the Platte River Recovery Implementation Program, 13 p.
- Karlinger, M.R., Mengis, R.C., Kircher, J.E. and Eschner, T. (1981). Application of theoretical equations to estimate the discharge needed to maintain channel width in a reach of the Platte River near Lexington, Nebraska. US Geol. Surv. Open File Rep, pp.81-697.
- Kircher, J.E. (1981a). Sediment analyses for selected sites on the South Platte River in Colorado and Nebraska, and the North Platte and Platte Rivers in Nebraska; Suspended sediment, bedload, and bed material (No. 81-207).
- Kircher, J.E. (1981b). Sediment transport and effective discharge of the North Platte, South Platte, and Platte Rivers in Nebraska (No. 81-53). US Geological Survey.
- Murphy, P.J., T.J. Randle, L.M. Fotherby, and J.A. Daraio. (2004). "Platte River channel: history and restoration". Bureau of Reclamation, Technical Service Center, Sedimentation and River Hydraulics Group, Denver, Colorado.
- Murphy, P.J., T.J. Randle, L.M. Fotherby, and R.K. Simons. (2006). Platte River sediment transport and vegetation model. Bureau of Reclamation, Technical Service Center. Denver, Colorado.
- O'Brien, J.S. and P.J. Currier. (1987). Channel morphology, channel maintenance, and riparian vegetation changes in the big bend reach of the Platte River in Nebraska. Unpublished report.



- 1 Platte River Recovery Implementation Program (PRRIP). (2006). Final Platte River Recovery
2 Implementation Program Adaptive Management Plan. U.S. Department of the Interior, State
3 of Wyoming, State of Nebraska, State of Colorado.
- 4 Platte River Recovery Implementation Program (PRRIP). (2018). Sediment Augmentation
5 Monitoring Brief.
- 6 Platte River Recovery Implementation Program (PRRIP). (2022). First Increment Extension
7 Science Plan.
- 8 Randle, T.J., Samad, M.A. (2003). Platte River Flow and Sediment Transport Between
9 North Platte and Grand Island, Nebraska (1895-1999). U.S. Dept. of Int., Bur. Of Reclamation
10 report, Denver, CO. 60 pp. Avail. online at: [http://www.usbr.gov/pmts/](http://www.usbr.gov/pmts/sediment/projects/index.html)
11 [sediment/projects/index.html](http://www.usbr.gov/pmts/sediment/projects/index.html).
- 12 Simons & Associates, Inc. and URS Greiner Woodward Clyde. (2000). Physical history of the
13 Platte River in Nebraska: Focusing upon flow, sediment transport, geomorphology, and
14 vegetation. Prepared for Bureau of Reclamation and Fish and Wildlife Service Platte River
15 EIS Office, dated August 2000.
- 16 Tetra Tech. (2014). Final 2013 Platte River Data Analysis Report Channel Geomorphology and
17 In Channel Vegetation. Prepared for the Platte River Recovery Implementation Program.
- 18 Tetra Tech. (2015). Draft Model Results, Platte River Sediment-transport Modeling, South
19 Channel at Jeffrey Island, prepared for the Platte River Recovery Implementation Program,
20 19 p.
- 21 Tetra Tech. (2017). Final Data Analysis Report Channel Geomorphology and In-Channel
22 Vegetation, prepared for the Platte River Recovery Implementation Program, 305 p.
- 23 The Flatwater Group, in association with Tetra Tech and HDR (2010). Sediment Augmentation
24 Experiment Alternatives Screening Study Summary Report, prepared for the Platte River
25 Recovery Implementation Program, 266 p.
- 26 The Flatwater Group, in association with Tetra Tech and HDR (2014). Sediment Augmentation
27 Final Pilot Study Report, prepared for the Platte River Recovery Implementation Program,
28 123 p.
- 29 Williams, Garnett P. (1978). The case of the shrinking channels: the North Platte and Platte Rivers
30 in Nebraska. M.S. Thesis. University of Wyoming, Laramie. In U.S. Geological Survey
31 Circular 781. 48 pp.



CHAPTER 2 Evaluation of trends in incision prior to full-scale sediment augmentation

2.1 Abstract

The Platte River Recovery Implementation Program (PRRIP or Program) is concerned that incision and narrowing downstream of the J2 Return may continue to progress downstream, negatively impacting the suitability of roosting habitat for the highly endangered whooping crane (*Grus americana*). Evaluating historical patterns and rates of incision provides insight into the potential magnitude of future impacts in absence of long-term augmentation of sediment supply. We conducted retrospective analyses to evaluate spatial and temporal patterns of incision. This included comparing current channel topography to the historical channel elevation (relative elevation model), evaluation of incision trends at repeat transect survey locations, development of specific gage analyses at the Overton Bridge and Cottonwood Ranch mid-channel stream gages, and estimation of changes in channel sinuosity through time using aerial imagery. These analyses indicated a wave of vertical incision propagated down through the study area after J2 Return began operations in the early 1940s. In the early 2000s, the primary mechanism of channel degradation shifted from incision to lateral migration, with the highest intensity of migration occurring in upper half of the J2 Return Channel.

2.2 Introduction

As discussed in Chapter 1 of this data synthesis, since the 1980s, stakeholders of the Platte River Recovery Implementation Program (PRRIP or Program) have been concerned about channel degradation due to clearwater hydropower returns near Lexington, NE. During the First Increment of the Program, the Governance Committee (GC) initiated monitoring, modeling, and research projects to explore the magnitude and extent of the problem. Those efforts resulted in three major conclusions:

- 1) There is a persistent sediment deficit downstream of the J2 Return that has resulted in incision and narrowing of the segment of channel that extends from the J2 Return to the Overton Bridge (J2 Return Channel).
- 2) Downstream of the Overton Bridge, there was no discernable degradational trend during the period of 2009-2016.
- 3) Over time, the degradation (incision and narrowing) observed in the J2 Return Channel could progress downstream beyond the Overton Bridge, decreasing the proportion of the central Platte River suitable as habitat for whooping crane roosting.

In response to these findings, the Program initiated a full-scale sediment augmentation experiment in 2017 to test the hypothesis that offsetting the sediment deficit downstream of the J2 Return is necessary to halt downstream progression of channel degradation (Extension Big Question 3). Implicit in this hypothesis is an unquantified level of risk relating to the rate that degradation is progressing downstream absent augmentation as well as the relationship between incision magnitude and degradation of habitat suitability. The objective of this chapter is to evaluate the magnitude and rate of channel degradation in the decades prior to augmentation and compare to stakeholder predictions. This is accomplished through four retrospective analyses that rely on historical aerial imagery, stream gaging data, repeat channel transect surveys, and remote sensing topographic data collected prior to implementation of full-scale augmentation.



2.2.1 Study area

The focus area for this study encompasses the western portion of the Program’s Associated Habitat Reach (AHR) extending from Lexington, NE downstream to the Kearney Canal Diversion (KCD), located two miles downstream of Elm Creek, NE. Figure 2.1 provides an overview of the study area including channel segments, stream gage locations, and landmarks referenced in this chapter.

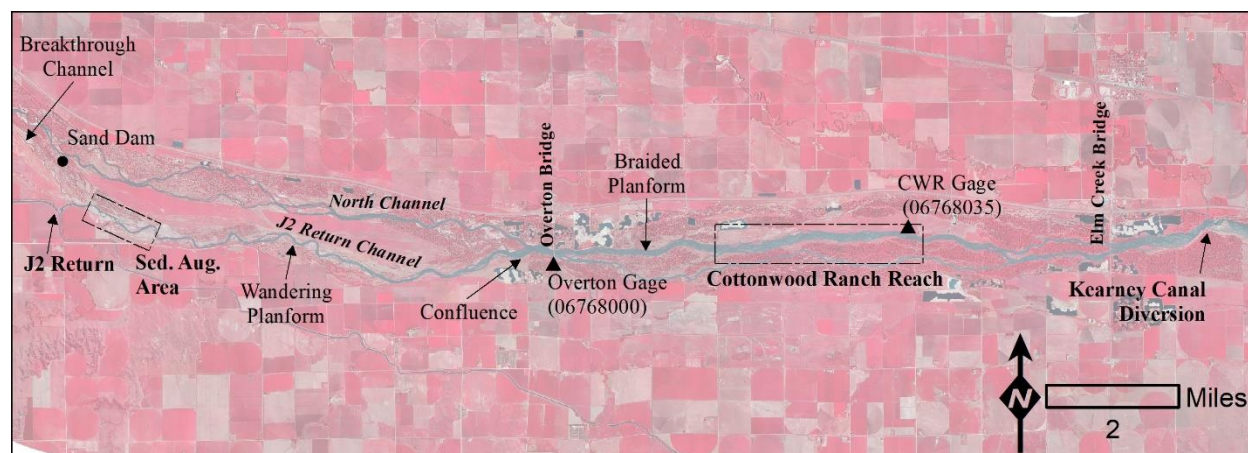


Figure 2.1. Map of the sediment augmentation study area including channel segments, stream gage locations and landmarks of interest.

To provide consistent spatial referencing (stationing) for all longitudinal analyses, we delineated the approximate centerline of the floodplain from the KCD upstream to the Lexington bridge (Figure 2.2) and cut transects across the entire floodplain perpendicular to centerline at five-foot intervals. Stationing starts at 0 at KCD and ends at station 113,780 at the Lexington bridge. Stationing for important landmarks is provided in Table 2.1.

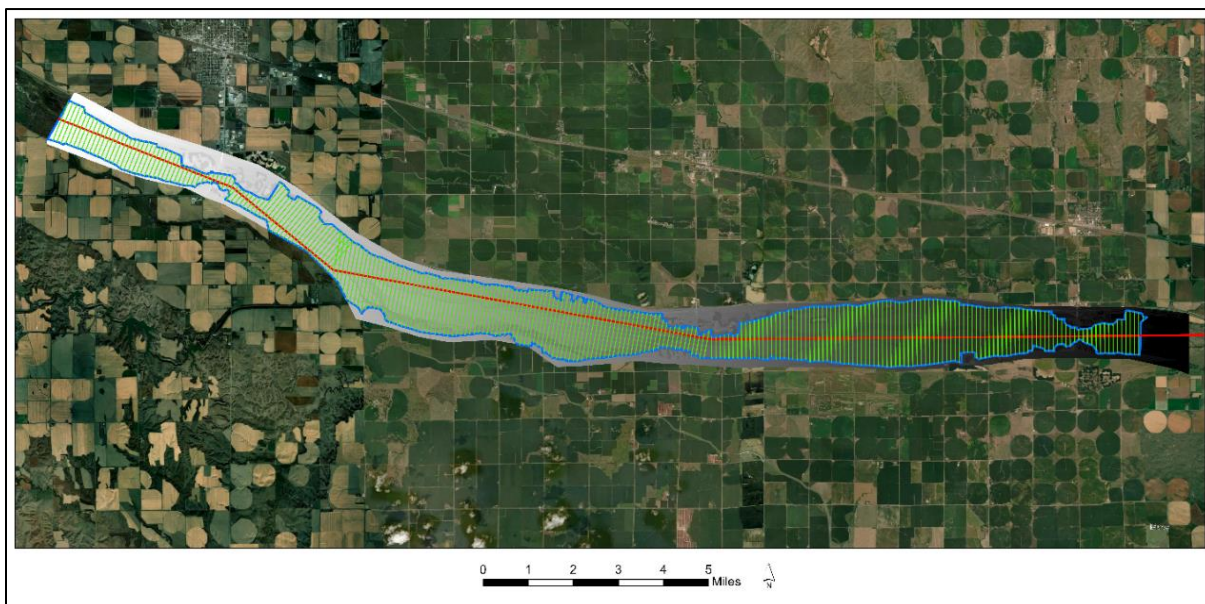


Figure 2.2. Floodplain centerline (red) and transects (green) through study area. Transects were generated perpendicular to centerline at five-foot intervals with example transects plotted at 500 ft spacing in this figure.

Table 2.1. Landmarks in the study area and associated stations.

Landmark	Station (ft)
Lexington Bridge	113,780
Berm at upstream North/J2 Return Channel split	101,890
J2 Return (Sand Dam is roughly same stationing)	91,955
Upstream extent of sediment augmentation area	89,360
Downstream extent of sediment augmentation area	84,000
North Channel/J2 Return Channel confluence	55,290
Overton Bridge	52,600
Cottonwood Ranch, upstream extent	39,925
Cottonwood Ranch, mid channel stream gage	25,120
Cottonwood Ranch, downstream extent	23,665
Elm Creek Bridge	8,395
Kearney Canal Diversion (KCD)	0

2.2.2 Overview of analyses

As stated in the introduction, the objective of this chapter is to explore historical incision and planform change downstream of the J2 Return prior to the initiation of full-scale sediment augmentation in the fall of 2017. The J2 Return began operations in the early 1940s but there was little focus on channel incision in this reach until the 1980s. Consequently, historical data is limited primarily to historical aerial photography, limited repeat cross section surveys collected in the late 1980s and early 2000s, and stream gaging records. In this chapter we utilized these



data in combination with contemporary remote sensing to explore patterns of channel incision through time. Specific analyses include:

- 1) development of a Geomorphic Grade Line and relative elevation model for 2016 to provide a snapshot of historical channel incision (relative to floodplain elevation) prior to implementation of full-scale augmentation,
- 2) analysis of historical repeat transect surveys and LiDAR data to evaluate spatial and temporal patterns of incision relative to those predicted in Murphy et al. (2004),
- 3) specific gage analyses at the Overton and Cottonwood Ranch Mid-Channel stream gages to identify temporal patterns of incision at those locations, and
- 4) estimation of channel sinuosity from aerial photography to quantify changes in channel length in the J2 Return Channel through time.

The results of these analyses are interpreted together to provide our assessment of spatial and temporal patterns of channel change prior to the implementation of the full-scale sediment augmentation management experiment and predict potential future patterns of incision in absence of augmentation.

2.3 Geomorphic Grade Line and relative elevation model

2.3.1 Methods

We utilized methods presented by Powers et al. (2019) to generate a Geomorphic Grade Line (GGL), or linear regression of valley slope, from fall 2021 Light Detection and Ranging (LiDAR) derived topography. The GGL is used as the reference plane for development of a relative elevation model (REM) of the study area. First, we hand delineated the geographical extent of the existing floodplain, which represents the pre-development channel. Mid-channel islands were not removed but human-made features like gravel mines, road embankments, and other development-related topographic features were clipped from the boundary. The fall 2021 LiDAR digital elevation model (DEM) was then sampled along transects at five-foot intervals within the floodplain, and we calculated average elevation for each transect (station). Mean transect elevations were regressed against station to establish the GGL for the study area.

Relative elevation models (REMs) provide a way to visualize and quantify channel elevations without influence of the overall valley slope and are commonly used in river restoration to determine areas of cut and fill when regrading the valley bottom (Powers et al., 2019). To develop a REM, we first generated a raster of the GGL for the study area. We then differenced the fall 2016 LiDAR DEM and GGL (DEM – GGL) to calculate the elevation of each raster cell relative to the GGL.

2.3.2 Results

The regression of average elevation versus river station (numbered downstream to upstream), or GGL, can be found in Figure 2.4. The slope of the GGL in the study area is 0.001276. Because stationing is from downstream to upstream, slope appears positive in the equation. The slope of the GGL is consistent with previous analyses of channel slope in the AHR (Murphy et al., 2004).

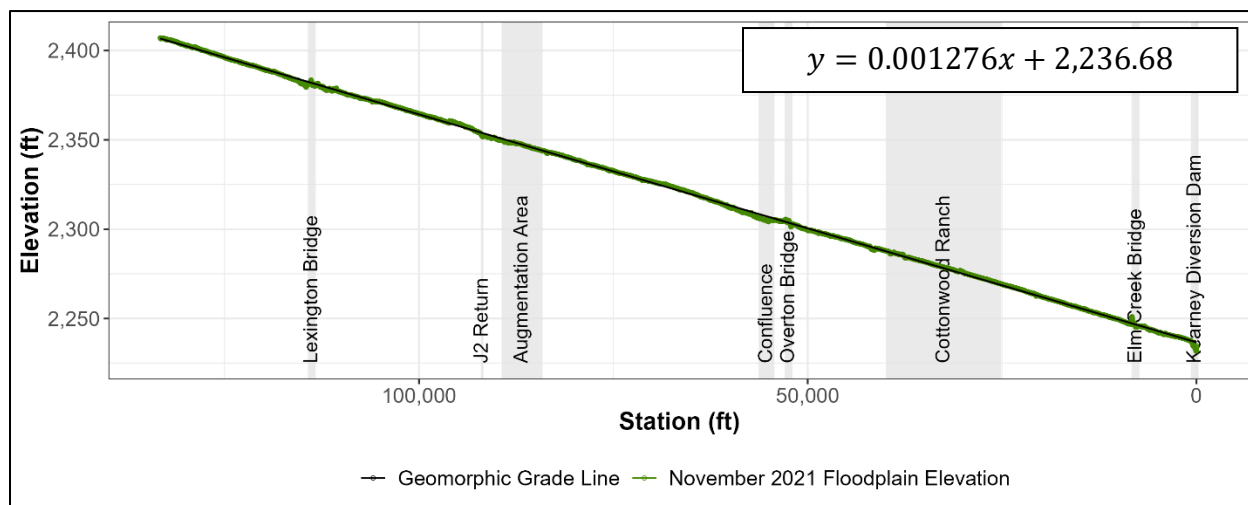


Figure 2.4. Geomorphic Grade Line (GGL) (black) of historical channel footprint in study area sensu Powers et al. (2019). Average elevation data sampled from 2021 LiDAR data (green) is plotted along with the GGL as presented in the equation.

The REM for 2016 is presented in Figure 2.5. A profile plot of REM elevations at lowest point in the channel (thalweg) is provided in Figure 2.6. The REM and REM thalweg profile provide a quantitative visualization of cumulative channel change downstream of the J2 Return to the extent that the GGL provides a good representation of pre-development channel elevations. As demonstrated in Figure 2.5, elevation deviation from GGL (incision) is greatest immediately downstream of the J2 Return. Channel elevation in that segment in 2016 was on the order of 15–20 ft below GGL. In comparison, the relative elevation of the North Channel in that same area, which is not affected by hydropower return flows, was only 2–4 ft below GGL.

In the highly incised upper half of the J2 Return Channel, the REM also indicates a change in planform to a narrower channel with high sinuosity that is visible in relative elevations ranging from 10 ft to 22 ft below GGL. This pattern becomes less obvious as the magnitude of J2 Return Channel incision decreases in a downstream direction. At the confluence of the North Channel and J2 Return Channels 6.5 miles downstream of the return, most of the channel is 4–6 ft below GGL and braiding is apparent with a limited amount of incision progressing back up the North Channel. Downstream of the North and J2 Return Channel confluence, a limited amount of incision can be observed in the mile of channel downstream of the Overton Bridge. Beyond that, the REM indicates channel elevations are generally consistent relative to the GGL.

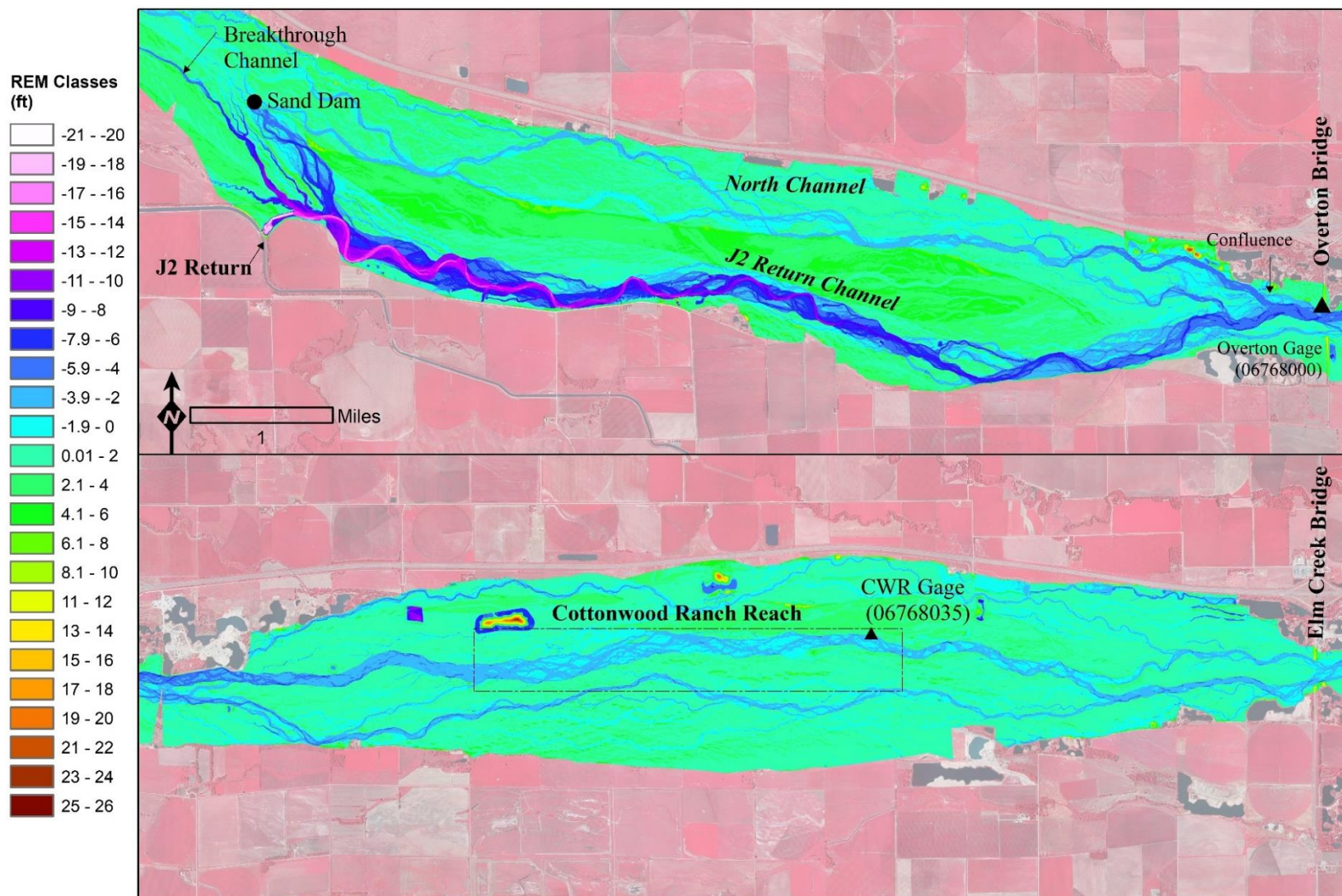
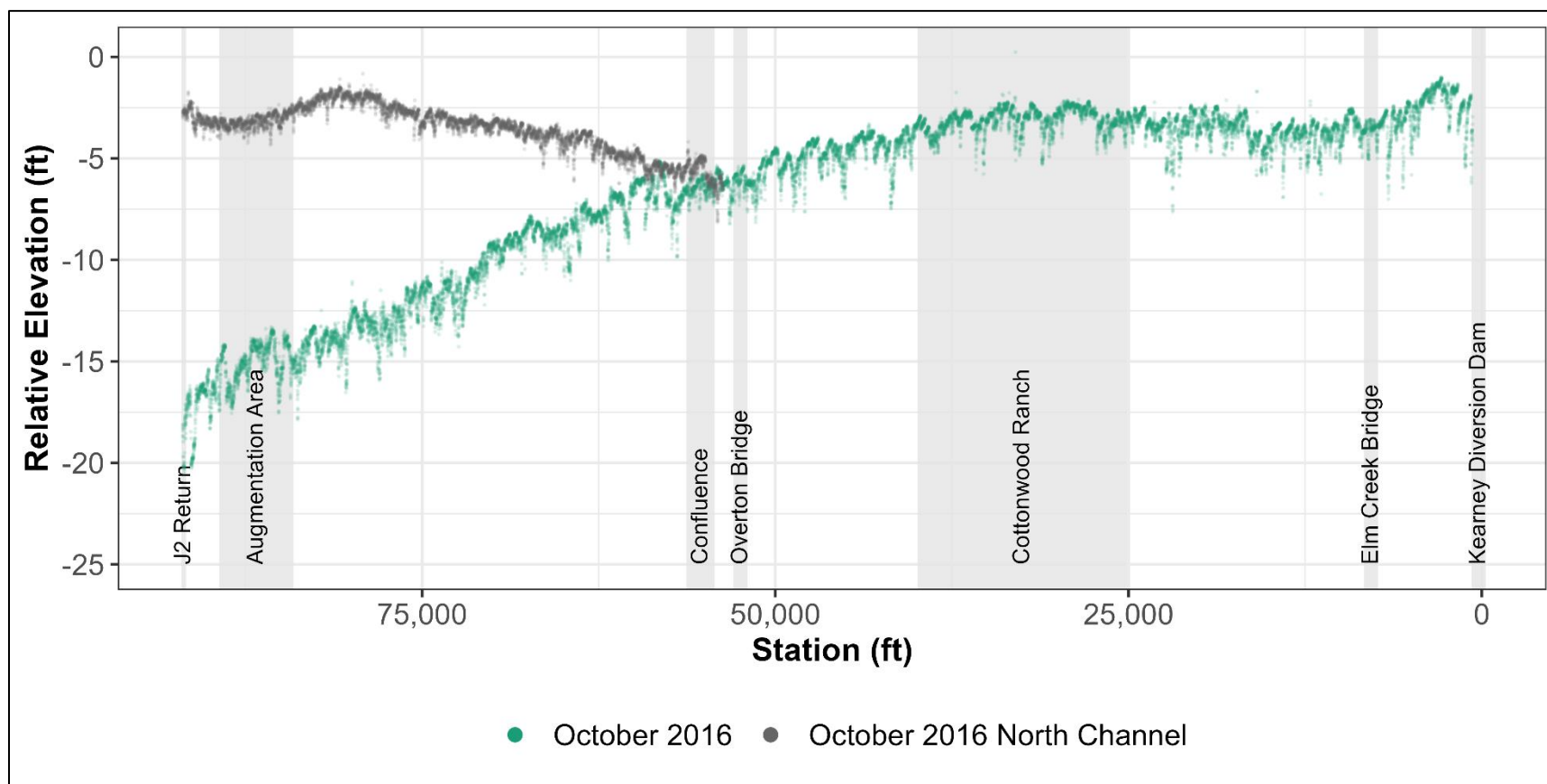


Figure 2.5. Relative elevation model (REM) of 2016 topography compared to the average elevation of the historical channel (GGL). The figure is split into J2 Return to Overton Bridge (top) and Overton Bridge to Elm Creek Bridge (bottom). Edges appear irregular due to clipping of ponds and other human-manipulated surfaces. Deviations from the GGL are much larger (10-20 ft below the floodplain) near the J2 Return and decrease to 1-6 ft below the floodplain toward the downstream extent of the study area.

1



2

Figure 2.6. Elevation of deepest point (thalweg) in the North Channel (gray) and J2 Return/Main Channel (green) relative to Geomorphic Grade Line (GGL). The segment of channel immediately downstream of the J2 Return is incised on the order of 15–20 feet lower than the North Channel at the same station. Magnitude of incision decreases in a downstream direction with the thalweg becoming roughly parallel to GGL (GGL has a value of 0) near the upper end of the Cottonwood Ranch habitat complex. North Channel incision is also apparent upstream of the confluence of the North and J2 Return Channels.

8

9

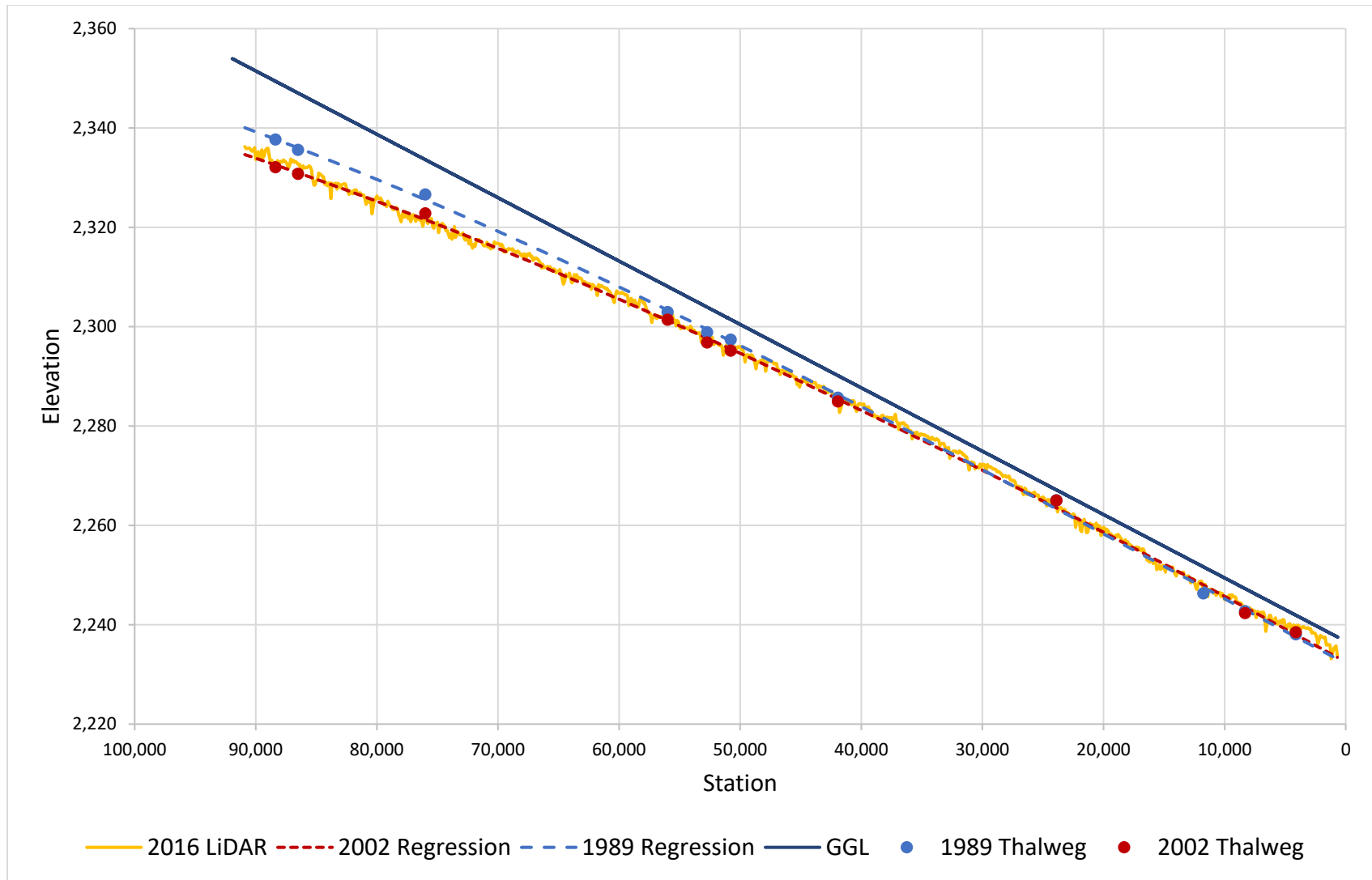


2.4 *Analysis of spatial and temporal trends in incision 1989-2016 relative to predictions*

2.4.1 Methods

Murphy et al. (2004) included predictions of incision downstream of the J2 Return over time based on an incision wave propagation model (de Vries 1973), later referenced in Graf (1998). The model predicted downstream propagation of incision through time based on a ratio of incision downstream of the J2 Return relative to maximum incision at the return. According to Murphy et al. (2004), the maximum incision relative to the North Channel thalweg elevation in 2002 was 13.3 ft. We compared to the Murphy et al. (2004) predictions of downstream spread of incision by plotting incision as the difference in elevation from modified GGLs that match the elevations of the 2002 North Channel thalweg and mean cross-sectional elevations. We used 1989 and 2002 channel cross sections and 2016 LiDAR data to compare observed and predicted incision patterns (Figure 2.8).

Repeat cross section data used in this analysis were collected by the United States Bureau of Reclamation (USBR) in 1989 and DJ&A consultants in 2002 (Holburn et al. 2006). These entities surveyed a total of 11 cross sections in 1989 between the J2 Return and KCD. Ten were repeated in 2002. We clipped the cross sections in ArcGIS to the extent of the active channel (5,000 cfs flow boundary) and calculated the minimum (thalweg) elevation and mean channel elevation at each survey cross section. The 2016 LiDAR DEM was also clipped and sampled to calculate thalweg and mean channel elevations at 5-foot intervals throughout the reach. Both mean and thalweg elevations were calculated and used in the analysis to evaluate maximum (thalweg) incision as well as general channel incision (mean). We used cubic (third order polynomial) regression to model full longitudinal profiles for thalweg and mean channel elevations from 1989 and 2002 with cross section data from 11 points in 1989 and 10 points in 2002 (Figure 2.7). Third order regression provided the best fit to the limited transect data and was consistent with the general shape of the 2016 LiDAR-derived profiles for mean cross-sectional elevation. We used a generalized additive mixed model (GAMM) for the 2016 thalweg elevations rather than a polynomial regression due to a more accurate fit. The methods for the GAMM are further described in Section 3.4.1.



1
2 **Figure 2.7.** Modeled longitudinal profiles (cubic regression) of thalweg from 1989, 2002 cross section data. Profiles plotted with
3 Geomorphic Grade Line (GGL) and thalweg profile from 2016 LiDAR data. Deviation from the GGL is evident between Stations
4 50,000 and 90,000 and increases between 1989 and 2002. No additional increase in deviation is observed between 2002 and 2016.



Incision was calculated at 100 ft intervals by differencing profile elevation from modified GGLs for both the thalweg profile and the mean channel elevation profile. We used Murphy et al.'s (2004) maximum incision value of 13.3 ft below the 2002 North Channel thalweg for our maximum potential thalweg incision. To validate the use of this value, we confirmed that 2016 channel elevations remained approximately 13 ft below the original 2002 North Channel thalweg elevation at the original USBR transect location. Mean channel elevations from 2016 did not match the minimum mean channel elevation in 2002, so we used the 2016 minimum mean cross-sectional elevation for our maximum possible incision of mean channel elevation. The modified GGLs were based on the original GGL, but reduced in elevation by 3.59 ft to meet the 2002 North Channel thalweg elevation for thalweg comparisons, and reduced by 0.59 ft for mean elevations. The final step in recreating Murphy et al.'s incision plot was calculating proportion of maximum incision depth by dividing profile incision depth by maximum incision depth at each station.

2.4.2 Results

Comparisons of observed incision relative to Murphy et al. (2004) predictions are provided in Figure 2.8. The top panel (panel a) presents thalweg (minimum channel elevation) incision relative to Murphy et al.'s predictions. The bottom panel (panel b) presents mean channel incision relative to predictions. Both panels begin one mile downstream of the J2 Return and end at the KCD. The number of years in both plots reference years since J2 Return was constructed.

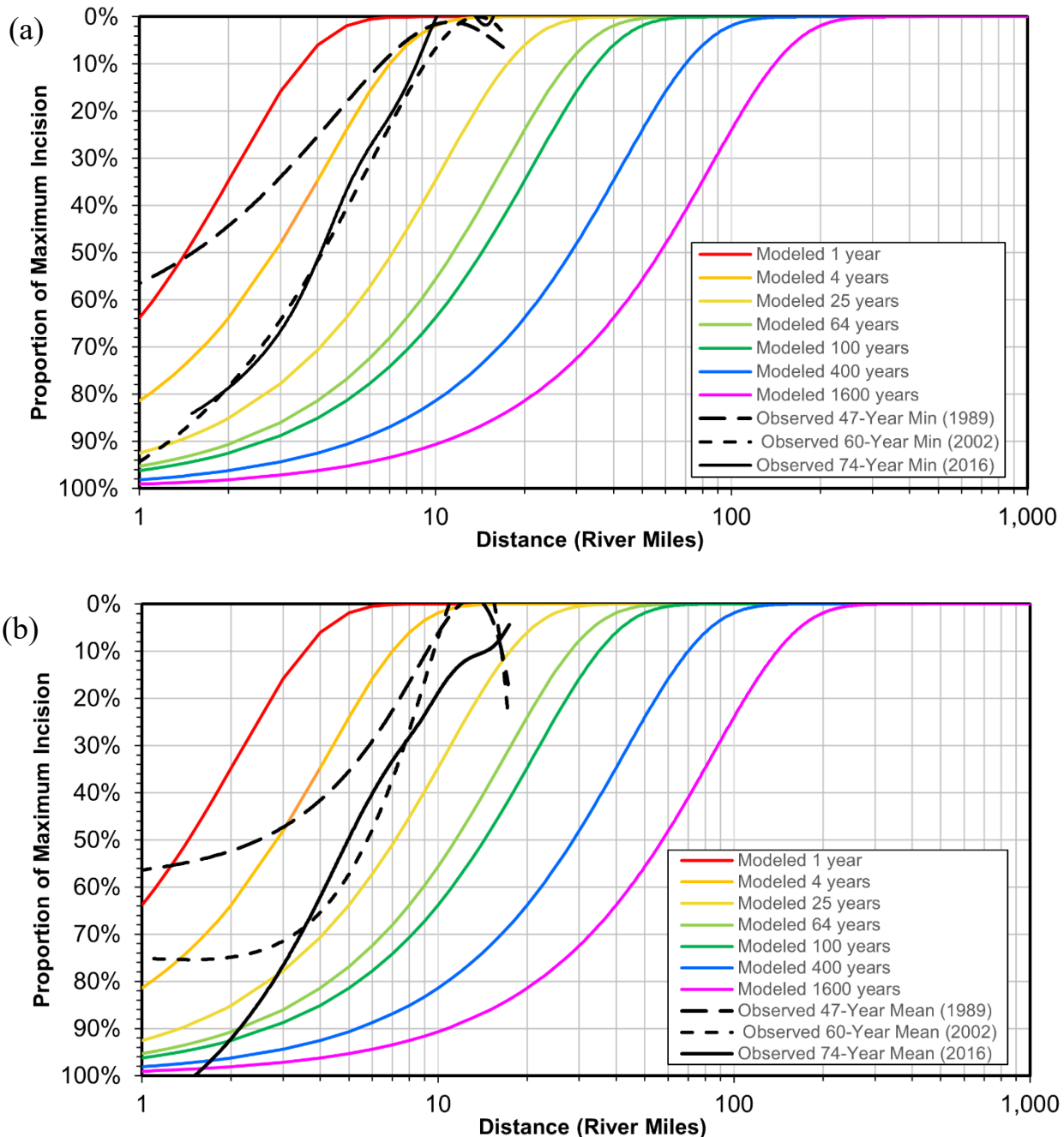
When observed incision is plotted on top of predictions, the observed extent of thalweg and mean channel incision propagation over the course of the 80 years since J2 Return operations began both fall between the 4-year and 25-year predictions for years 2002 and 2016. This indicates downstream propagation of incision has occurred substantially more slowly than predicted. Beyond the similarity in slower rate of observed progression of incision relative to predictions, the temporal incision patterns differ substantially.

The thalweg incision plot (panel a) indicates that approximately 55% of thalweg incision immediately downstream of the J2 Return occurred prior to 1989 and the remainder occurred prior to 2002. Between 2002 and 2016, the thalweg was stable, with little vertical incision occurring during that period. The mean channel elevation plot (panel b) indicates that mean channel incision did not stabilize after 2002, especially in the three-mile segment below the J2 Return, where mean channel elevation continued to decrease despite thalweg stability. Taken together, the panels indicate a shift from incision to erosion through lateral channel movement (lateral erosion) after 2002.

The 1989, 2002, and 2016 incision plots all terminate slightly less than 20 miles downstream of the J2 Return at the KCD. The plotted portion of maximum incision depth between approximately 10 and 20 miles downstream of the diversion is highly variable indicating inconsistent trends in that reach. This may be due to differing patterns of sediment accumulation and transport upstream or through KCD during wet and dry periods. A longer study period may be needed to reduce variability and increase sample size.



1



2 **Figure 2.8.** Channel incision estimates below J2 Return plotted on top of incision propagation
3 estimates from Murphy et al. (2004). Minimum cross section elevation (thalweg) incision is
4 shown in (a) and the mean channel elevation incision is shown in (b). Number of years
5 represents years since operation started at J2 Return. Observed values from 1989 and 2002 were



estimated with a 3rd order polynomial model through 10 transect locations, while 2016 observed values are based on a Generalized Additive Mixed Model made with LiDAR data (thalweg) and a 3rd order polynomial through LiDAR data (mean).

Our use of Murphy et al.'s estimate of 13.3 ft for maximum thalweg incision below the North Channel allows for calculation of estimated thalweg elevation after 74 years (1942 to 2016) and subsequent comparison to 2016 LiDAR data (Figure 2.9). The model-predicted and measured thalweg elevation values diverge in the J2 Return Channel. The incision propagation model does not account for any changes in channel slope, sinuosity, or sediment discharge through time, and is therefore an oversimplified prediction of channel response to clearwater release from the J2 Return.

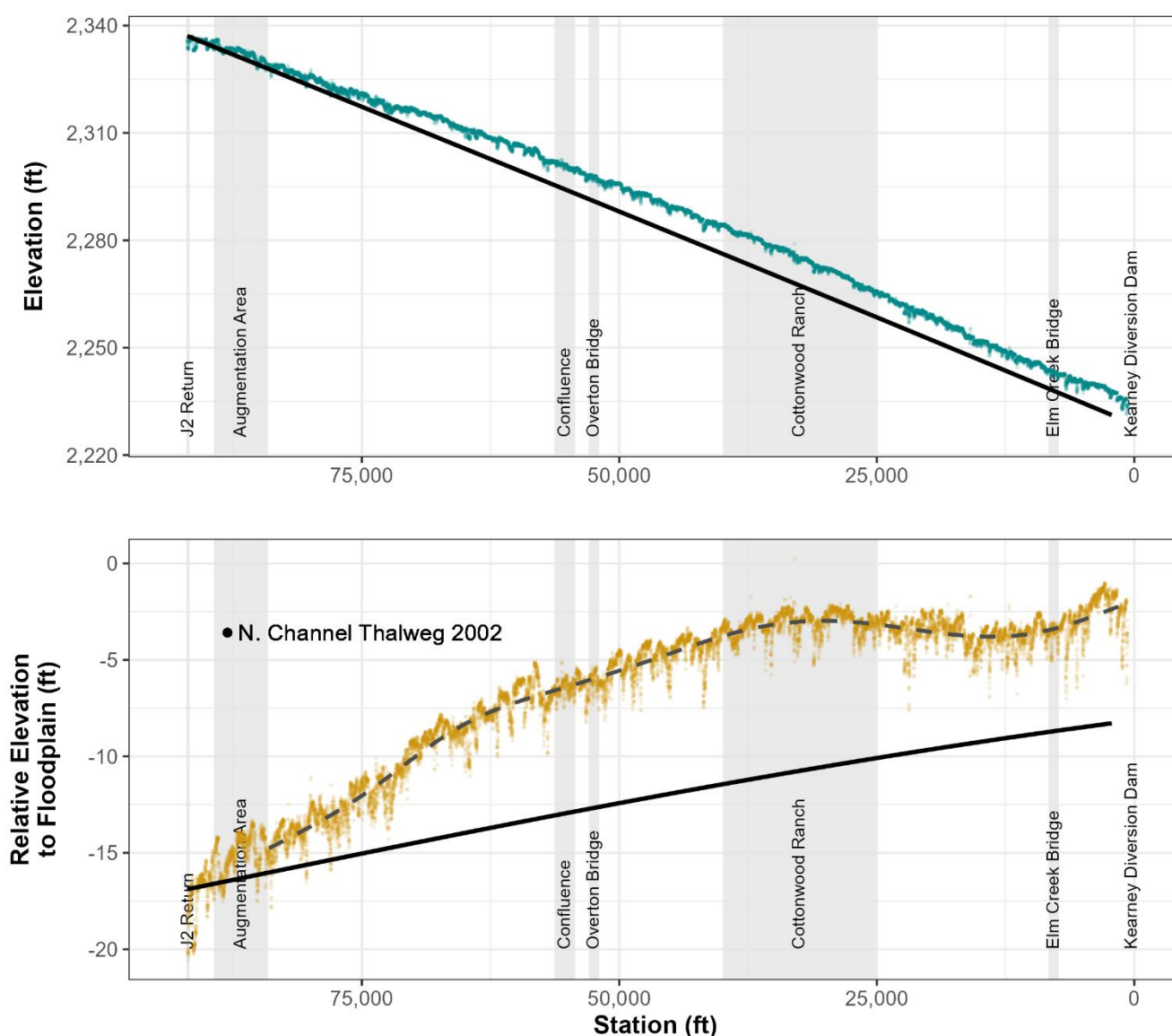


Figure 2.9. Observed and predicted channel thalweg elevations (a) and relative elevations to the floodplain (b) according to incision models presented in Murphy et al. (2004). The bold black



lines in both plots show predicted elevations, while the dashed line in (b) is a modeled thalweg from a generalized additive mixed model (GAMM). We used a maximum potential thalweg incision value of 13.3 ft below the 2002 North Channel thalweg to be consistent with historical estimates.

2.5 *Specific gage analysis*

2.5.1 Methods

The presence of USGS stream gages at the Overton Bridge and the downstream end of Cottonwood Ranch (see location Figure 2.1) provide an opportunity to assess incision patterns through time at those locations via a specific gage analysis. Trends of increasing or decreasing water surface elevation at a constant discharge can be linked to a variety of complex processes and are associated with sediment supply and vegetation dynamics. Increasing water surface elevation at a constant discharge through time is an indication that the channel at that location is aggradational, whether width changes or remains static. Declining water surface elevation could indicate several channel responses, including channel degradation alone, channel degradation and narrowing (e.g. due to vegetation encroachment and/or decreased sediment supply), or channel widening. In this study, we interpret decline in water surface elevations to be generally indicative of channel degradation.

Specific gage analyses can be conducted using either stage-discharge records or physical measurements that are used to develop and adjust stage-discharge rating curves. This analysis relies solely on physical measurement data to eliminate potential biasing related to stages that are estimated from rating curves (Samaranayake 2009, Biedenharn et al. 2017). Physical measurements include an unknown but low uncertainty in stage. Discharge at stage is estimated using current-meters or acoustic doppler current profilers (ADCP). USGS rates measurements as excellent, good, fair or poor, which correspond to potential errors of less than 2%, 5%, 8%, and greater than 8% respectively (Turnipseed and Sauer 2010). For the purpose of this analysis we filtered physical measurement data to remove measurements with poor ratings as well as all measurements in the months of December through February, which are often ice-affected.

Specific gage analyses examine trends in water surface elevation through time at a discharge. We chose to evaluate three discharges at each gage including the 10th and 50th percentile of mean daily discharge and median of instantaneous annual peak discharge during the period when physical measurements were available. These three discharges allowed us to evaluate trends in stage at low flows, normal flows, and at approximate bankfull discharge.

Most specific gage analyses involve development of simple linear regressions of stage through time for a range of discharges around a target discharge (Chen et al. 1999, Biedenharn et al. 2017). This is done to obtain a sufficient sample size to meet linear regression assumptions. For example, a specific gage analysis at 1,000 cfs would generally include all measurements collected from 800 to 1,200 cfs. If actual discharges are skewed above/below target through time, this approach can provide a biased estimate of stage change. Using simple linear regression also has other limitations including inability to model non-linear relationships and lack of meaningful estimates of uncertainty.



1 To address these issues, we developed generalized additive models (GAMs) for all physical
2 measurement data at each gage with smoothed relationships limited to five degrees of freedom
3 (Hastie and Tibshirani 1990). GAMs allowed us to estimate possible non-linear relationships of
4 stage-discharge relationships using all appropriate physical measurement data. We then plotted
5 the estimated relationships of stage-discharge for the three discharges described above with 95%
6 confidence intervals.

7 8 2.5.2 Results

9 2.5.2.1 *Overton Gage (06768000)*

10 The period of record for the Overton stream gage extends from October 1, 1930, to present.
11 However, the gage has been relocated several times and was moved to the present location on
12 October 10, 1986. At the current location, operation has been continuous with one major datum
13 adjustment (lowered by 2.0 ft) on September 30, 2004. Specific gage analysis results cover the
14 period from October 1986 to present with an adjustment to bring the entire period of record onto
15 a single datum. Figures 2.10 through 2.12 provide a time series of aerial imagery at the gage
16 location.

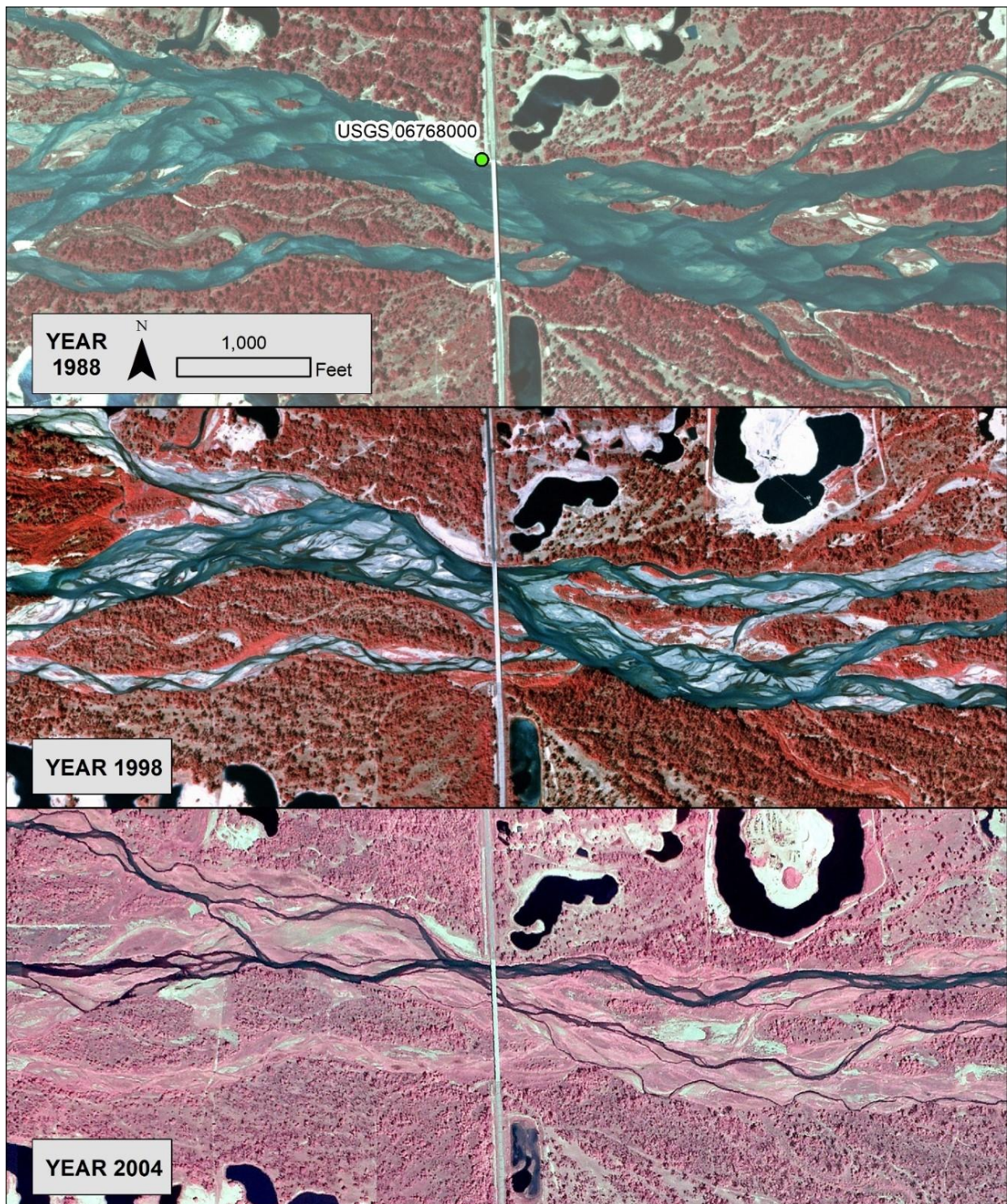


Figure 2.10. Imagery at Overton Gage (USGS 06768000) 1998 through 2004.

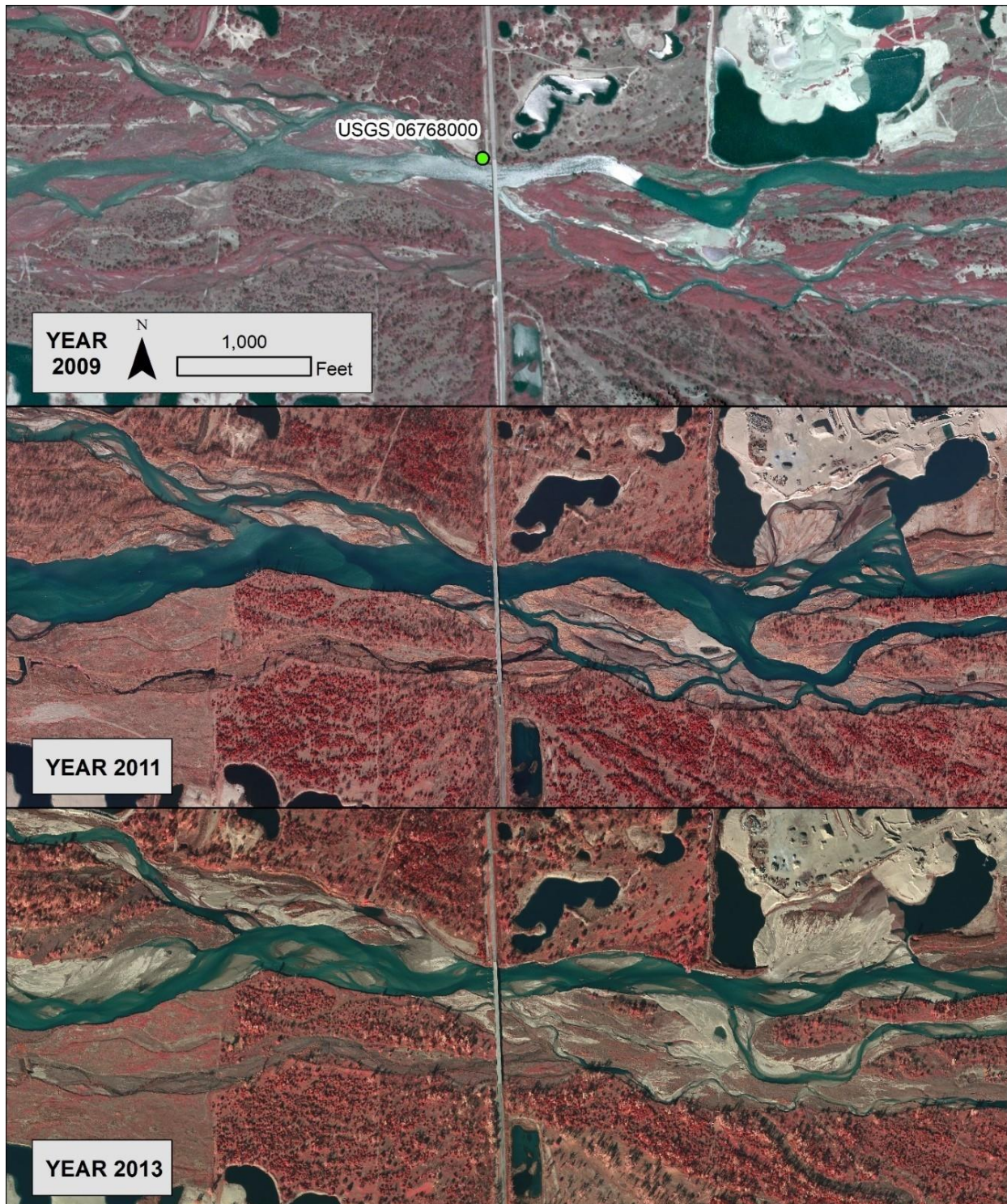


Figure 2.11. Imagery at Overton Gage (USGS 06768000) 2009 through 2013.

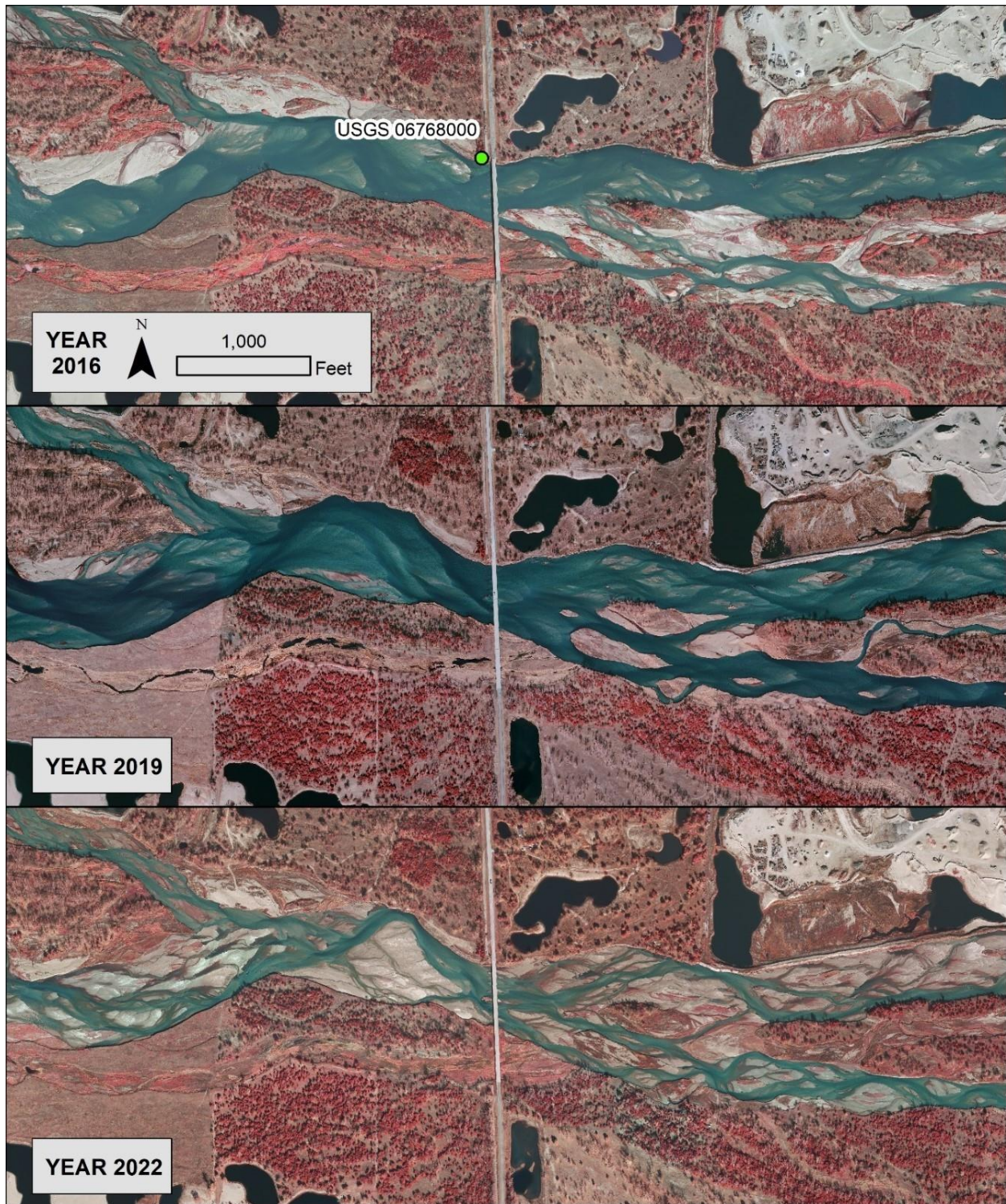


Figure 2.12. Imagery at Overton Gage (USGS 06768000) 2016 through 2022.



Figure 2.13 provides physical stage measurement data for the study period at the current Overton gage location along with trailing 30-day mean discharge. In the figure, stages are binned by discharge. The measurement data indicates slight decline in stage for discharges below 3,000 cfs until the late 1990s when the decline began to accelerate, especially at lower discharges. The trend of declining stage continued through approximately 2013 when it reversed and stage began to increase at low discharges (<1,000 cfs). Stage trends at higher discharges are less clear but appear to indicate a long term decline.

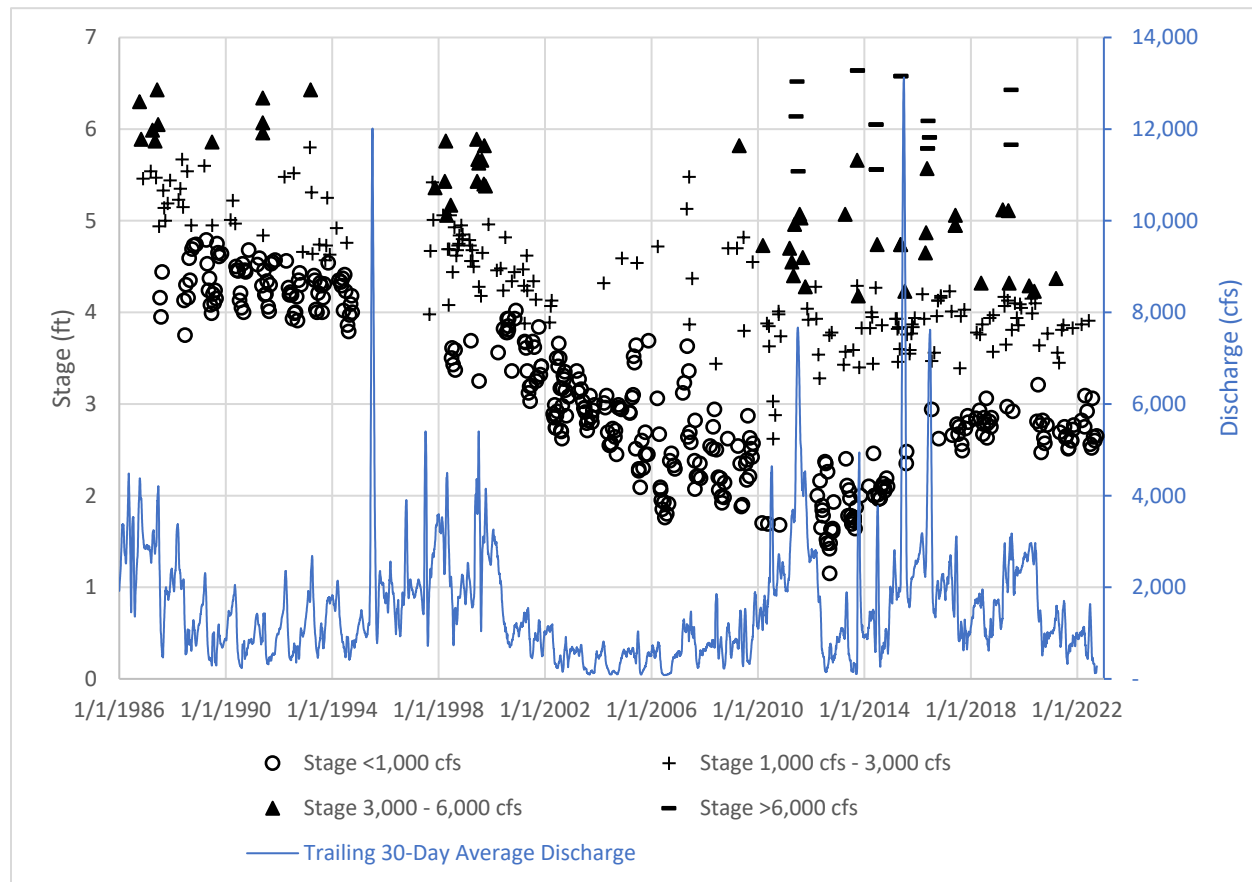


Figure 2.13. Physical measurement stage data at Overton Gage (USGS 06768000) and trailing 30-day average discharge.

Figure 2.14 provides specific gage analysis results. The specific gage analysis indicates decreasing stage at the Overton Bridge at low and median discharges from 1986-2013 with a total magnitude of approximately two feet. That trend is reversed in 2014 with stage increasing, especially at the 10th percentile discharge. Stage at the median annual peak discharge has declined throughout the period of record. This indicates that approximately two feet of incision occurred at the bridge between 1990 to 2014 with the greatest rate of change in the 2000s. The specific gage analysis results can be observed in Figures 2.9 through 2.11 which show narrowing, incision and side channel deactivation between 1988 and 2009, relative stability from 2009–2013, and pronounced widening in 2016 and beyond.

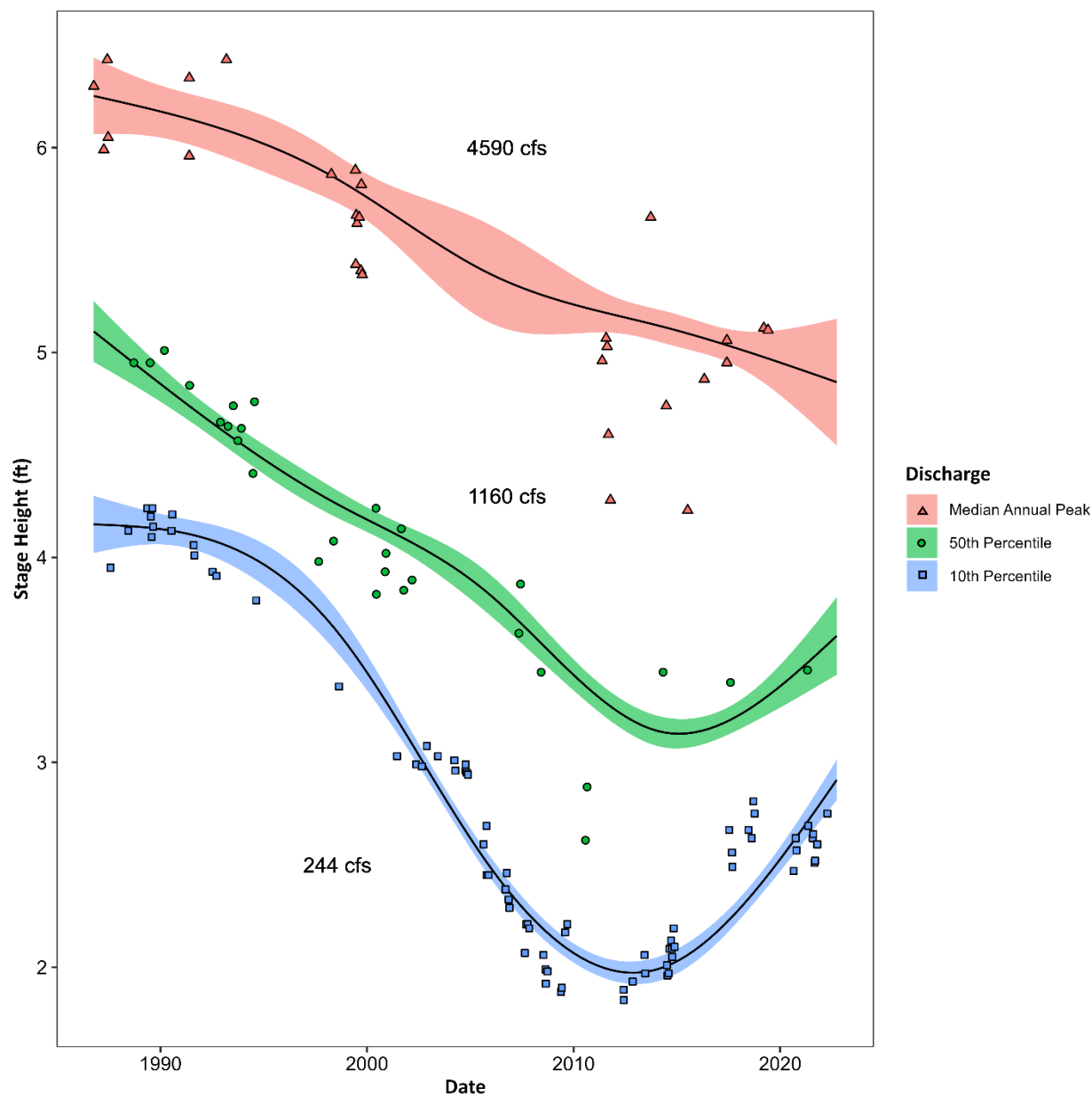


Figure 2.14. Specific Gage analysis for Overton Gage (USGS 06768000) at 10th percentile discharge of 244 cfs, median discharge of 1,160 cfs, and median annual peak discharge of 4,590 cfs. Shaded regions represent 95% confidence intervals for each discharge. Results indicate that elevations at this gage have decreased since 1986, though a rebound may be occurring beginning in 2013.



2.5.2.2 *Cottonwood Ranch Mid-Channel Gage (06768035)*

The period of record for the Cottonwood Ranch Mid-Channel stream gage extends from October 1, 2001 to present. The gage has operated at the current location through that entire period and there have been no datum adjustments. Figures 2.15 and 2.16 provide a time series of aerial imagery at the gage location.

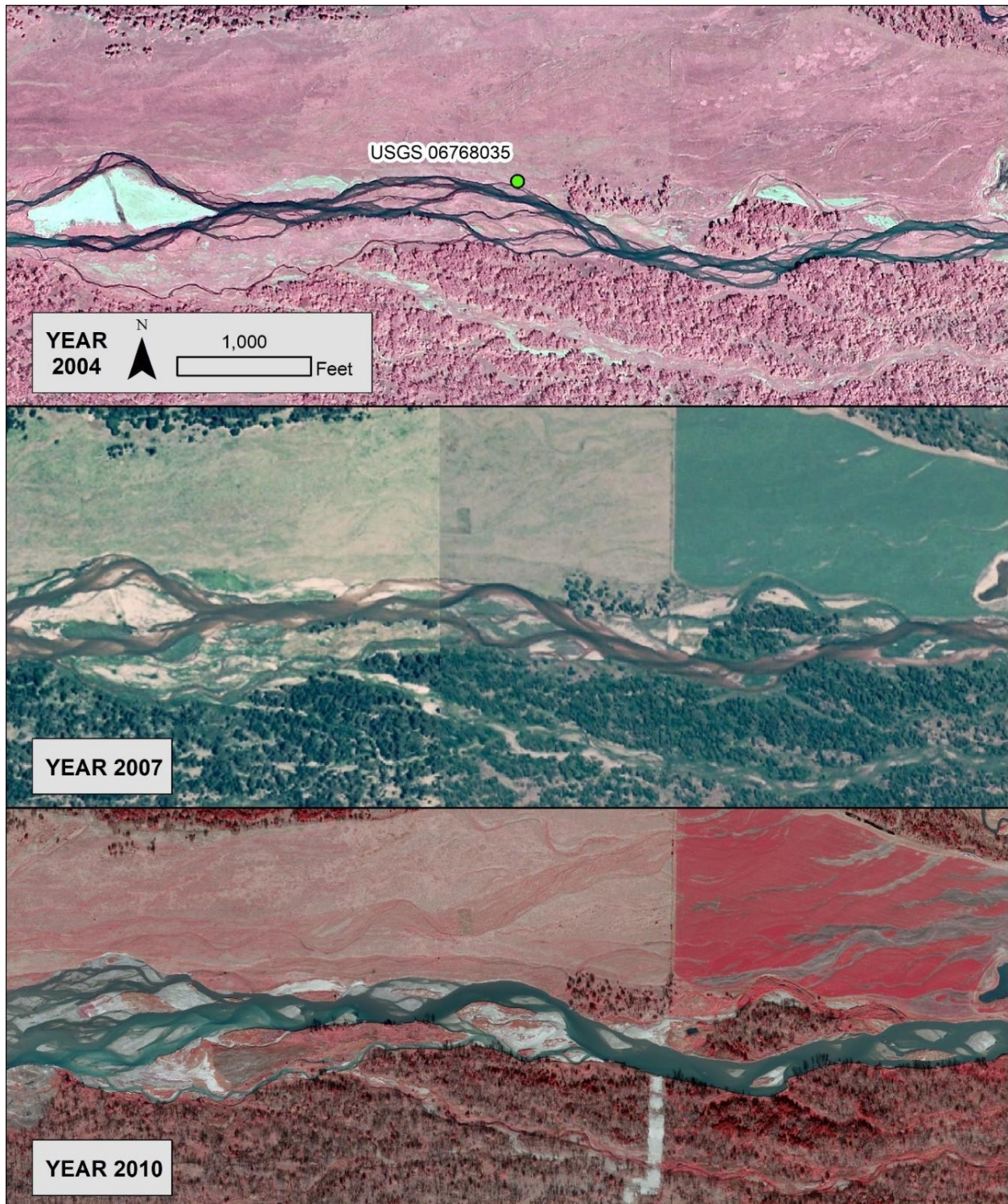


Figure 2.15. Imagery at Cottonwood Ranch Mid-Channel Gage (USGS 06768035) 2004 through 2010.

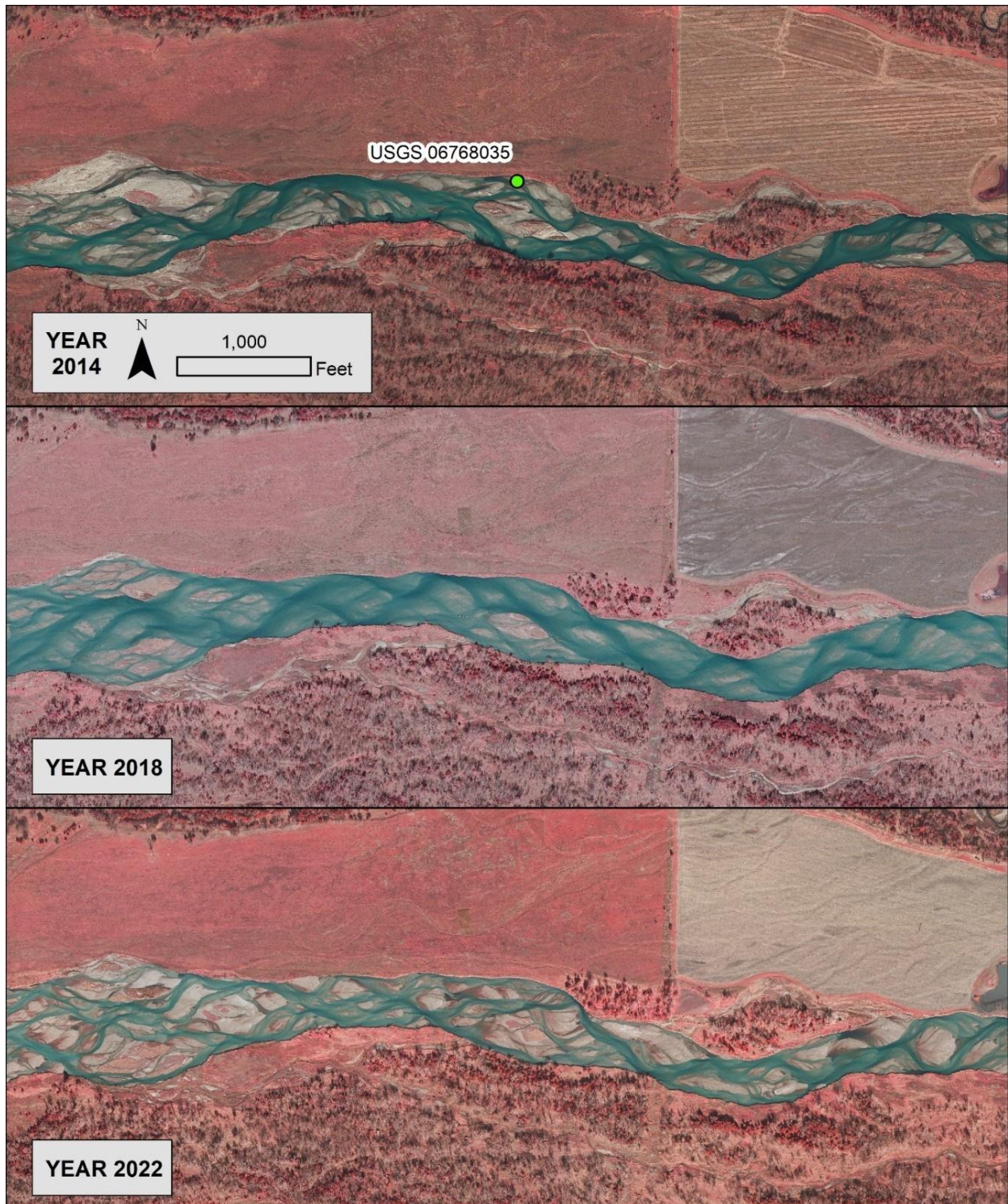


Figure 2.16. Imagery at Cottonwood Ranch Mid-Channel Gage (USGS 06768035) 2014 through 2022.



Figure 2.17 provides physical stage measurement data for the period of record at Cottonwood Ranch Mid-Channel gage along with trailing 30-day mean discharge. The raw stage measurements indicate relative stability at low discharges (<1,000 cfs) until 2007, increasing stage from 2007 to 2011, and stability since 2012. The lack of stage measurements at discharges exceeding 3,000 cfs limit ability to interpret trends in stage for peak flows.

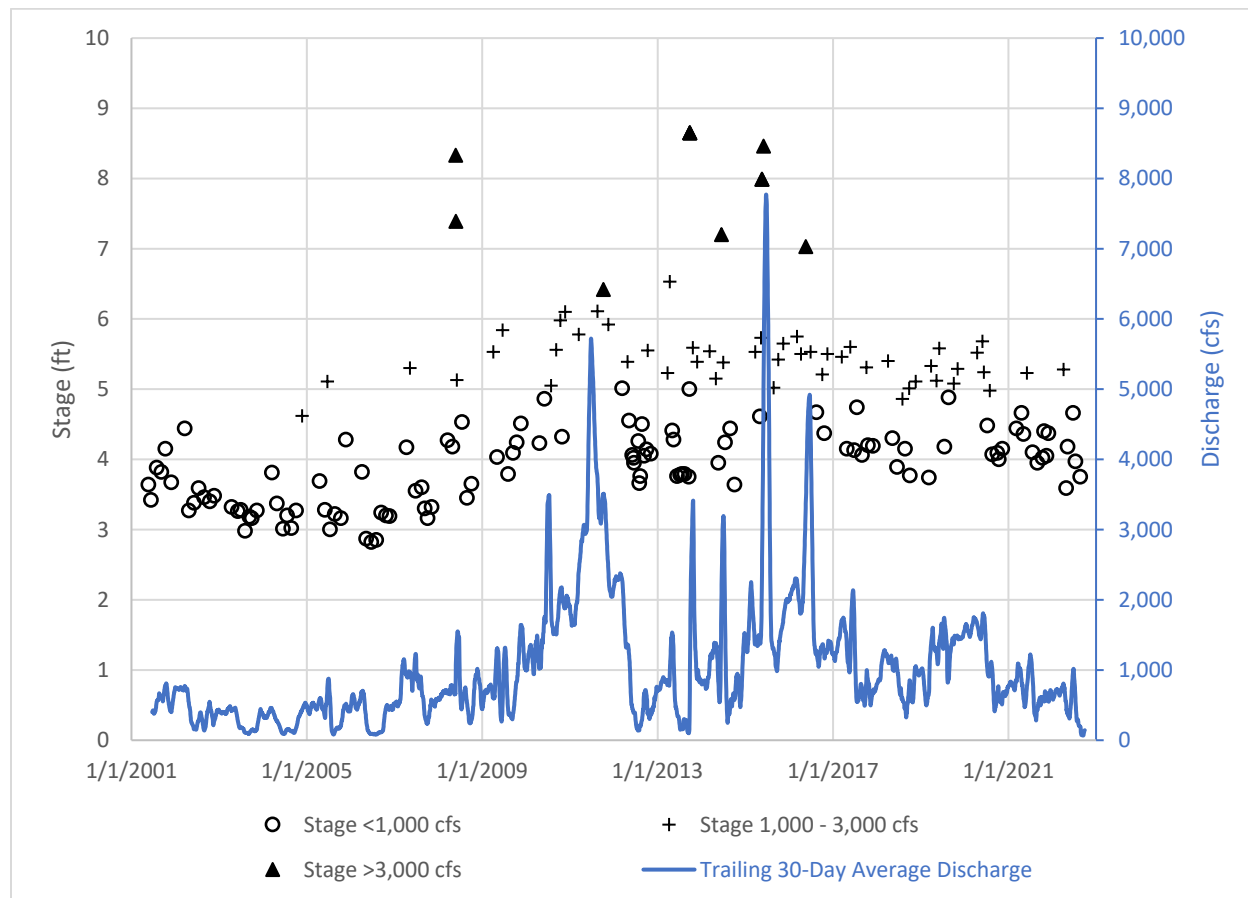


Figure 2.17. Physical measurement stage data at Cottonwood Ranch Mid-Channel gage (06768035) and trailing 30-day average discharge.

Figure 2.18 provides specific gage analysis results. The specific gage analysis indicates stable to slightly increasing stage at low and median discharges during the period of record. There are an inadequate number of stage measurements at the median annual peak discharge to establish any trends in stage at approximate bankfull discharges.

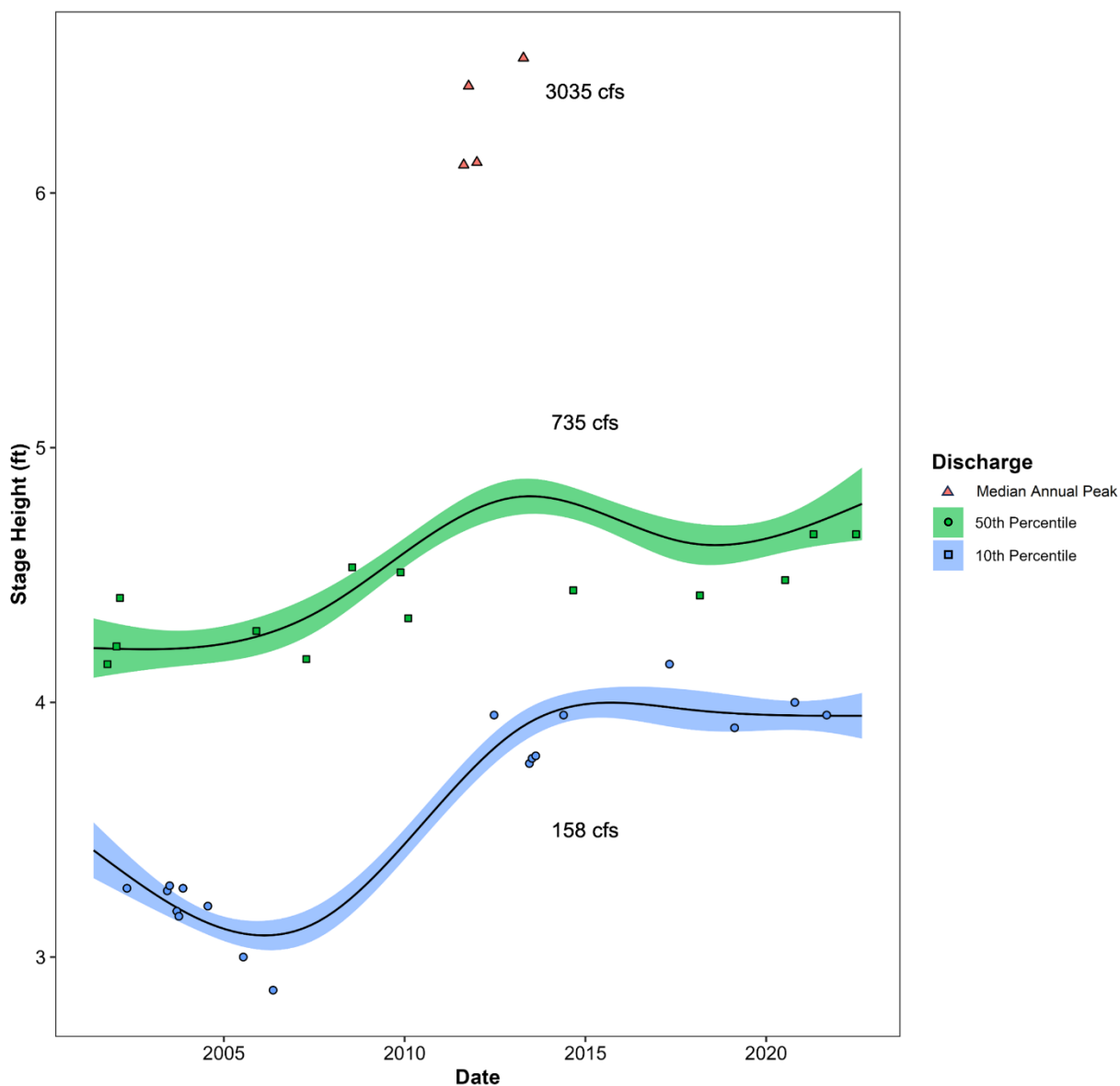


Figure 2.18. Specific Gage analysis for Cottonwood Ranch Mid-Channel Gage (USGS 06768035) at 10th percentile discharge of 158 cfs, median discharge of 735 cfs, and median annual peak discharge 3,035 cfs. Shaded regions represent 95% confidence intervals for each discharge. Results indicate that elevation at this gage increased slightly until approximately 2012 and 2015 for median and 10th percentile discharge, respectively, and remained relatively stable afterward.



2.6 *Channel sinuosity upstream of the Overton Bridge*

2.6.1 Methods

As discussed in Section 2.3, the REM appears to show a shift in channel geometry upstream of the Overton Bridge, especially in the upper half of the J2 Return Channel. In that section, the channel shifted from a braided planform (historically) to narrower and more sinuous wandering form. The results of the incision analysis presented in Section 2.4 indicated minimal vertical incision after 2002 with continuing decline in mean channel elevation in the upper portion of the reach. Taken together, these findings indicate that after 2002 the channel adjustment is occurring primarily through lateral channel movement with increasing meander intensity.

We attempted to quantify this increase in meandering by estimating annual sinuosity in the reach between the J2 Return and Overton Bridge using aerial imagery. The first step in this analysis involved hand-delineating channel length by tracing the thalweg from the Overton Bridge to the J2 Return in a series of primarily color-infrared imagery spanning the period of 1969 to 2016. Imagery series captured at high discharge were not included as the thalweg could not be identified. We then calculated straight-line distances between the starting and ending points of each year's thalweg and divided total thalweg channel length by the straight-line distance producing an estimate of sinuosity for each year/image.

2.6.2 Results

Sinuosity analysis results are presented in Figure 2.19. Sinuosity ranged from 1.1 – 1.15 during the late 1960s through the late 1990s. Sinuosity began to increase in the early 2000s with that trend continuing up to the initiation of full-scale sediment augmentation in 2017. Many systems of stream classification (Leopold, 1957; Rosgen, 1994; Fryirs, K. & Brierley, G, 2005) include measures of sinuosity as part of their distinction between braided and meandering streams or rivers. In these systems, threshold sinuosity to transition from a braided to meandering channel ranges from 1.2 -1.5. By 2016, mean sinuosity in the J2 Return Channel had increased to the lower end of this threshold, consistent with a transition toward a meandering planform.

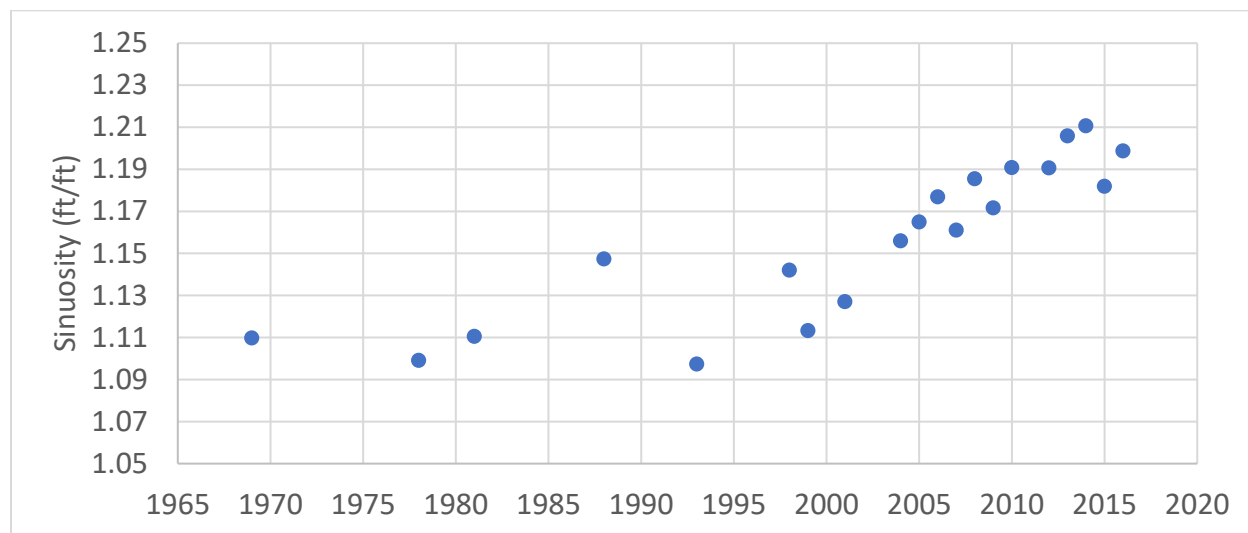


Figure 2.19. Ratio of total channel length to straight-line length (sinuosity) between the J2 Return and the Overton Bridge 1969 to 2016. Figure shows an increase in sinuosity starting in the early 2000s.

2.7 Discussion

The Program's Extension Big Question 3 asks whether augmentation is necessary to keep incision and narrowing from progressing downstream past the Overton Bridge and negatively impacting the suitability of habitat for whooping cranes. The retrospective analyses presented above provide information about historical incision patterns in the study area. The first analysis (2016 REM) indicates there has been approximately 16 ft of incision immediately downstream of the J2 Return. The magnitude of incision declines to about four ft at the confluence of the North and J2 Return Channels near the Overton Bridge and is negligible at the upper end of the Cottonwood Ranch habitat complex. Patterns of incision that can be observed in the REM also indicate the most incised segment in the J2 Return Channel (upper half) has transitioned from braided to a wandering planform that is narrower with higher sinuosity.

Thalweg and mean channel elevation profiles created from 1989 and 2002 repeat cross section surveys, along with 2016 LiDAR profiles, indicate that incision stabilized by the early 2000s. The 2016 and 2002 channel thalweg profiles are topographically similar along the interpolated profile between the ten available thalweg points from 2002. However, comparison of mean channel profiles indicates mean channel elevation continued to decline in the reach downstream of the J2 Return, signaling a shift from a pattern of vertical incision to lateral migration. This is consistent with the trend of increasing sinuosity upstream of the Overton Bridge starting in the early 2000s.

The specific gage analysis at the Overton Bridge indicated approximately two ft of incision occurred at the bridge between 1990 to 2014 with the greatest rate of change in the 2000s. After 2014, stage increased somewhat at the 10th percentile flow (low flow) increasing back to early 2000s levels by 2016. The similarity in low flow stage in early 2000s and 2016 is consistent with the similarity in 2002 and 2016 thalweg profiles but it should be noted that the profile analysis misses the cycle of incision followed by deposition that was observed in the gage data. The



1 specific gage at Cottonwood Ranch indicates that reach has been stable to slightly aggradational
2 since the mid-2000s. However, it should be noted that pilot-scale sediment augmentation
3 occurred one mile upstream of the Overton gage in late 2012 and early 2013 and a considerable
4 amount of channel widening though mechanical augmentation occurred upstream of that gage on
5 Cottonwood Ranch during the period of 2005-2013. Those actions likely affected trends in stage
6 at the gage locations.

7 Beyond documenting incision rates and patterns, the Program is interested in the rate of incision
8 progression. How long until incision and narrowing progress downstream of Overton and that
9 segment begins to transition to the kind wandering channel observed below the J2 Return? These
10 analyses indicate that vertical incision slowed dramatically by 2002 with the channel continuing
11 to evolve via increasing meandering (lateral migration) in the three-mile reach below the J2
12 Return. This shift from vertical to lateral change was likely caused by a number of factors,
13 including but not limited to: channel slope dropping below the threshold for transition from
14 braided to meandering, armoring of the channel bed in the J2 Return Channel that limited
15 vertical incision, and degradation of the channel below the root depth of bank vegetation which
16 increased bank erodibility.

17 Overall, the retrospective analyses indicated the first wave of channel degradation (vertical
18 incision) appears to have propagated down through the study area by 2002 with a total
19 magnitude of incision of 16 feet at the J2 Return, four ft at the Overton Bridge and negligible
20 incision at the upper end of Cottonwood Ranch. The second wave of channel degradation via
21 lateral migration has been dominant since the early 2000s. The second wave relationships
22 between incision, channel slope, and planform evolution are explored further in Chapters 3 and
23 4.

24



2.8 References

- Biedenharn, D. S., Allison, M. A., Little Jr, C. D., Thorne, C. R., & Watson, C. C. (2017). *Large-scale geomorphic change in the Mississippi River from St. Louis, MO, to Donaldsonville, LA, as revealed by specific gage records*. US Army Corps of Engineers, Mississippi Valley Division, Engineer Research and Development Center.
- Chen, A.H., D.L. Rus, and C.P. Stanton (1999). Trends in Channel Gradation in Nebraska Streams, 1913-95. (Vol. 99, No. 4103). US Department of the Interior, US Geological Survey.
- de Vries, M. (1973). "River-bed Variations - Aggradation and Degradation," Delft Hydraulic Laboratory Publication No. 107, Delft, Netherlands.
- Fryirs, K. A., Brierley, G. J. (2005). *Geomorphology and River Management: Applications of the River Styles Framework*. Germany: Wiley
- Graf, W. (1998). *Fluvial Hydraulics, Flow and Transport Processes in Channels of Simple Geometry*, John Wiley & Sons, New York, New York, 681 pp.
- Hastie, T., and Tibshirani, R. (1990). Exploring the nature of covariate effects in the proportional hazards model. *Biometrics*, 1005-1016.
- Holburn, E.R., Fotherby, L.M, Randle, and D.E. Carlson. (2006). Trends of Aggradation and Degradation Along the Central Platte River: 1985 to 2005. United States Bureau of Reclamation.
- Leopold, L. B., & Wolman, M. G. (1957). *River channel patterns: braided, meandering, and straight*. US Government Printing Office.
- Murphy, P.J., T.J. Randle, L.M. Fotherby, and J.A. Daraio. (2004). "Platte River channel: history and restoration". Bureau of Reclamation, Technical Service Center, Sedimentation and River Hydraulics Group, Denver, Colorado.
- Powers, P.D., Helstab, M. & Niezgoda, S.L. (2019). A process-based approach to restoring depositional river valleys to Stage 0, an anastomosing channel network. *River Research and Applications*, 35(1), 3– 13. Available from: <https://doi.org/10.1002/rra.3378>
- Rosgen, D. L. (1994). A classification of natural rivers. *Catena*, 22(3), 169-199.
- Samaranayake, V. A. (2009). The statistical review of three papers on specific gage analysis. *Rep., US Army Corps of Engineers*.
- Turnipseed, D.P., and Sauer, V.B. (2010). Discharge measurements at gaging stations: U.S. Geological Survey Techniques and Methods book 3, chap. A8, 87 p. (Also available at <http://pubs.usgs.gov/tm/tm3-a8/>.)



CHAPTER 3 Evaluation of longitudinal change after sediment augmentation in the Central Platte River, NE, USA

3.1 Abstract

Incision and narrowing downstream of the J2 Return near Lexington, NE, led to channel planform transition from braided to wandering in a seven-mile stretch of river between the J2 Return and Overton Bridge near Overton, NE. The Platte River Recovery Implementation Program (PRRIP) implemented sediment augmentation as a management strategy to address the possibility of incision and planform change affecting habitat management areas downstream of Overton (such as Cottonwood Ranch management area) that provide habitat for endangered species such as whooping cranes (*Grus americana*). We evaluate changes during the first five years of sediment augmentation and one year prior to augmentation (2016–2021) with analyses of longitudinal change in elevation relative to the floodplain, thalweg elevation, cross-sectional elevation, and channel geometry (slope, width, and sinuosity). Aggradational response from augmentation is present in the first two miles downstream of the augmentation area. Downstream of the aggradational response, the channel remains degradational until the confluence with the North Channel, a large branch of channel that rejoins near the Overton Bridge. Downstream of Overton, changes are subtle and the braided channel is relatively stable compared to upstream of Overton Bridge.

3.2 Introduction

Water infrastructure often leads to longitudinal discontinuity of water and sediment in rivers (Wohl et al., 2015; Schmidt and Wilcock, 2008; Poff et al.; 1997, Kondolf 1997; Ligon et al., 1995). In response, rivers adjust toward new states of equilibrium after infrastructure-related disturbances to water and sediment supply (Howard, 1982). Adjustments to river planform, slope, width, and longitudinal profile occur abruptly at the sites of dams (Ward and Stanford, 1995), or in the case of our study area, the J2 Return. The J2 Return releases clear, sediment-free water into the south channel of the Platte River near Lexington, NE. River adjustments to lack of sediment supply extend and dissipate downstream for significant distances and tend to incise the upper portion of channel toward a convex profile (Smith and Mohrig, 2017; Graf, 2006; Williams, 1978). Over time, effects of the disturbance can propagate for large distances downstream (Smith and Mohrig, 2017). As a management strategy to balance the needs for human water use with river ecosystem function, sediment augmentation can help mitigate sediment imbalance that causes channel incision (Mortl and Cesare, 2021).

In this chapter, we aim to help address Big Question #3 from the PRRIP Science Plan (Chapter 1) and evaluate the effectiveness of sediment augmentation in the central Platte River near Overton, Nebraska, USA. We further specify our goal to answer the following question: What are the measurable effects of sediment augmentation and/or continued sediment deficit after five years of implementation, and how do the effects change with distance downstream?

In this chapter, our objective is to answer this question by examining longitudinal changes between the J2 Return and Kearney Canal Diversion (KCD) during the first five years of sediment augmentation implementation, 2017–2021. We compare to 2016 pre-augmentation conditions when data from topobathymetric LiDAR were available.



In the following sections, we present methods and results for four analyses used to evaluate the effectiveness of sediment augmentation. We first evaluate changes in channel elevation relative to the floodplain elevation as a measure of incision. Then, we present longitudinal analyses of thalweg elevation, mean channel elevation, wetted width, and sinuosity. We follow with a more detailed evaluation of channel change that occurred during the augmentation experiment near the midpoint between augmentation and the Overton Bridge.

3.3 Relative elevation model

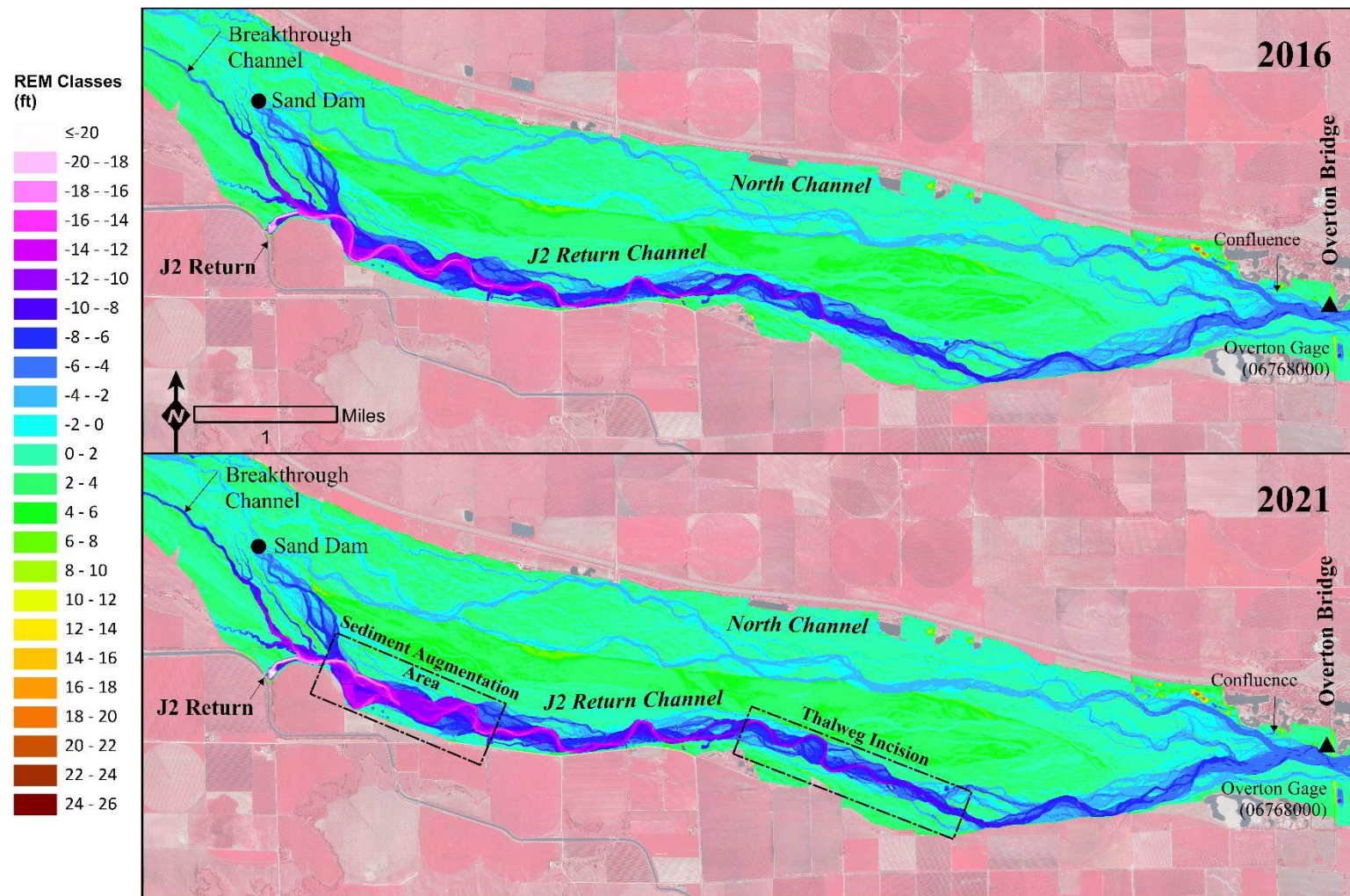
In Chapter 2, we introduced relative elevation models (REMs) as a tool to visualize channel planform and incision relative to the elevation of the floodplain. That chapter discussed incision patterns prior to augmentation. In this chapter, we extended the REM analysis through the augmentation experiment to evaluate change during augmentation.

3.3.1 Methods

We developed annual (2016–2021) REMs of channel topography relative to average floodplain elevation using the methods described in Chapter 2 derived from Powers et al. (2019). In general, REMs were generated by differencing annual LiDAR from the Geomorphic Grade Line (GGL) surface that approximates the elevation of the valley-scale floodplain in the reach. The resulting REM rasters were classified into two-foot intervals to observe topographic changes during the sediment augmentation experiment.

3.3.2 Results

The 2016 and 2021 REMs for the segments of the study area upstream and downstream of the Overton Bridge are included in Figure 3.1 and Figure 3.2. In general, the pattern of incision downstream of the J2 Return extends the length of the J2 Return Channel to the Overton Bridge (Figure 3.1). At the upper end of the J2 Return Channel, the planform has transitioned to a wandering planform with concentrated and mainly single-threaded flow paths. The J2 Return Channel begins to braid near Station 70,000. Headcutting (incision) is present in the lower section of the North Channel, in the breakthrough channel upstream of the J2 Return, and in the sand-dammed channel that was formerly connected to the North Channel upstream of Jeffrey Island. This headcutting is generally due to the elevation of the affected channel segments adjusting to match the base level of the incising J2 Return Channel.



1 **Figure 3.1.** Relative elevation models (REMs) of the portion of the study area upstream of Overton in 2016 (top) and 2021 (bottom).
 2 The topographic signature of sediment augmentation is apparent in the 2021 REM as is a segment of thalweg incision midway
 3 between the J2 Return and Overton Bridge. More change occurred from 2016-2021 upstream of Overton Bridge than downstream
 4 (comparing Figure 3.1 to Figure 3.2 below).

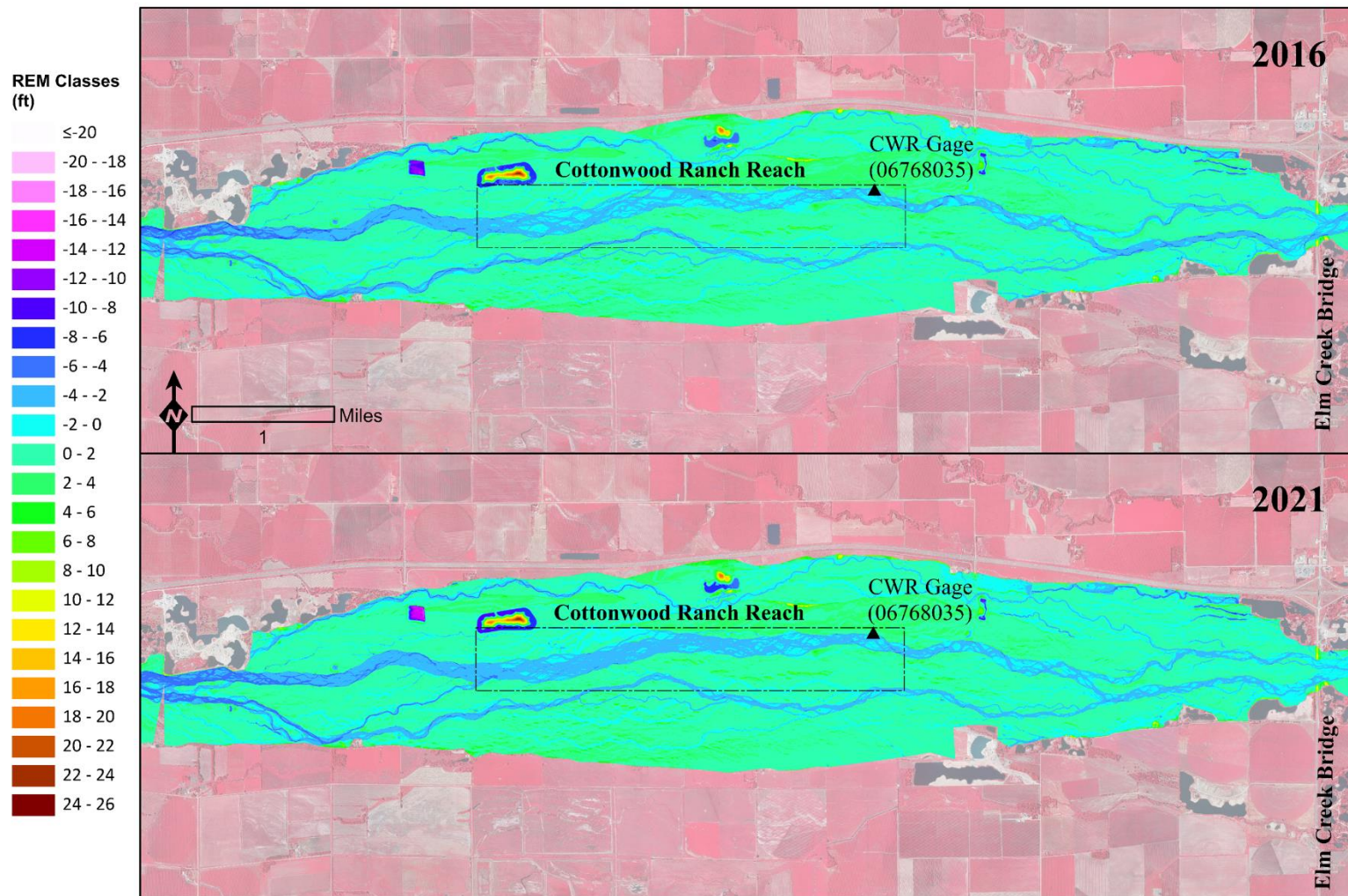
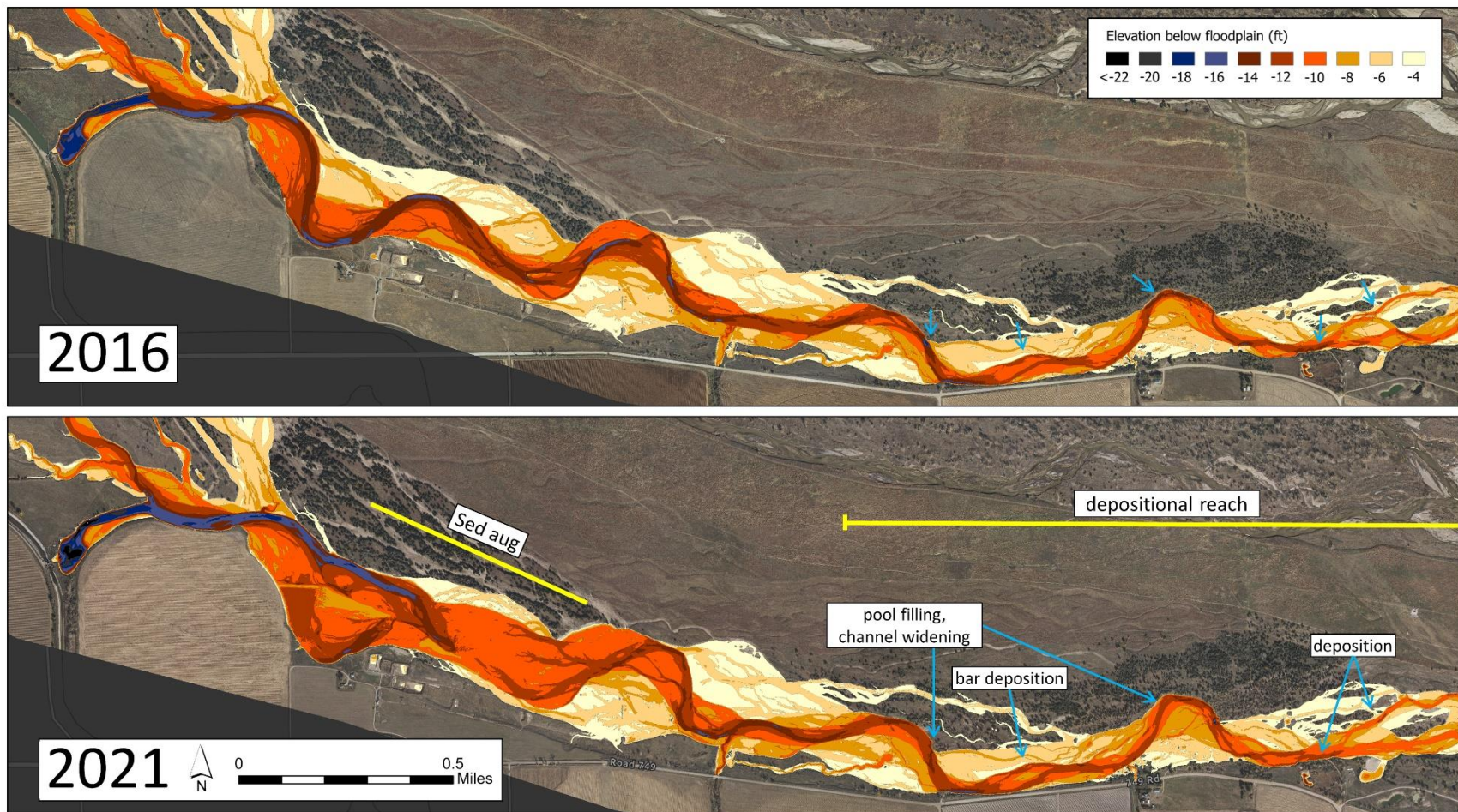


Figure 3.2. Relative elevation models (REMs) of the portion of the study area downstream of Overton to the Elm Creek Bridge in 2016 and 2021. A greater proportion of the Cottonwood Ranch Reach fell into the -2 ft to -4 ft class in 2021 than in 2016, indicating potential degradation in that reach.

1



2 **Figure 3.3.** Annotated relative elevation model of the sediment augmentation area and downstream. The color scale illustrates four
 3 feet or more below the average floodplain and omits higher elevations. Incision occurred upstream of augmentation (blue) and
 4 deposition occurred downstream of augmentation.

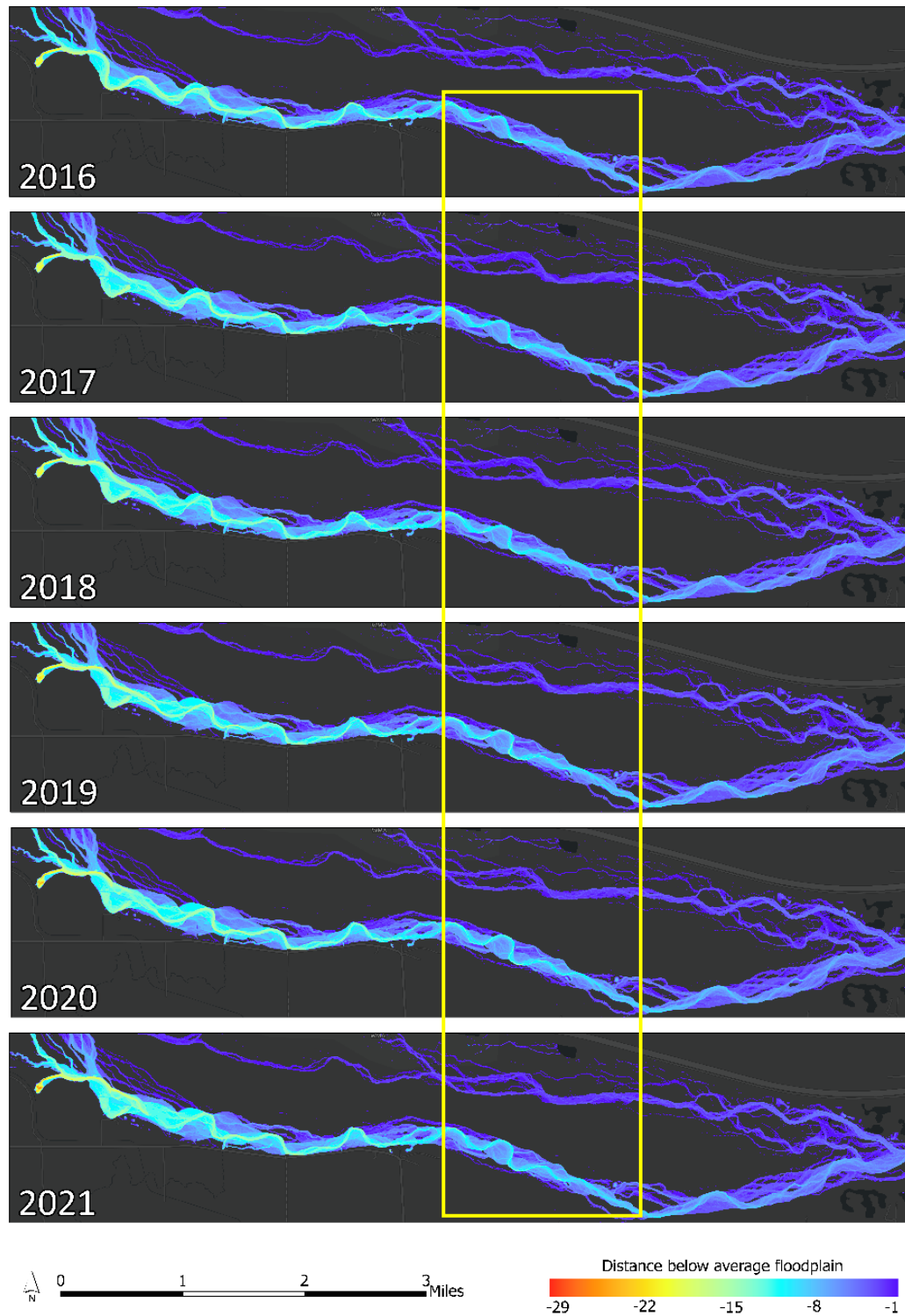


1 When comparing 2016 and 2021 REMs upstream of Overton, changes are apparent in three areas
2 of the J2 Return Channel. Farthest upstream, channel straightening, incision within the
3 straightened channel, and terrace removal can be seen in the sediment augmentation area. To
4 protect private property in 2017, the channel was straightened to eliminate a meander bend in the
5 augmentation area. Since then, the straightened channel incised (Figure 3.3). Downstream of the
6 augmentation area, deposition occurred in the form of pool filling, channel widening, and bar
7 deposition (Figure 3.3). Midway through the J2 Return Channel, an area of thalweg incision
8 extends toward the Overton Bridge (Figure 3.1). At the upper end of the area of incision,
9 meander growth and migration are visible, and it appears the channel transitioned from multiple
10 threads into a single wandering channel. This downstream progression of incision is discussed in
11 more detail in Section 3.8.

12 Below Overton (Figure 3.2), a small amount of pronounced incision is present downstream of the
13 bridge but subsides near the upstream boundary of Cottonwood Ranch with thalweg elevation
14 stabilizing at approximately 3 ft below the GGL. In the Cottonwood Ranch reach, a greater
15 proportion of the channel fell in the -2 ft to -4 ft class in 2021 than 2016, indicating potential
16 degradation in that reach. In 2018, vegetated bars in the Cottonwood Ranch reach were disked.
17 Without root stabilization, the bars were more susceptible to erosion. Finally, a small amount of
18 aggradation can be observed in the channel segment upstream of the Elm Creek Bridge.

19 Given most channel change during the sediment augmentation experiment occurred in the
20 segment upstream of the Overton Bridge, all annual REMs for that area are plotted together in
21 Figure 3.4 with a continuous color scale ranging from -1 ft to -29 ft below GGL. In the sediment
22 augmentation area, the sediment source locations for annual augmentation operations along the
23 left (North) bank are apparent starting near the upper end of the augmentation area in 2017 and
24 moving downstream through 2019. Augmentation operations subsequently moved back upstream
25 in 2020 and 2021. Downstream, the area of channel incision and planform transition is located
26 near Station 70,000 (Figure 3.4, outlined in yellow). Meandering intensity progressively
27 increased in that area from 2016–2021.

28



1
2 **Figure 3.4.** Annual relative elevation models (REMs) of the J2 Return Channel (2016 to 2021).
3 Meander development and thalweg incision can be observed near Station 70,000 (yellow box).



3.4 Longitudinal profile of channel thalweg 2016–2021

While visual comparison of REMs is useful for identification of areas of changes during sediment augmentation, longitudinal profiles of the deepest point of the channel (thalweg) provide a more specific numerical measure of spatial and temporal patterns of aggradation or degradation during the sediment augmentation experiment.

3.4.1 Methods

The physical location or alignment of the thalweg was identified for each year (2016–2021) using the Hydrology Toolbox in ArcGIS Pro 2.9.3 to generate flow direction and flow accumulation rasters from annual DEMs derived from topobathymetric LiDAR. We delineated a stream network of connected flow paths in the channel and filtered the flow paths to select the highest stream order flow path through the study area to designate as the channel thalweg. Visual inspection of aerial imagery validated the use of these accumulated flow paths as reasonable thalweg lines except for 2018 and 2021, where thalwegs were originally routed in secondary channels. To maintain consistency with other years, we manually confined the alignment of the 2018 and 2021 thalwegs to the main channel using the highest order streamline in that fell within the main channel.

Thalweg lines were processed into longitudinal profiles by sampling DEM elevations at the intersection of the thalweg lines and stationed transects spaced every 5 ft perpendicular to the stationing centerline (transect methods are described in Chapter 2). We calculated at-a-station change in thalweg elevation between consecutive years and for the study period as a whole (2016–2021). Changepoint analysis, a method of detecting statistically similar segments, was used to identify patterns in measured changes in mean thalweg elevations for the reach extending from the downstream end of the sediment augmentation area (Station 84,000) to Station 15,000¹³. Changepoints were calculated using the changepoint package in R version 4.2.2 (Killick et al., 2022; R Core Team 2022; Killick & Eckley 2014). We used the Pruned Exact Linear Time (PELT) method to detect multiple changepoints of sample mean, and the Changepoints for a Range of Penalties (CROPS) process to determine a manual penalty value of 200 on the log likelihood scale with diagnostic plots (Haynes et al., 2017 Killick et al., 2012). PELT is a dynamic programming technique that sequentially and iteratively optimizes changepoint locations, and CROPS automatically calculates all changepoint locations according to a variety of penalty values to assist with optimal penalty selection.

As discussed in Chapters 1 and 2, evaluating channel slope, and change in slope through time, is an important objective of this synthesis. Thalweg elevation at-a-station is highly variable through space and time (± 2.5 ft) even in areas of relative channel stability. This is due to the dynamic nature of the channel with constantly moving transverse bars, dunes and other bedforms. The presence of these topographic features makes it difficult to evaluate trends in slope without 1) calculating slope at a segment scale or 2) deriving at-a-station slope from a model of the channel profile that “smooths” out topographic variability due to bedforms. We evaluated slope with the second option. We used Generalized Additive Mixed Models (GAMM) with a sampling distance of 100 ft to fit a line to the thalweg profile for each year, and calculated slope with a moving window. The generalized additive model structure allowed for inclusion of a cubic regression

¹³ Analysis ended at Station 15,000 to eliminate backwater effects from the Kearney Canal Diversion.



spline because elevation data are nonlinear. The mixed model component allowed for inclusion of an exponential spatial correlation function to account for spatial autocorrelation among thalweg points. GAMM output includes model-predicted lines of best fit. Slopes are calculated based on model-predicted channel elevations; therefore, uncertainty in our slope calculations depends on the accuracy of the model.

Because our longitudinal profiles are stationed the same way each year, slope estimates assume the same along-channel distance for all years. In reality, extension of the channel thalweg via lateral migration and meandering leads to our measurements of slope along the thalweg to be slight over-estimates. However, stationed slope calculations provide a sufficient general representation of the channel slope throughout the study area.

3.4.2 Results

Figure 3.5 provides annual thalweg alignments for 2016–2021. Annual alignments in the upper half of the J2 Return Channel were highly stable, except for the sediment augmentation area where thalweg location varied with augmented sediment placement and a meander was cut off in 2017. The planform transition from single thread wandering (upstream) to braided (downstream) is also apparent in Figure 3.5. Approximately two miles upstream of the Overton Bridge, annual alignments begin to diverge with annual differences increasing spatially with channel width and braiding intensity. Annual differences are most apparent in the Cottonwood Ranch Reach in the Overton to Elm Creek Bridge segment and in the reach immediately upstream of the KCD (below the Elm Creek Bridge).

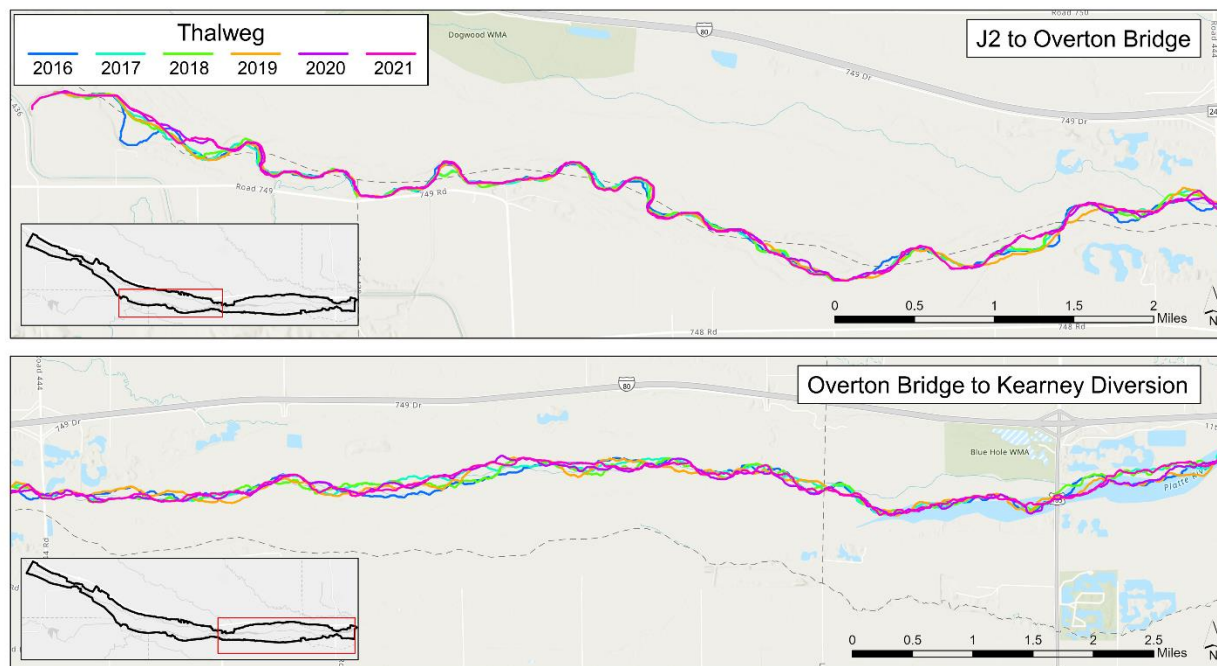


Figure 3.5. Annual thalweg alignments (2016–2021) derived from flow accumulation rasters. In the top panel, the transition from wandering to braided planform is present midway through the J2 Return Channel.

The longitudinal profiles for 2016 and 2021 are plotted in Figure 3.6 along with the Geomorphic Grade Line (GGL) for the study area. Both longitudinal profiles are convex in shape, with slope generally increasing in a downstream direction, away from the area of maximum incision immediately below the J2 Return. Differences in 2016 and 2021 thalweg profiles are apparent in the sediment augmentation area (upstream of Station 84,000) where the 2021 thalweg is higher than 2016 because of augmentation operations. Downstream in the J2 Return Channel, a segment between Stations 72,000 and 66,000 shows incision relative to the rest of the channel. Below the Overton Bridge, thalweg elevations appear to have been stable through Cottonwood Ranch and increased upstream of the Elm Creek Bridge (Station 25,000 to 15,000), indicating the bed aggraded in that area.

Figure 3.7 provides annual thalweg profiles for the J2 Return Channel smoothed using 1,005 ft centered running average elevations to highlight annual profile changes. Thalweg elevations in the sediment augmentation area generally increased during the augmentation experiment as sediment from floodplain terraces was mechanically spread across the active channel. Downstream near Station 70,000, the highest magnitude of incision occurred between 2018 and 2019, with more stability from 2019 through 2021. We explore this segment in greater detail in Section 3.8.

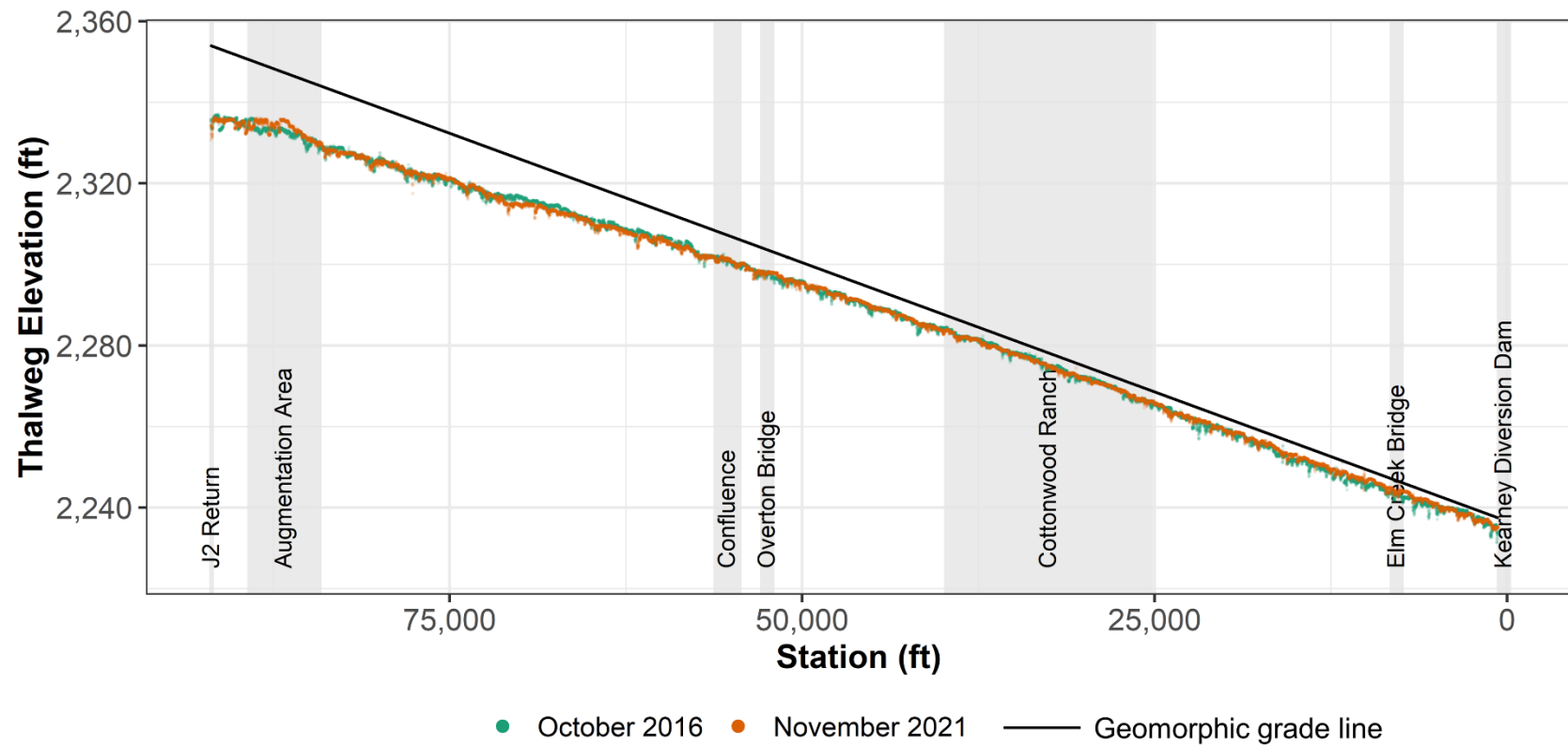


Figure 3.6. Longitudinal profile of thalweg elevation in 2016 (green) and 2021 (orange). The Geomorphic Grade Line (GGL) is shown in black as a reference for the magnitude of channel incision.

1
2
3



1

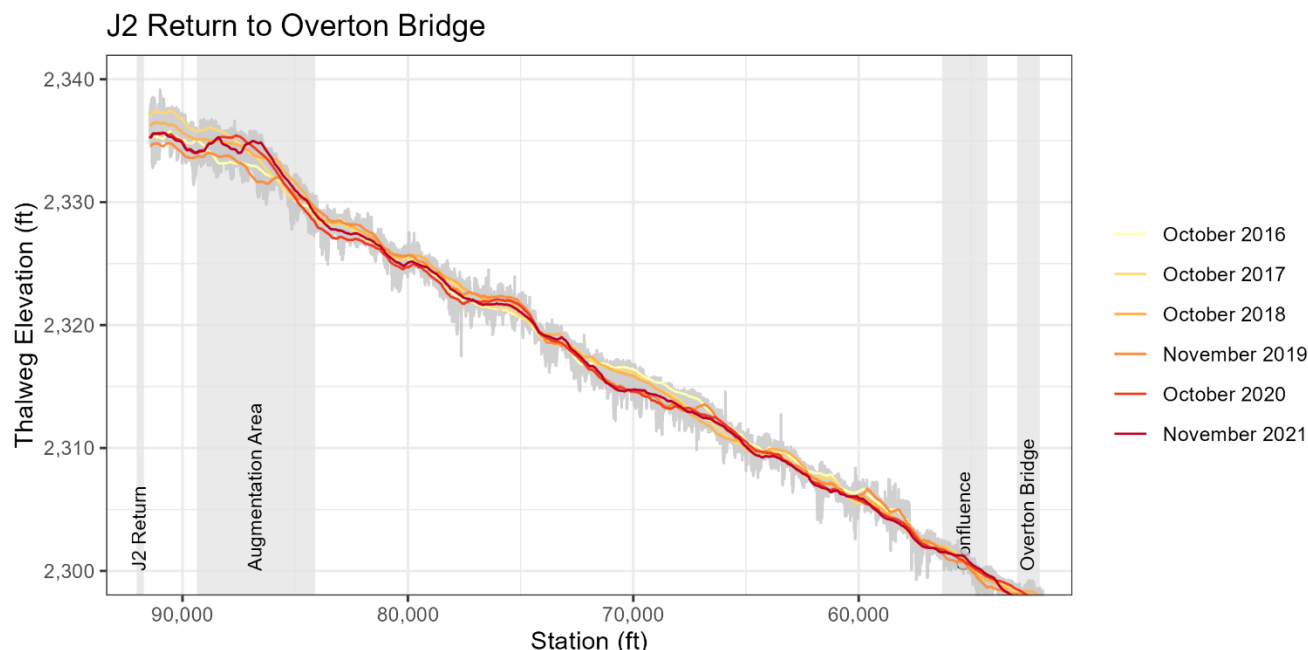


Figure 3.7. 2016–2021 annual moving average (1,005 ft) longitudinal profiles between J2 Return and Overton Bridge. Grey area behind profiles indicates the range of values for 2016–2021. Progressive thalweg aggradation is apparent in the sediment augmentation area and progressive degradation is apparent downstream in the vicinity of Station 70,000.

2 Segments of mean change derived from the changepoint analysis for the entire augmentation
3 period (2016–2021) are presented in Figure 3.8 and mean change values are provided in Table
4 3.1. After five years of augmentation, mean change in thalweg elevation in the first 2.3 miles
5 downstream of the augmentation area ranged from -0.3 to +0.4 ft. This is followed by an
6 approximately one-mile reach with the most prominent incisional trend in the study area. The
7 incisional reach extends from roughly Station 72,000 downstream to Station 66,000 with mean
8 thalweg incision of -1.3 ft. The thalweg also incised in the reach immediately downstream with
9 mean thalweg elevation loss of -0.64 ft. Continuing downstream, the channel transitioned to
10 slight aggradation (+0.2 ft) near the J2 Return Channel confluence with the North Channel. Near
11 Cottonwood Ranch, mean change shifted to slight thalweg incision (-0.2 ft). Downstream of
12 Cottonwood Ranch, thalweg elevation increased by an average of 0.5 ft.

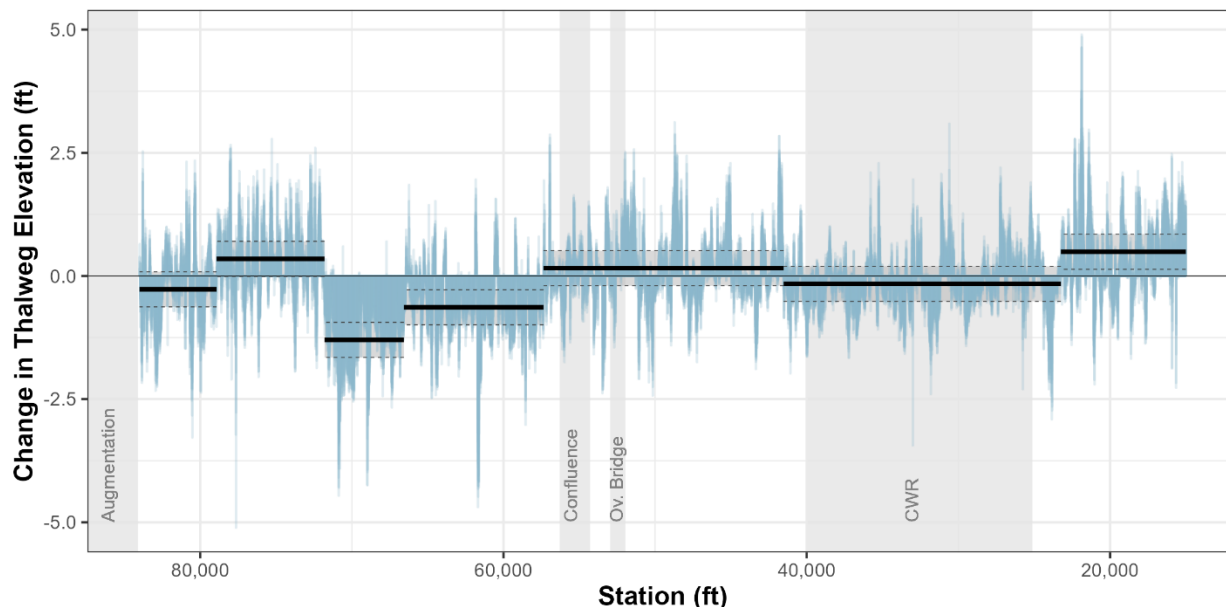


Figure 3.8 2016–2021 thalweg changepoint analysis results. Differences in thalweg elevations shown in blue. Mean segment change values shown in black. Negative numbers indicate thalweg incision and positive indicate thalweg aggradation. Shaded areas with bounding dotted lines represent the propagated error from LiDAR collection for 2016 and 2021 (0.356 ft).

Table 3.1. 2016–2021 thalweg changepoint analysis results.

Station Range	Segment Length (mi)	Thalweg Elevation Change (ft)		
		Mean	Minimum	Maximum
84,000–78,915	1.0	-0.3	-2.3	4.9
78,915–71,805	1.3	0.4	-3.4	3.1
71,805–66,570	1.0	-1.3	-2.4	3.1
66,570–57,360	1.7	-0.6	-4.7	2.0
57,360–41,520	3.0	0.2	-4.5	0.7
41,520–23,240	3.5	-0.2	-5.1	2.8
23,240–15,000	1.6	0.5	-3.3	2.5

Changepoint analyses were also utilized to detect segments of mean change for each set of consecutive years during the augmentation experiment to evaluate inter-annual variability (Figure 3.9). In the J2 Return Channel, the segment around Station 70,000 shows persistent loss from 2016 to 2019, with the most loss occurring in 2019. The thalweg was stable in that area in 2020 and aggraded slightly in 2021. Downstream of the Overton Bridge, the annual changepoints indicate relative thalweg stability. Table 3.2 shows annual mean thalweg changes summarized by their location either upstream or downstream of Overton Bridge.

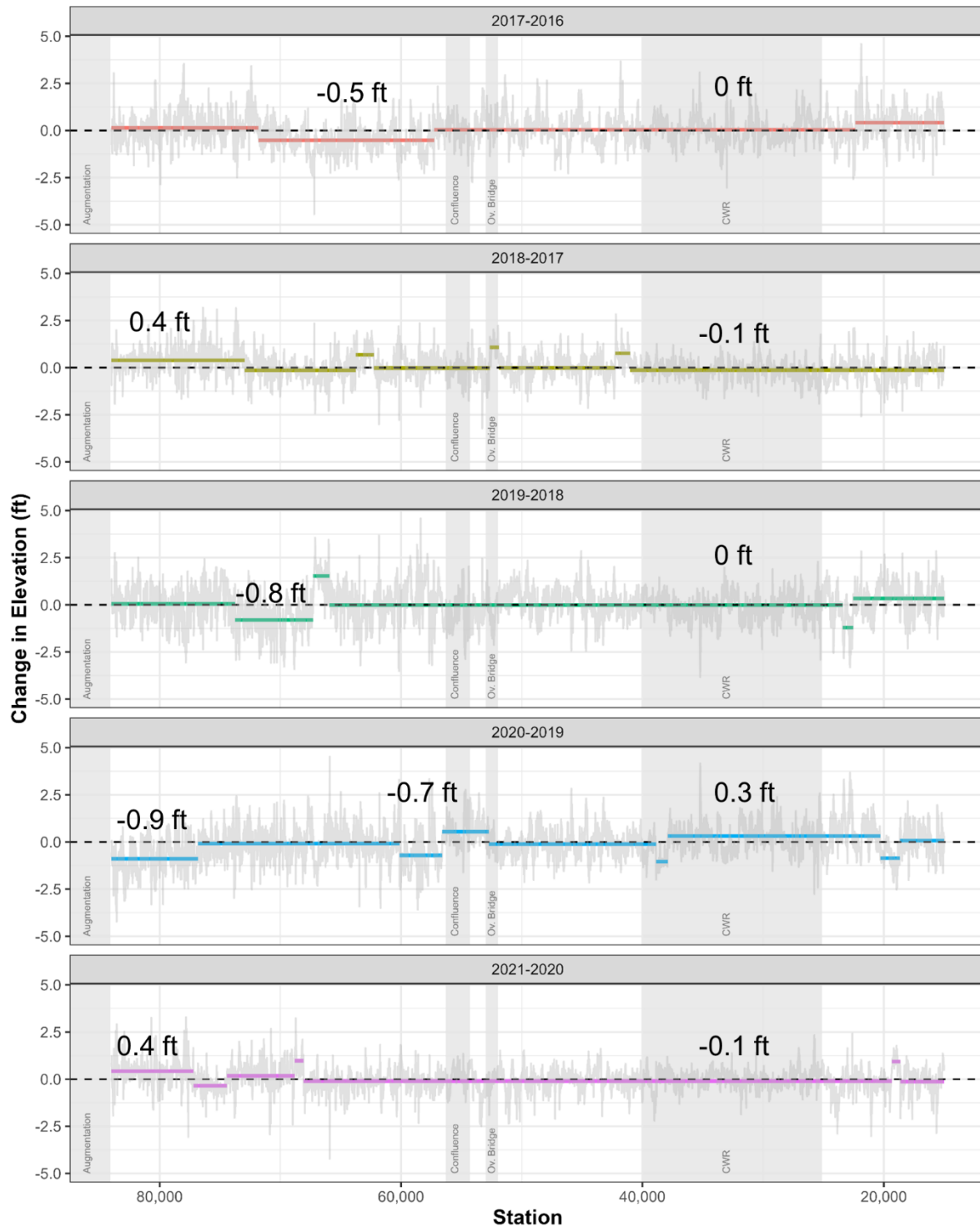


Figure 3.9. Annual changepoint analysis results of change in thalweg elevation between years. Colored lines show mean change values of changepoint segments. Light grey lines show at-a-station thalweg elevation difference.

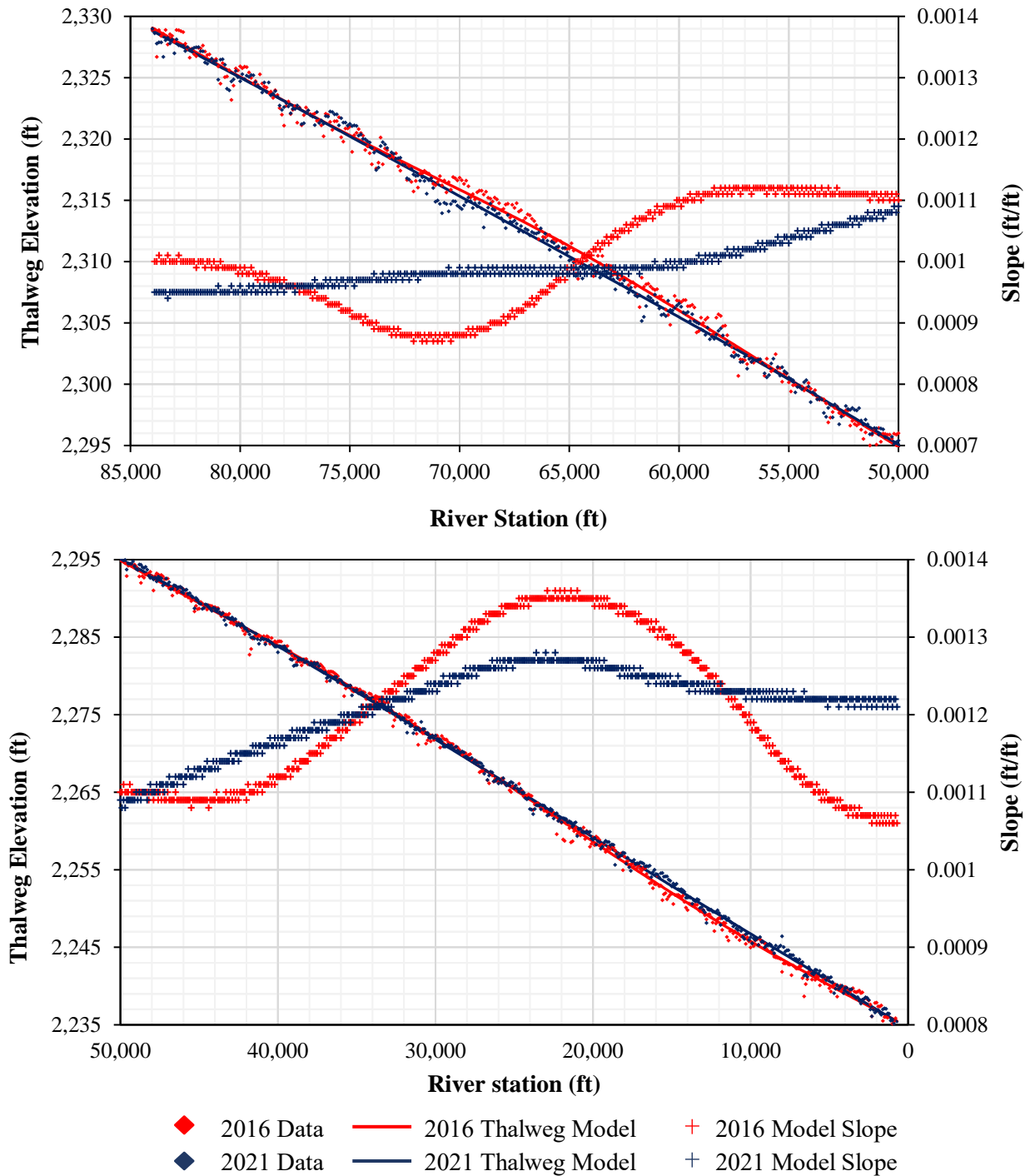


Table 3.2. Average thalweg changes upstream and downstream of Overton Bridge with mean flow for comparison.

Year	Mean Thalweg Change (ft)		Mean Discharge at Overton Bridge (cfs)	Mean J2 Return Flow (cfs)
	J2 Return Channel	Downstream of Overton		
2016–2017	-0.17	0.11	1,780	1,099
2017–2018	0.13	-0.05	1,289	807
2018–2019	-0.10	0.04	2,082	1,155
2019–2020	-0.26	0.05	2,127	1,225
2020–2021	0.04	-0.06	1,008	589

Channel slope and the relationship between slope and planform are important focus areas of this investigation. As discussed above, the thalweg in our study reach is convex, with slope increasing in a downstream direction away from the J2 Return. Given this non-linearity and the highly variable thalweg longitudinal profile elevations, slope was calculated from moving window slope calculations of GAMM model-derived annual thalweg profiles. The moving window size was two points for Figure 3.10 and ten points for Figure 3.11. Results for 2016 and 2021 are provided in Figure 3.10. Upstream of the Overton Bridge, the models reflect the previously described incision that occurred in the vicinity of Station 70,000. When slope is calculated from the 2016 profile, it becomes apparent that slope was highly variable in this area with slope decreasing from 0.001 to 0.0009 between Station 80,000 to 72,000 and increasing to 0.0011 at Station 58,000. Taken together, the profile (Figure 3.6) and associated slopes (Figure 3.10) describe a “high point” between Stations 72,000 and 58,000 of the J2 Return Channel. Between 2016 and 2021, the thalweg incised through this high point and slope stabilized between 0.00095 and 0.00099. The 2021 slope change near Station 60,000 is likely an important discriminator for planform change as it is the location where thalweg alignments begin to diverge and the channel begins to braid.

Downstream of Station 58,000, slope was stable at 0.0011 to approximately the upper end of the Cottonwood Ranch Reach at Station 42,000. Slope increased to 0.00135 at lower end of the Cottonwood Ranch Reach (Station 22,000) and declined back to 0.0011 at the KCD. By 2021, slope had stabilized in this reach as well, increasing gradually from 0.001 to 0.00127 at the lower end of the Cottonwood Ranch Reach. Downstream of Cottonwood Ranch, slope was stable to slightly declining.



1 **Figure 3.10.** Modeled (GAMM) thalweg profiles and model-derived slopes for 2016 and 2021.
2 Top panel (sediment augmentation area to Overton Bridge) and bottom panel (Overton Bridge to
3 KCD) both indicate stabilization in slope over the period of 2016-2021.



When all annual modeled slope profiles are plotted together (Figure 3.11), it appears that most of the slope stabilization upstream of Overton occurred between 2016 and 2017. Below Overton, slope stabilized more incrementally. The oscillation in slope observed in 2016 between Cottonwood Ranch and the KCD slowly stabilized over the course of the augmentation experiment with slope declining at the upper end of that segment and increasing at the lower end of the segment.

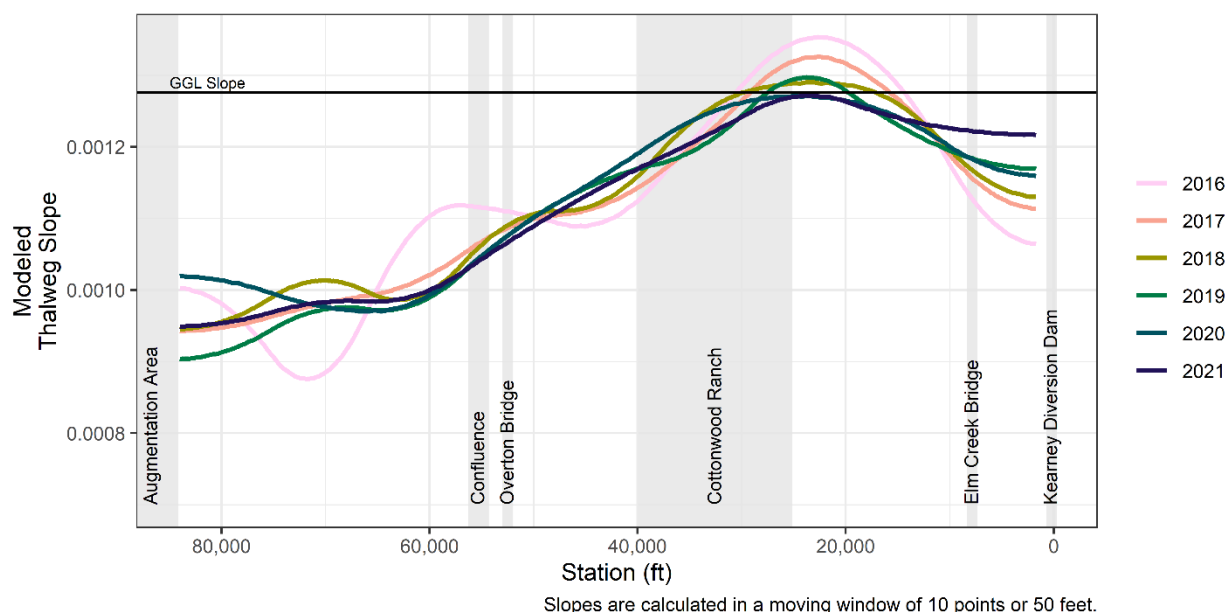


Figure 3.11. Annual slope profiles (2016–2021) derived from GAMM thalweg models. Slope profiles show rapid stabilization of channel slope upstream of the Overton Bridge (2016 to 2017) and progressive stabilization downstream of Cottonwood Ranch throughout the experiment (2017–2021).

3.5 Longitudinal profile of mean channel elevation 2016–2021

Longitudinal profiles of thalweg elevations are useful in evaluating incision and slope change during the sediment augmentation experiment. However, they only describe changes to the deepest part of the channel. We also examined longitudinal profiles of average cross-sectional elevation to quantify dispersed channel change beyond the thalweg.

3.5.1 Methods

To calculate average cross-sectional elevation, we first clipped stationed channel transects to confine them to the active channel, defined as the portion of the channel wetted at a discharge of 2,500 cfs upstream and 5,000 cfs downstream of Overton. Wetted area was modeled for each year with SRH-2D (Lai, 2008), using 2016–2021 LiDAR (PRRIP 2022b). Flow area polygons for each year were merged into a single polygon capturing the entire wetted area during the management experiment. After transects were clipped to the limits of the active channel, we sampled LiDAR DEM elevations at 3 ft intervals along each clipped transect and calculated the average elevation. Mean elevations were plotted by station for each year. At-a-station differences were calculated for each pair of consecutive years from 2016 through 2021, and for the



1 difference between 2021 and 2016. The merged polygon used to clip our transects includes
2 inactive floodplain elevations that may have been incorporated into the active floodplain via
3 lateral erosion over the course of the study period. As a result, reductions in mean channel
4 elevation through time can be the result of either lateral erosion or bed erosion.

5 3.5.2 Results

6 The longitudinal profiles of average cross-sectional elevation for 2016 and 2021 are plotted in
7 Figure 3.12 along with the GGL. Like the channel thalweg, the longitudinal profile of average
8 cross-sectional elevation is convex in shape due to incision downstream of J2 Return. Maximum
9 divergence from the GGL occurs near the J2 Return. The profile gradually converges with the
10 GGL in a downstream direction. Through the Cottonwood Ranch Reach, the average cross-
11 sectional elevation is nearly parallel with the GGL and close to the predicted GGL elevation.
12 Downstream of Station 12,000 (near Elm Creek Bridge) the profile of mean elevation converges
13 with GGL due to the backwater effect and consequent upstream aggradational influence of the
14 KCD.

15 When mean elevation profiles are compared to thalweg profiles using 2021 as an example, there
16 is a larger difference between average cross-sectional elevation and thalweg elevation in the J2
17 Return Channel compared to downstream of Overton (Figure 3.12). This is a result of incision
18 and the difference in channel geometry between the single-thread J2 Return Channel versus the
19 wide braided reach downstream of Overton.

20 The average elevation in the sediment augmentation area (above Station 84,000) decreased
21 between 2016 and 2021 as a result of augmentation (Figure 3.12). Station 71,250 also
22 experienced a decrease in mean elevation. Overall, elevation change from 2016 to 2021 was
23 more evident in the J2 Return Channel than downstream of Overton Bridge.

1
2

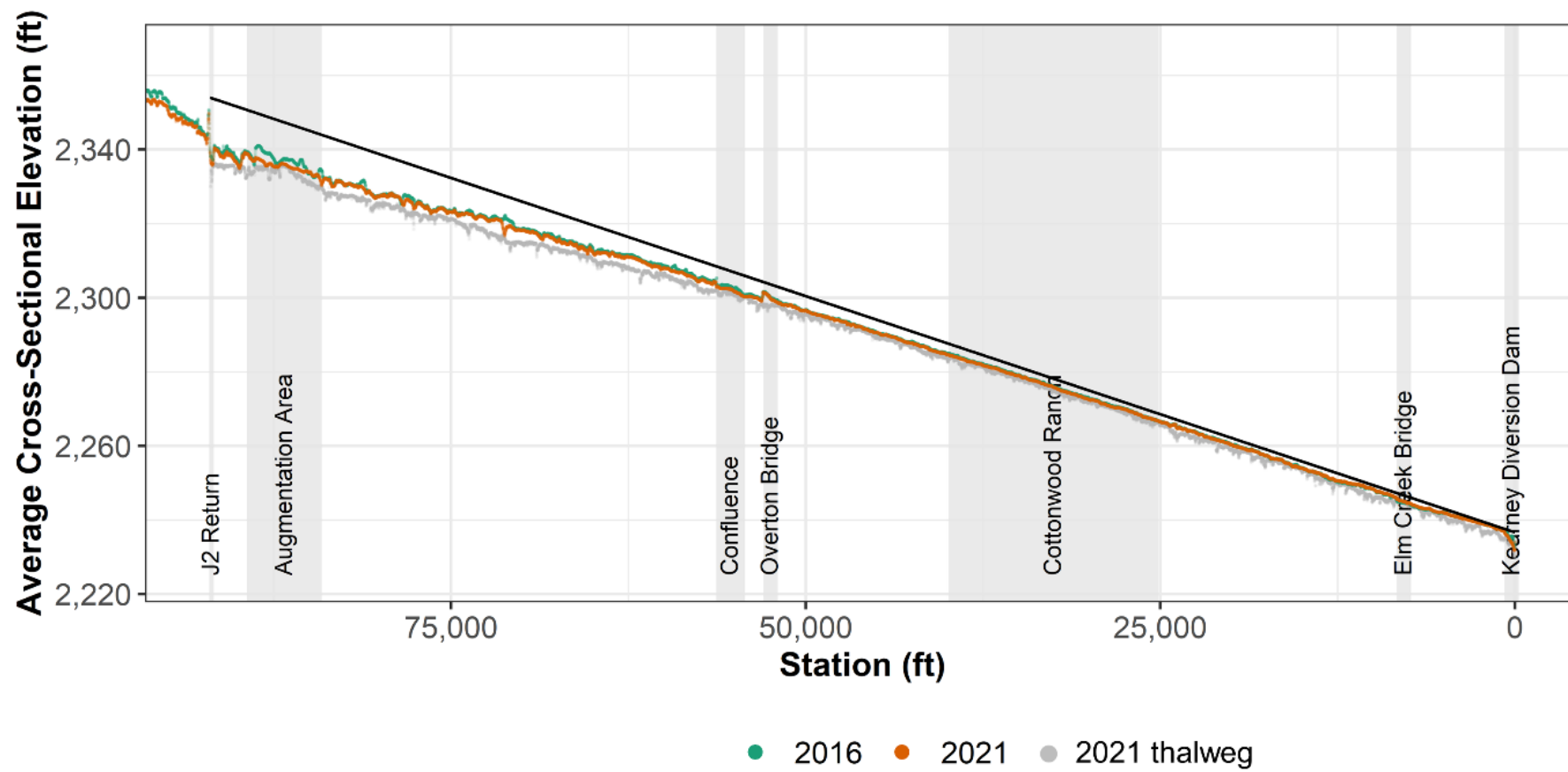


Figure 3.12. Average cross-sectional elevation longitudinal profile. The geomorphic grade line and 2021 thalweg are shown for reference.

3



Figure 3.13 provides annual mean channel elevation profiles for the J2 Return Channel smoothed using 1,005 ft centered running average elevations to highlight annual profile changes. Mean channel elevation decreased in the sediment augmentation area through the augmentation experiment due to mechanical removal of sediment from floodplain terraces and placement into the active channel. Downstream of the augmentation area, areas of large progressive decline in mean channel elevation are apparent near Stations 82,000, 78,000 and 72,000. These are areas with meanders that are actively migrating via lateral erosion.

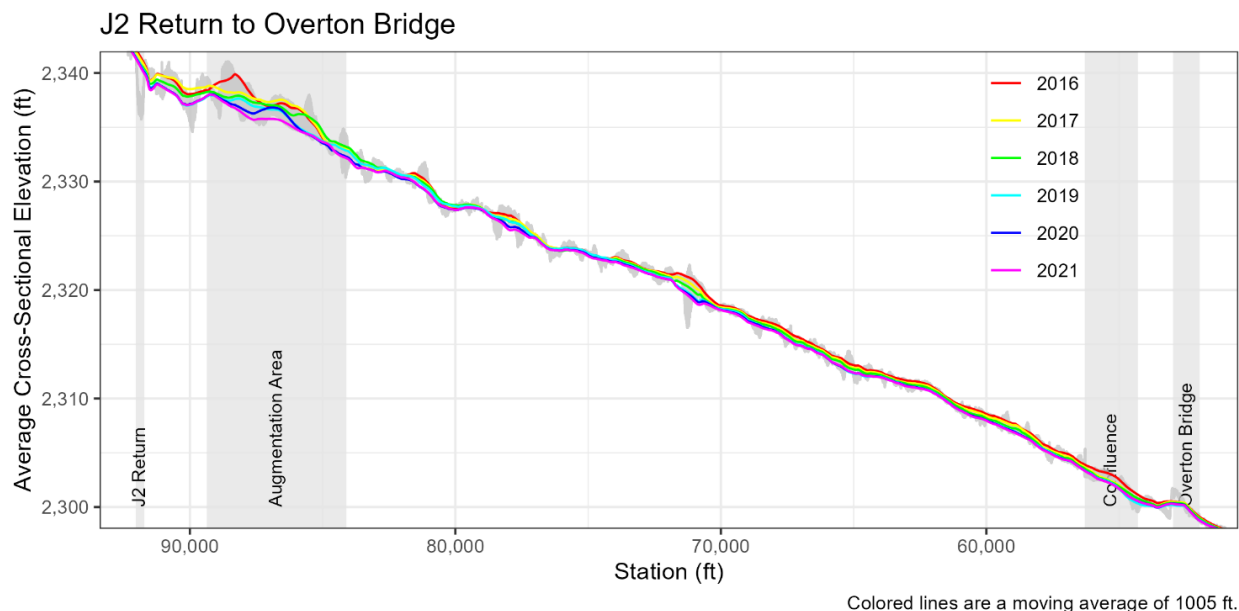


Figure 3.13. Average cross-sectional elevation longitudinal profile in the J2 Return channel. Colored lines are a moving average of 1005 ft and grey lines show the range of values for 2016–2021.

At-a-station change in thalweg and mean channel elevations during the augmentation experiment provide a comprehensive view of in-channel changes during the augmentation experiment (Figure 3.14). In the sediment augmentation area, mean channel elevation decreased, and thalweg elevations increased. This is consistent with the mechanical augmentation of bank sediment into the active channel. The increase in thalweg elevations persists downstream of the augmentation area to approximately Station 72,000 but the decrease in mean channel elevation is lower magnitude except in previously identified areas of lateral channel erosion. The change in mean and thalweg elevations are both generally negative from Station 72,000 to the Overton Bridge. This is an indicator of general channel degradation in that reach.

Below the Overton Bridge, thalweg elevation increased upstream of Cottonwood Ranch and decreased within Cottonwood Ranch, while mean channel elevation decreased throughout the reach except for increases near Elm Creek Bridge. Decreasing mean channel elevation paired with increasing thalweg elevation is an indicator of channel widening. Increasing thalweg and mean channel elevation is an indication of deposition or aggradation. Accordingly, we interpret the reach between the Overton Bridge and Cottonwood Ranch to be stable to widening, Cottonwood Ranch



to be slightly degradational, and the reach downstream to be aggradational. These patterns of erosion and deposition can be more directly assessed through a three-dimensional analysis of volume change that discriminates between lateral and bed erosion. That analysis is presented in Chapter 4.

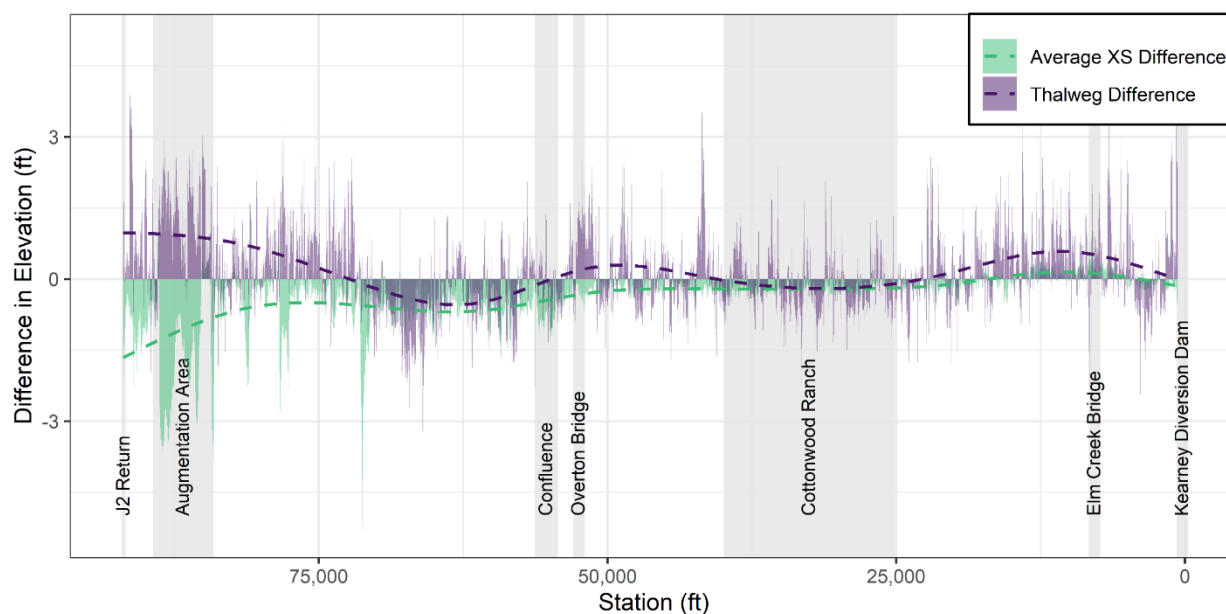


Figure 3.14. Differences in thalweg and average cross-sectional elevation from 2016 to 2021. A line depicting general trends was estimated with a generalized additive model.

3.6 Wetted Width

As discussed previously, a portion of the J2 Return Channel transitioned from a historically wide braided planform to a narrow wandering planform over several decades after the J2 Return began operations in the 1940s. Evaluating spatial and temporal trends in wetted width, or the width of channel inundated by water during a reference flow, provides clues about the progression of incision and narrowing in the J2 Return Channel as well as potential effects of sediment augmentation.

3.6.1 Methods

Analyses of wetted widths are necessarily tied to one or more reference flows. For this analysis, we used a flow of 2,000 cfs to remain consistent with ongoing system-scale monitoring efforts (PRRIP EDO, 2022a). In general, 2,000 cfs is the approximate flow in the J2 Return Channel when the return is operating at full capacity.¹⁴ Downstream of Overton, a flow of 2,000 cfs was chosen for system-scale analyses of wetted width as it is sufficient to inundate bedforms and fill the entire channel without overtopping banks.

Wetted widths prior to and during the augmentation experiment were modeled using a combination of one-dimensional (1D) and two-dimensional (2D) hydraulic models of the study

¹⁴ J2 Return flow of approximately 1,800 cfs and an additional 200 cfs of groundwater return flows.



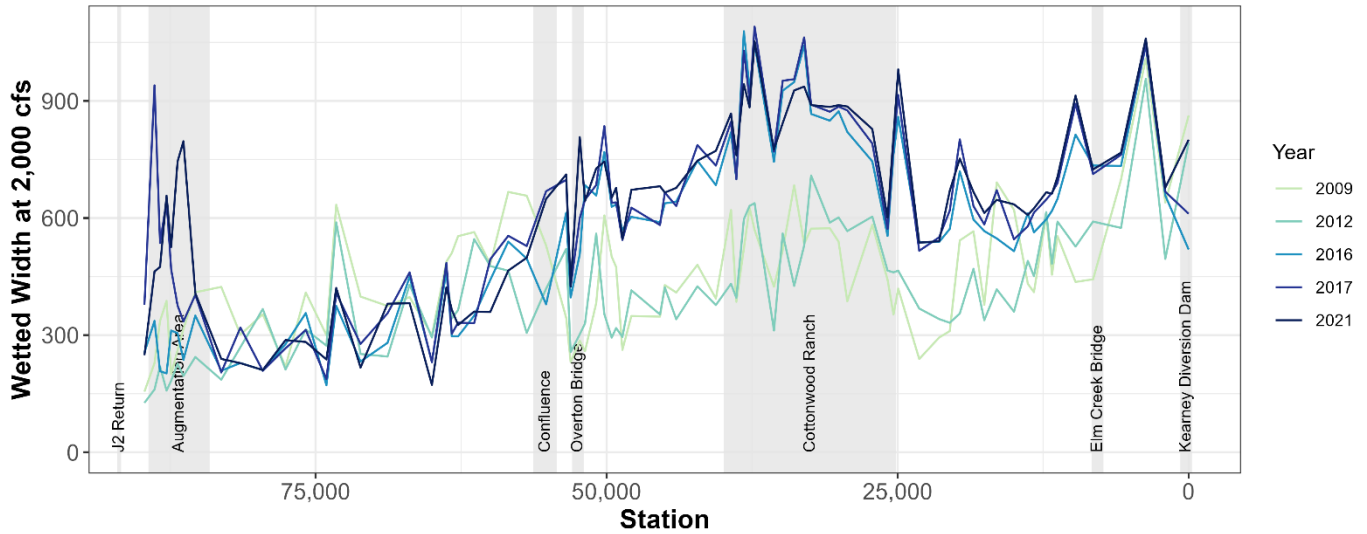
1 area. Wetted widths in 2009 and 2012 were modeled in 1D HEC-RAS at 78 cross-sections
2 (PRRIP 2022a, HEC-RAS 2008) spaced an average of 1,165 ft apart through the study area.
3 These models pre-dated topobathymetric LiDAR and relied on a combination of terrestrial
4 LiDAR and supplemental field surveys. Once topo-bathymetric LiDAR were available in 2016,
5 the Program shifted to annual two-dimensional hydraulic modeling using the Bureau of
6 Reclamation SRH-2D modeling platform (Lai 2008). To provide for a direct comparison of
7 HEC-RAS and SRH-2D wetted widths, we clipped HEC-RAS cross station lines to SRH-2D
8 water surface polygons (2016, 2017, 2021) which allowed us to report 2D wetted widths at 1D
9 cross section locations. Statistical tests of differences between mean width in three reaches
10 (augmentation area, J2 Return Channel, and downstream of Overton) were completed with the
11 emmeans package in R version 4.2.2 (Lenth 2023).

12 3.6.2 Results

13 The results of the wetted width analysis can be viewed as a continuum from upstream to
14 downstream (Figure 3.15) or broken into three reaches and averaged (Table 3.3). The first reach
15 is from the J2 Return to the downstream boundary of the augmentation area. This is the reach in
16 which the channel was mechanically widened by bulldozing terraces and spreading the terrace
17 sediment over the channel bed. Because of augmentation activities, widths in this reach increased
18 dramatically in 2017, the first year of sediment augmentation. The second reach extends from the
19 downstream boundary of the augmentation area to the Overton Bridge. This reach shows year-to-
20 year width variations, but on average no progressive widening or narrowing (Table 3.3). In this
21 reach, Tukey-adjusted pairwise comparisons of mean width between years do not reveal
22 significant change in sequential years but do detect a significant difference between 2009 and
23 2016 wetted widths, with 2009 having higher width on average in the J2 Return Channel
24 between stations 84,000 and 55,000 (mean difference 120 ft, $p < 0.025$ at the 95% confidence
25 level). Pre-2016 widths are derived from a 1D model while post-2016 widths are derived from a
26 2D model. While this inconsistency should not obfuscate large changes, it precludes fine-scale
27 analysis of year-to-year variation. Downstream of the Overton Bridge, the channel receives water
28 inputs from both the J2 Return Channel and the North Channel, making it subject to natural high
29 flow events in a way that the J2 Return Channel is not. A high flow event in 2015 had a large
30 morphological impact on the reach downstream of Overton including substantial bank erosion.
31 The result of this event can be seen in the 50% increase in width from 2012 to 2016 below the



1 confluence. This increase in width was maintained with additional slight increases during the
2 sediment augmentation experiment.



3 **Figure 3.15** Wetted width at HEC-RAS cross-sections in 2009–2021. Widening due to
4 augmentation (2017, 2021) is visible upstream of the Augmentation Boundary and widening due
5 to the 2015 flood visible downstream of Overton Bridge.

6 **Table 3.3** Mean wetted width and standard deviation (SD) in three reaches, measured at 78 HEC-
7 RAS cross-section locations. Augmentation beginning in 2017 increased width in Reach 1.
8 Flooding in 2015 caused Reach 3 to widen between 2012 and 2016.

	Reach 1 J2 to Augmentation Boundary		Reach 2 Augmentation Boundary to Overton		Reach 3 Overton to KCD	
Year	Mean (ft)	SD (ft)	Mean (ft)	SD (ft)	Mean (ft)	SD (ft)
2009	290	90	440	130	490	150
2012	190	40	360	120	480	140
2016	280	60	350	120	720	160
2017	510	200	380	150	740	150
2021	540	180	360	140	760	130

9

10 We compared 2021 wetted width with modeled channel slope to identify slope-width
11 relationships in the study area (Figure 3.16). In 2021, there is an upward inflection in both slope
12 and wetted width near Station 60,000. Between Station 60,000 and 30,000, both width and slope
13 appear to increase together. Below Station 30,000, both width and slope decrease. However,
14 width decreases more substantially than slope.



In terms of the relationship between slope and planform (with width as an indicator), it appears that both slope and width increase at a higher rate once slope exceeds 0.001. Slope and width are correlated throughout the study area between Stations 84,000 and 0 (Pearson correlation coefficient 0.71; $R^2 = 0.51$, correlation p-value $< 2.2E-16$). This is an indication that 0.001 could be the threshold slope between wandering and braided planforms in this section of the Platte River. Once slope exceeds 0.001, the channel begins to braid with the amount of braiding (width as proxy) increasing with increasing slope. The relationship between width and slope is less clear below Station 30,000. This is likely due to the presence of a major flow split in that reach where flow is distributed between two channels separated by a large permanent island.

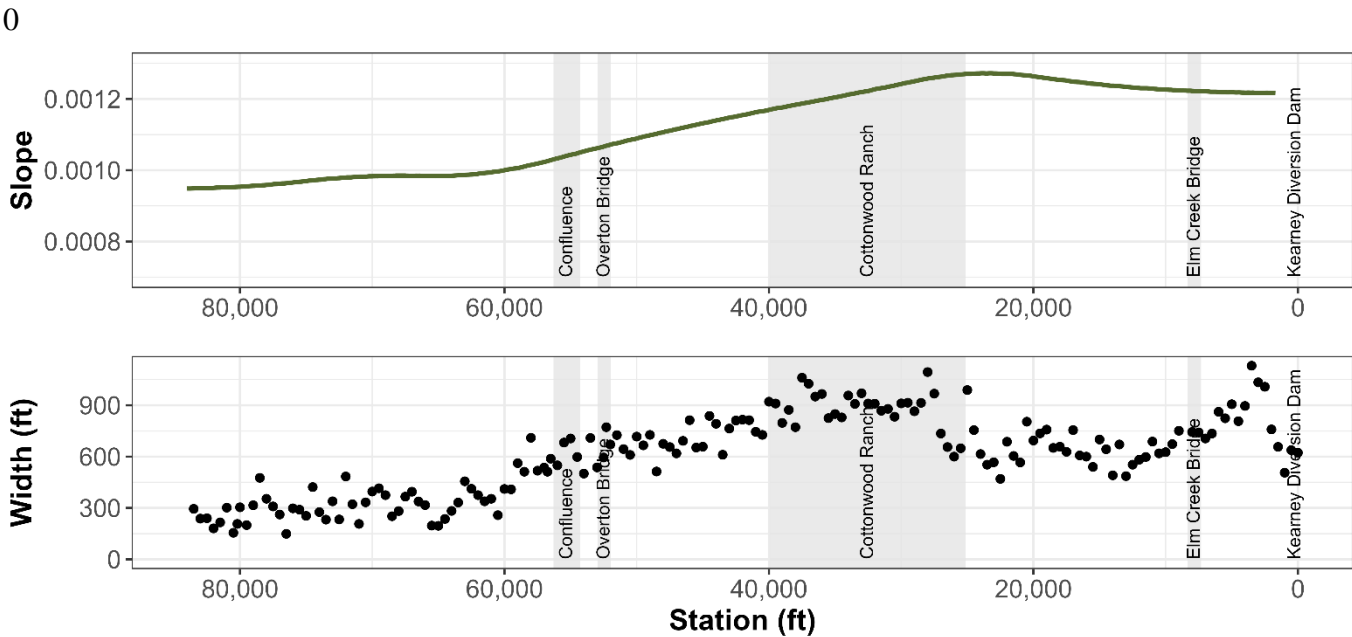


Figure 3.16. 2021 channel slope of the GAMM-modeled thalweg (top) and wetted width at 2,000 cfs (bottom). Width and slope increase together between Station 60,000 and 30,000.



3.7 *Sinuosity of the J2 Return Channel*

Similar to wetted width, evaluating spatial and temporal trends in sinuosity provides clues about the progression of incision and narrowing in the J2 Return Channel as well as potential effects of sediment augmentation.

3.7.1 Methods

We analyzed pre-augmentation changes in channel sinuosity in the J2 Return Channel between 1969 and 2016 using hand-delineated channel thalwegs from aerial imagery (see Chapter 2). For the analysis of post-augmentation sinuosity, we used geoprocessing techniques described in Section 3.4.1 to delineate thalwegs from topobathymetric LiDAR. These lines were then smoothed in ArcGIS Pro version 3.0.3 using polynomial approximation with an exponential kernel smoothing algorithm and a tolerance of 300 ft. We compared the smoothed LiDAR-derived thalwegs to hand-delineations for overlapping years and found results to be similar, although hand-delineations yielded a higher average sinuosity by 0.01. Therefore, we plot and interpret sinuosity derived from both methods together.

3.7.2 Results

Sinuosity results are presented in Figure 3.17. Prior to initiation of sediment augmentation, sinuosity of the J2 Return Channel had increased steadily since the early 2000s. Sinuosity declined in 2017 due to the construction of a meander cutoff immediately below the J2 Return (see Chapter 1). The cutoff rerouted the channel to avoid erosion of private property and straightened the alignment of the channel, decreasing length by about 1,300 ft. After 2017, sinuosity continued to increase throughout the duration of the augmentation management experiment. This is due to the continued development of meanders in the wandering segment of channel.

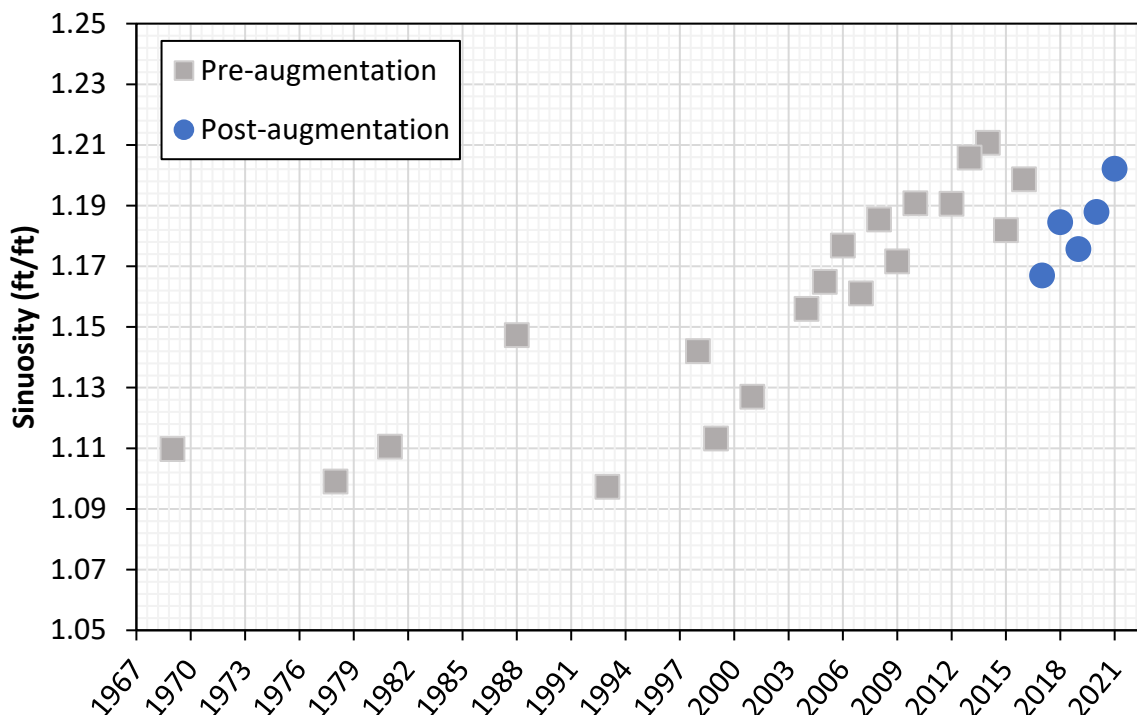


Figure 3.17 Ratio of thalweg to straight-line length (sinuosity) in the J2 Return Channel between 1969 and 2021. Figure shows a trend in increasing sinuosity beginning in the early 2000s. Sinuosity declined in 2017 due to the construction of a meander cutoff as part of augmentation operations. Despite the cutoff, the trend of increasing sinuosity continued during the augmentation experiment.

3.8 Focused analysis of incision in the vicinity of Station 70,000

We identified a reach of river extending from Station 72,000 to 65,000 that required deeper investigation due to higher magnitude of change relative to other river segments. The reach is referred to as Reach 70,000 due to its proximity to River Station 70,000. In addition to a more detailed evaluation of prior analyses, we measured six channel cross sections from LiDAR data in this reach to provide a cross-sectional view of channel change during the augmentation experiment.

A detailed plot of 2016 and 2021 longitudinal profiles of the thalweg, 1,005 ft centered moving average thalweg elevations, and GAMM-predicted thalweg elevations is presented in Figure 3.18. A comparison of thalweg profiles indicates at-a-station change was highly variable with the highest magnitude of incision near Station 71,000 at the apex of a meander. Overall, the modeled thalweg profiles indicate significant incision of the thalweg beginning at Station 73,000 and ending at approximately Station 57,000. Within this reach the maximum magnitude of modeled thalweg incision (> 2 ft) occurred in the vicinity of Station 70,000.

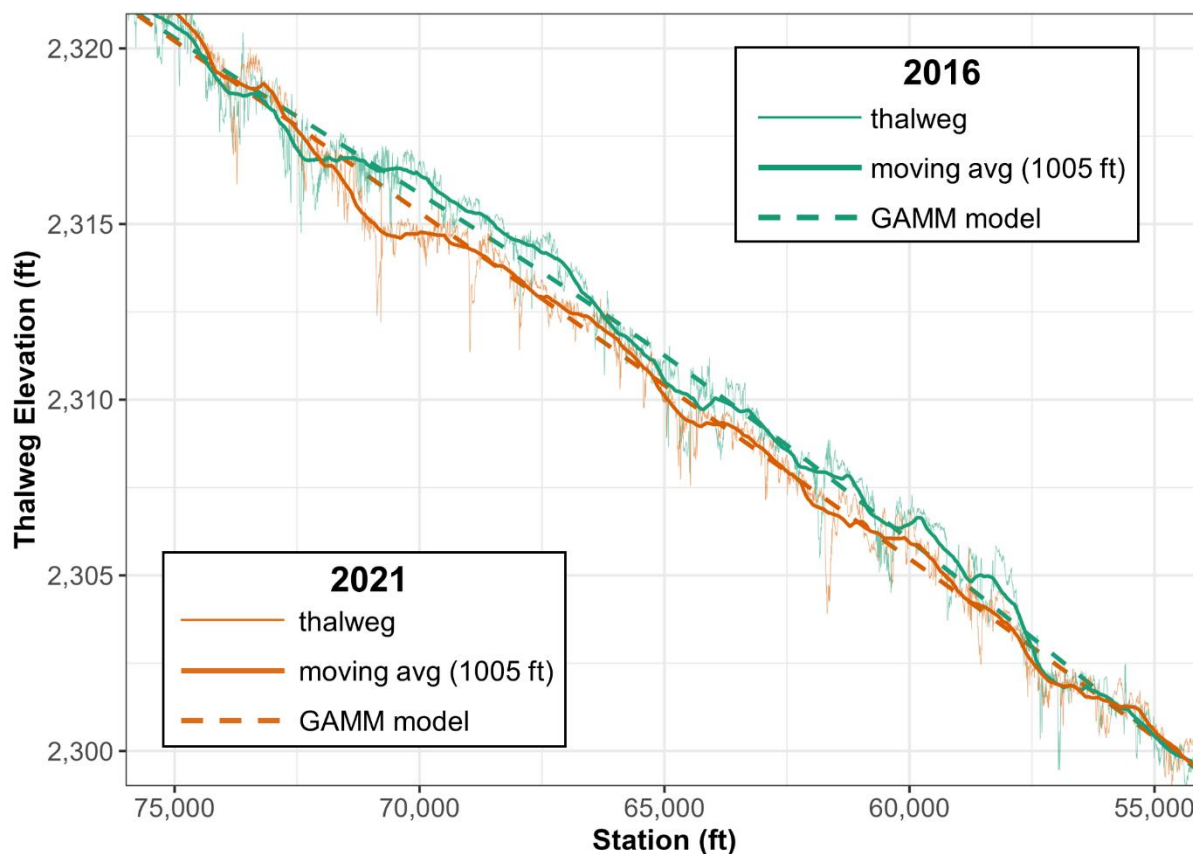
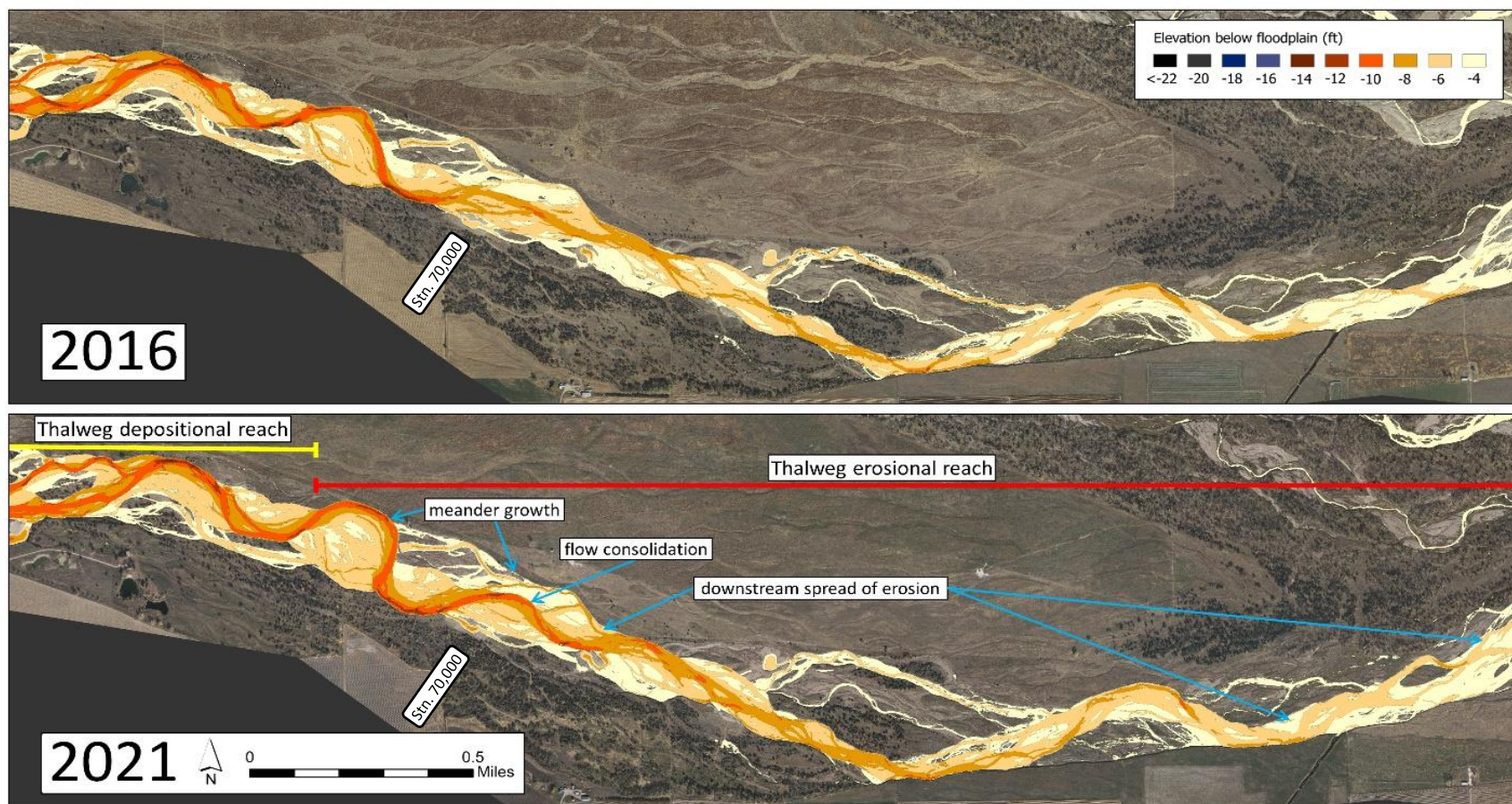


Figure 3.18. Longitudinal thalweg profiles and thalweg models (GAMMs) for 2016 and 2021 between Station 75,000 and 55,000.

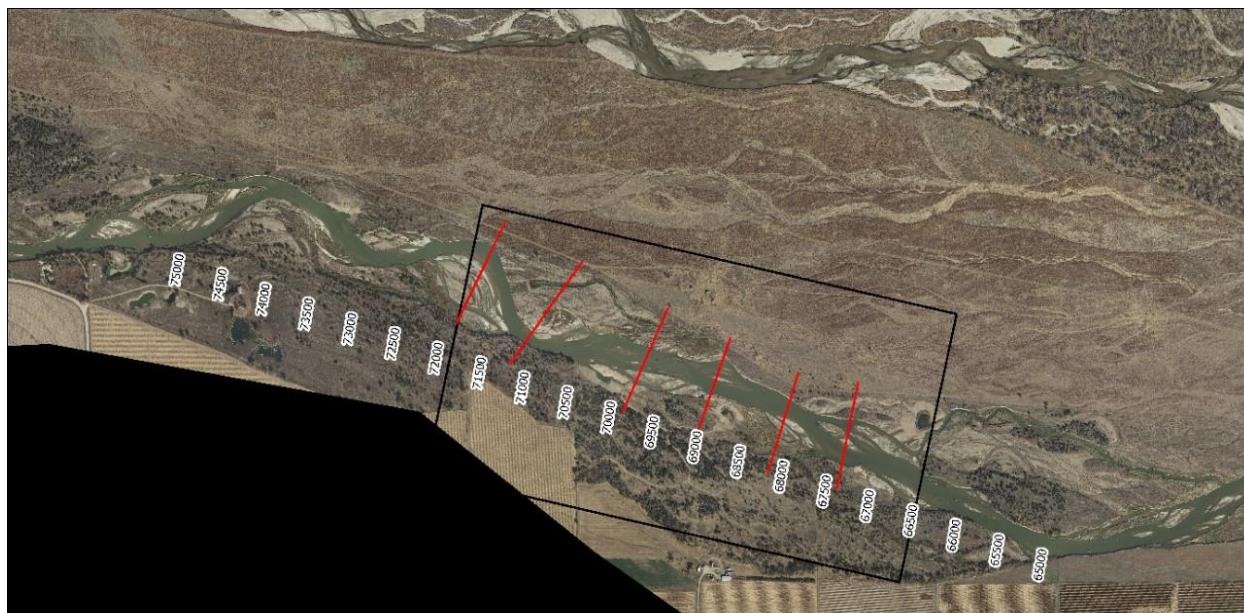
Annotated Reach 70,000 REMs for 2016 and 2021 are presented in Figure 3.19. The REMs indicate intensification of the existing meander and formation of a new meander just downstream of Station 70,000. Incision is apparent in the downstream extension of the eight ft and ten ft REM classes between 2016 and 2021. Figure 3.20 provides the location of cross sections between Station 71,580 and 68,940 within 2016 and 2021 aerial imagery.

1



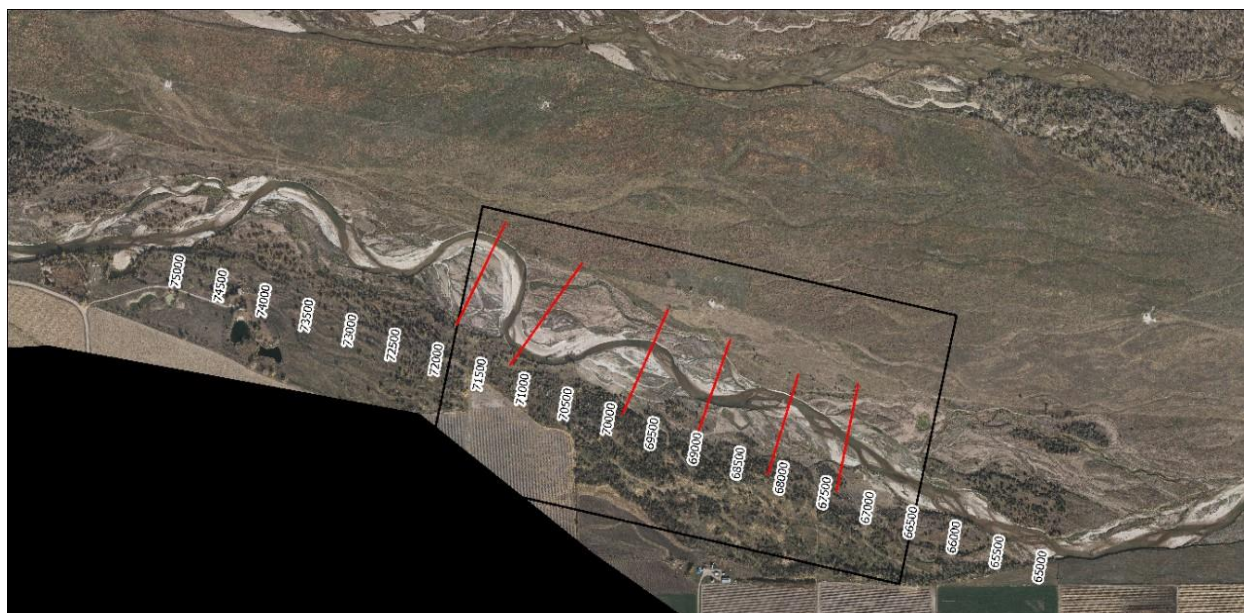
2

3 **Figure 3.19.** Annotated relative elevation models (REMs) of the downstream section of J2 Return Channel ending at Station 58,000.
 4 The relative elevation model is contoured into 2 ft intervals below -4 ft relative to the floodplain. Blue arrows in the bottom panel
 5 highlight changes since sediment augmentation. Yellow and red lines indicate regions of erosion and deposition detected by
 6 changepoint analysis.



0 0.25 0.5 0.75 1 Mile

2016



0 0.25 0.5 0.75 1 Mile

2021

Figure 3.20. Aerial imagery of Reach 70,000 in 2016 (top) and 2021 (bottom). A black rectangle extends from Station 71,835 to Station 66,435 and delineates the reach with the most change. Cross section locations are noted in red.



1 LiDAR-derived transect plots for the six cross sections between Station 71,580 and 68,940 are
 2 provided in Figure 3.21. All cross sections show some degree of lateral erosion between 2016
 3 and 2021. This is most apparent at Station 71,580, 71,070, 68,940 and 68,050 transects which are
 4 all located at or near the apices of developing meanders. In terms of thalweg incision, the three
 5 most upstream cross sections experienced the highest magnitudes of incision in 2019 with some
 6 thalweg infilling in subsequent years. The three downstream cross sections did not experience
 7 thalweg infilling after 2019. Change in channel geometry at the furthest downstream cross
 8 section (67,355) indicates a planform shift at that location in 2019 with the development of an
 9 incised low flow channel near the midpoint of the cross section that persisted through 2021.

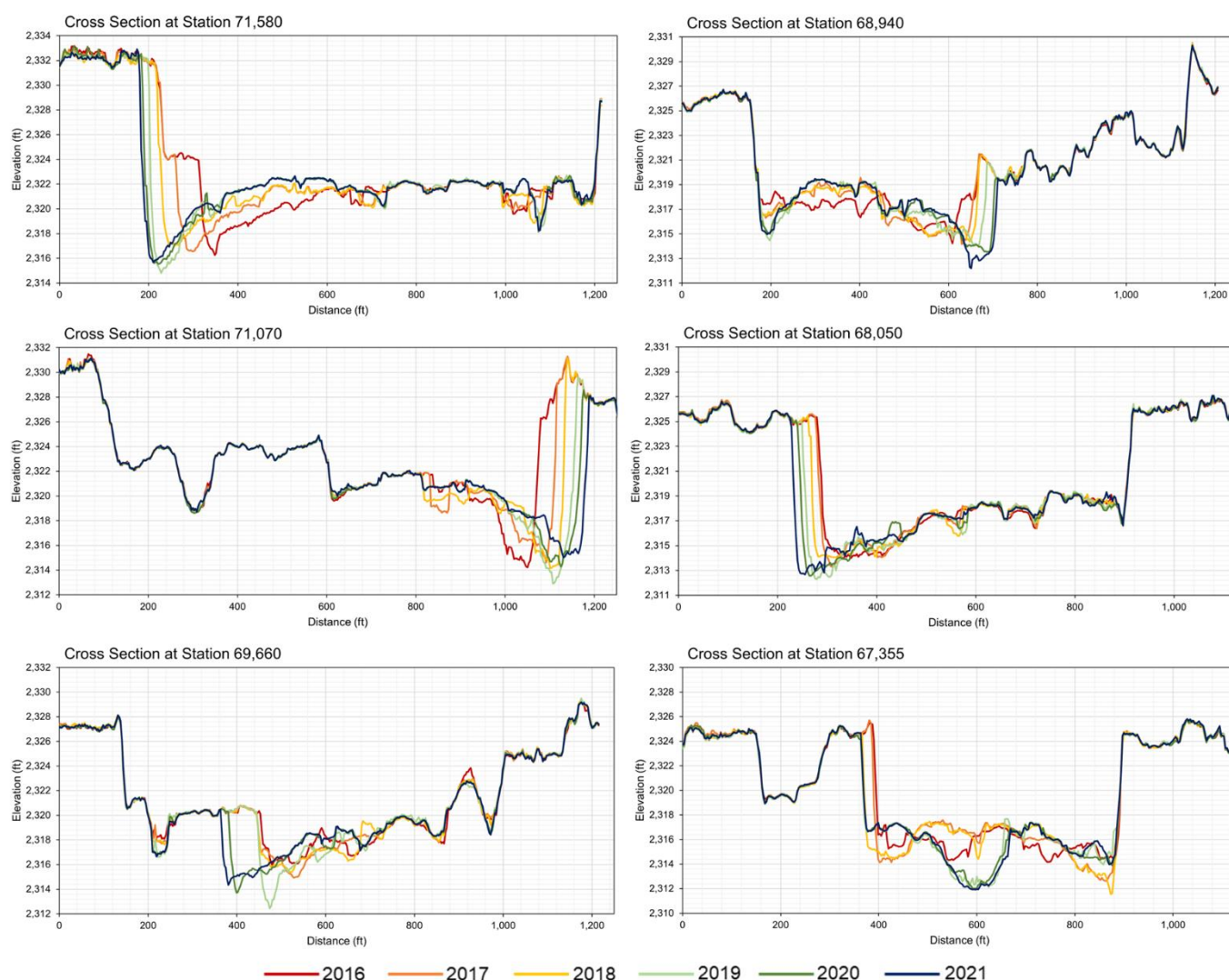


Figure 3.21. Cross sections viewed from river left to right, looking in the downstream direction at 6 locations in Reach 70,000 of the J2 Return Channel.



- 1 Sinuosity in Reach 70,000, calculated as thalweg length within the black rectangle in Figure
- 2 3.19, increased from 2016 to 2021 (Figure 3.22a). This is evident in REMs and aerial imagery as

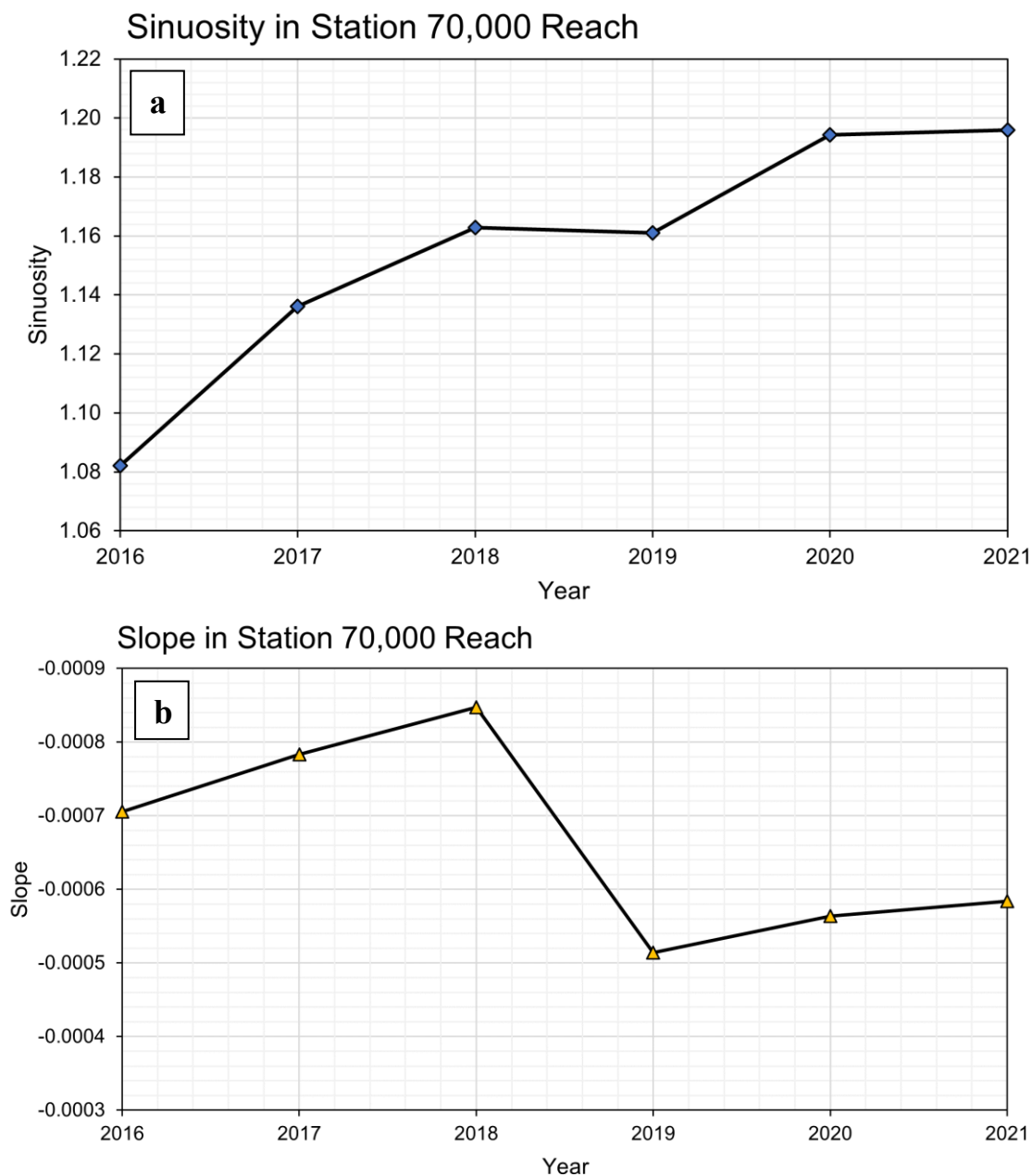


Figure 3.22. (a) Sinuosity of Reach 70,000, measured in the area delineated by the black rectangle in Figure 3.20. Sinuosity is the ratio of along-channel distance to straight line distance. (b) Slope of reach 70,000, measured as the slope of a linear regression between elevation and along-thalweg distance within the black rectangle in Figure 3.20. Note that slope presented here is calculated with actual distance along the thalweg, rather than stationed distance or the GAMM-derived thalweg estimate.



meanders expanded during this period (Figures 3.19–3.20). Over the same period, channel slope decreased in this area due to events in 2019, although slight increases occurred before and after 2019 (Figure 3.22b). Spatially, slope from Station 76,000 to 65,000 increased (Section 3.4.2; Figure 3.10 top) and slope decreased from Station 65,000 to 50,000 as the thalweg incised through a “high point” in the channel profile.

This area is evolving and appears to have been the focal point of incision and planform change in the J2 Return Channel during the sediment augmentation experiment. The pace of this migration should be monitored, especially in absence of sediment augmentation, to evaluate how the channel continues to evolve.

3.9 Discussion

To evaluate sediment augmentation effectiveness since sediment augmentation began below the J2 Return, we examined longitudinal change starting in 2016, the year immediately prior to sediment augmentation. Analyses extended through 2021 to incorporate the first five years of the sediment augmentation management experiment. Using results from relative elevation to the floodplain, thalweg elevation, average cross-sectional elevation, and channel geometry, we found evidence of aggradational augmentation response in the upper portion of the J2 Return Channel. The lower portion of the J2 Return Channel degraded during augmentation, especially as a result of high flows in 2019. Downstream of Overton Bridge, minor aggradation and degradation was observed at much smaller magnitudes than in the J2 Return Channel.

Upstream of Station 70,000 (the first 2.3 miles below sediment augmentation), the channel elevation increased. Sediment inputs during this time formed bars, decreased pool depths, and generally aggraded the channel. Though low magnitude when averaged through the reach, this gain in elevation could be partially attributed to sediment augmentation efforts, with some additional sediment inputs from the breakthrough channel prior to 2019. The breakthrough channel is discussed further in Chapter 4.

Moving downstream of the aggradational reach within the J2 Return Channel, the remaining length of channel upstream of the North Channel confluence continued to degrade during the first few years of the sediment augmentation experiment. Thalweg and average cross-sectional elevation decreased, and the reach surrounding Station 70,000 experienced the most negative change. Within this reach, meanders grew and migrated downstream. Although already incising, the reach experienced a large magnitude incisional event in 2019. Since 2019, when high flows occurred and the breakthrough channel was closed, bed elevations in this reach have been stable though sinuosity has continued to increase.

Lateral migration recruits additional sediment to the channel and is therefore not considered a negative outcome, but increased lateral migration can result in lowered channel slope, which in turn may affect planform. In the remaining braided section of the J2 Return Channel, both width and slope increase steadily in the downstream direction. We estimate that the increase reflects an approximate slope threshold of 0.001 for channel planform transition between wandering and braided in this area (Station 65,000–60,000). As meanders continue to expand and add channel length in this vicinity, slope is expected to decrease accordingly and shift the planform transition further downstream. It is possible that upstream portions of the J2 Return Channel have adjusted to a relatively constant slope that yields a consistent wandering planform and may not evolve



1 further under the current discharge and sediment regime. However, without sediment
2 augmentation, and with the 2019 blockage of sediment and flow inputs from the breakthrough
3 channel, the previously adjusted channel length is subject to additional change.

4 Changes downstream of Overton Bridge were generally subtle and lower magnitude than
5 changes within the J2 Return Channel. Some bars dissipated during the study period. This
6 change could be attributed to low magnitude degradation and management actions (e.g.
7 vegetation disking in 2018) between 2016 and 2021. Generally, the reach downstream of
8 Overton retained high wetted widths since 2015 with little to no detectable change in channel
9 elevations and geometry. The channel is aggrading upstream of Elm Creek Bridge. This
10 aggradation is potentially associated with the buildup of sediment upstream of the constriction at
11 Elm Creek Bridge and behind KCD.

12 The J2 Return Channel, especially Reach 70,000, is sensitive to high flows and experienced
13 overall average loss in elevation during the three highest flow years within the study period
14 (2016–2017, 2018–2019, and 2019–2020; Table 3.2). During the two drier years (2017–2018 and
15 2020–2021), elevation gained on average in the J2 Return Channel. During all years measured,
16 reach-averaged losses and gains have opposite signs in the J2 Return Channel versus
17 downstream of Overton Bridge, i.e., when the J2 Return Channel experiences elevation loss, the
18 channel downstream of Overton experiences elevation gain. Losses versus gains relative to flow
19 magnitudes are reversed within the reach downstream of Overton Bridge. During lower flow
20 years, the channel degraded downstream of Overton, and during high flow years the channel
21 aggraded. This behavior can assist future assessment of the general fate of augmented sediment.
22 During dry years, more augmented sediment remains within the J2 Return Channel, and during
23 wet years more sediment (both augmented and stored) is transported downstream of Overton.
24 Because the system upstream of Overton Bridge continues to receive insufficient sediment
25 supply for sediment balance, high sediment transport years lead to channel degradation and
26 threat of planform migration downstream within the J2 Return Channel. Though incision may be
27 present in the J2 Return Channel during years with high flow, high transport years also yield
28 important sediment inputs to downstream habitat.

29 A primary goal of sediment augmentation is to halt downstream progression of incision and
30 narrowing. The transition from wandering to braided planform is roughly 3 miles upstream of
31 Overton Bridge. Here, the wandering planform migrated downstream during the augmentation
32 experiment by roughly 2,000 ft. This length estimate of channel planform migration over 5 years,
33 and the approximate distance of 3 miles downstream to Overton Bridge, indicate that a
34 wandering planform could migrate to the Overton Bridge on the order of 40 years. Though this
35 estimate is general, it implies that the timescale for complete planform transition of the J2 Return
36 Channel is decadal. Incision and planform change are measurable threats to habitat downstream
37 of the Overton Bridge, but the confluence with the North Channel provides significant sediment
38 inputs which are not quantified in this study. Analogous to sediment inputs from tributary
39 confluences (Benda et al., 2004), water and sediment inputs from the North Channel offset some
40 of the risk associated with incision caused by the J2 Return. Thus, related channel changes
41 downstream of the confluence are likely to occur at a slower pace than within the J2 Return
42 Channel.



1 Future analyses to advance our understanding of channel behavior downstream of the J2 Return
2 include more detailed analysis of changes in channel width and slope, quantification of lateral
3 migration of the channel thalweg, and statistical or morphodynamic models to relate channel
4 response to sediment supply and flow. There are limitations to examining change with one metric
5 at a time longitudinally. For example, confining analysis of change within the channel thalweg
6 leads to continued uncertainty regarding the active channel and floodplain outside of the deepest
7 portion of the channel and omits information about overbank deposition and secondary flow
8 paths. Thus, we extend our analyses in the following chapter with examination of volume change
9 to quantify sediment erosion and deposition within the study reach.

10



3.10 References

- Benda, L.E.E., Poff, N.L., Miller, D., Dunne, T., Reeves, G., Pess, G. and Pollock, M., (2004). The network dynamics hypothesis: how channel networks structure riverine habitats. *BioScience*, 54(5), pp.413-427.
- Graf, W.L., (2006). Downstream hydrologic and geomorphic effects of large dams on American rivers. *Geomorphology*, 79(3-4), pp.336-360.
- Haynes, K., Eckley, I.A. and Fearnhead, P. (2017). Computationally efficient changepoint detection for a range of penalties. *Journal of Computational and Graphical Statistics* 26(1):134-143.
- Howard, A.D., (1982). Equilibrium and time scales in geomorphology: Application to sand-bed alluvial streams. *Earth Surface Processes and Landforms*, 7(4), pp.303-325.
- HEC-RAS. (2008). Hydraulic Reference Manual. U.S. Army Corps of Engineers, Hydrologic Engineering Center.
- Killick, R., Eckley, I.A. (2014). changepoint: An R Package for Changepoint Analysis. *Journal of Statistical Software* 58(3): 1-19. <https://www.jstatsoft.org/article/view/v058i03>.
- Killick, R., Fearnhead, P. and Eckley, I.A. (2012). Optimal detection of changepoints with a linear computational cost. *Journal of the American Statistical Association* 107(500):1590-1598.
- Killick, R., Haynes, K., Eckley, I.A. (2022). changepoint: An R package for changepoint analysis. R package version 2.2.4. <https://CRAN.R-project.org/package=changepoint>.
- Kondolf, G. M. (1997). Hungry water: Effects of dams and gravel mining on river channels. *Environmental Management* 21 (4): 533–551. <https://doi.org/10.1007/s002679900048>.
- Lai, Y. (2008). SRH-2D Version 2: Theory and User's Manual. Bureau of Reclamation Technical Service Center Sedimentation and River Hydraulics Group.
- Lenth R (2023). emmeans: Estimated Marginal Means, aka Least-Squares Means. R package version 1.8.5. <https://CRAN.R-project.org/package=emmeans>.
- Ligon, F.K., Dietrich, W.E. and Trush, W.J., (1995). Downstream ecological effects of dams. *BioScience*, 45(3), pp.183-192.
- Mörtl, C. and De Cesare, G., (2021). Sediment Augmentation for River Rehabilitation and Management—A Review. *Land*, 10(12), p.1309.
- Platte River Recovery Implementation Program (PRRIP). (2022a). System-scale geomorphology and vegetation monitoring report. Prepared for PRRIP Governance Committee, June 2022.
- Platte River Recovery Implementation Program (PRRIP) Executive Director's Office (EDO). (2022b). First Increment Extension Science Plan.



- 1 Poff, N. LeRoy, J. David Allan, Mark B. Bain, James R. Karr, Karen L. Prestegard, Brian D.
2 Richter, Richard E. Sparks, and Julie C. Stromberg (1997). The natural flow regime.
3 BioScience 47 (11): 769-784.
- 4 Powers, P.D., Helstab, M. and Niezgoda, S.L. (2019). A process-based approach to restoring
5 depositional river valleys to Stage 0, an anastomosing channel network. River Research
6 and Applications 35(1): 3-13.
- 7 R Core Team (2022). R: A language and environment for statistical computing. R Foundation for
8 Statistical Computing, Vienna, Austria. <https://www.R-project.org/>.
- 9 Schmidt, J. C., & Wilcock, P. R. (2008). Metrics for assessing the downstream effects of
10 dams. Water Resources Research, 44(4).
- 11 Smith, V.B. and Mohrig, D., (2017). Geomorphic signature of a dammed Sandy River: the lower
12 Trinity River downstream of Livingston Dam in Texas, USA. Geomorphology, 297,
13 pp.122-136.
- 14 Ward, J.V. and Stanford, J.A., (1995). The serial discontinuity concept: extending the model to
15 floodplain rivers. Regulated rivers: research & management, 10(2-4), pp.159-168.
- 16 Williams, G.P., (1978). The case of the shrinking channels: the North Platte and Platte Rivers in
17 Nebraska (Vol. 781). US Department of the Interior, Geological Survey.
- 18 Wohl, E., Bledsoe, B. P., Jacobson, R. B., Poff, N. L., Rathburn, S. L., Walters, D. M., & Wilcox,
19 A. C. (2015). The natural sediment regime in rivers: Broadening the foundation for
20 ecosystem management. BioScience, 65(4), 358-371.

21

22



CHAPTER 4 Volume change analysis

4.1 Abstract

We used topobathymetric elevation data to calculate volumes of sediment that deposited or eroded between the Johnson No. 2 Hydropower Return (J2 Return) and the Kearney Canal Diversion (KCD). Using hydraulic modeling results, we separated lateral erosion from bed aggradation and degradation. We found that the study reach became less degradational in years since sediment augmentation began. Bed erosion has decreased 45% to 60% upstream of Overton Bridge. Our data indicate that a combination of hydrology, natural sediment sources, and augmented sediment have played a role in this reduction.

4.2 Introduction

As discussed in Chapter 1, the Platte River Recovery Implementation Program (PRRIP or Program) attempted to estimate the sediment deficit in the Program's Associated Habitat Reach (AHR) created by the J2 Return structure using various measured and theoretical sediment transport functions that tie transport to flow. The estimated deficit ranged from 50,000 tons per year (35,000 yd³/yr) between Overton Bridge and Kearney (Tetra Tech, 2017), to a 109,000 tons per year (73,000 yd³/yr) deficit between Overton and Elm Creek (The Flatwater Group, Inc, 2010). The 2017 estimate is less than half that of the 2010 estimate, despite covering a longer stretch of river with no major sediment sources. This disparity underlines the uncertainty and difficulty in comparing theoretical and field sediment data.

The Program began a full-scale sediment augmentation management experiment in 2017 with the purpose of offsetting the deficit and assessing effectiveness of augmentation in stabilizing the J2 Return Channel. Specifically, the Program began to augment 60,000–80,000 tons (40,000 – 60,000 yd³) of sediment immediately downstream of the J2 Return each year. Effectiveness is assessed using Light Detection and Ranging (LiDAR) topographic data and hydraulic modeling data to measure actual volumetric change in our study area. This approach, dubbed the “morphological approach” (Anderson, 2019; Vericat, et al., 2017), makes the most of our high-resolution LiDAR data to calculate change under known (or mostly known) circumstances.

Chapter 3 focuses on evaluation of longitudinal change in channel morphology during full-scale augmentation operations. Two of the primary limitations of that effort were 1) inability to quantify sediment flux through the study area and 2) lack of differentiation between lateral and bed erosion. Lateral erosion is sediment removal from banks and islands due to horizontal stress, while bed erosion is sediment removal from the riverbed due to vertical stress. Lateral erosion is a natural result of channel migration or width adjustment due to increased flow. With lateral erosion, sediment that was previously stored in the bank is added to the system. This sediment is incorporated into downstream bars and may reduce downstream deficits. In this way, lateral erosion is fundamentally different from bed erosion which signals channel deepening and further disconnection from the floodplain.

In this chapter, we expand LiDAR-derived longitudinal analysis into three-dimensional estimates of annual volume change during the sediment augmentation experiment that differentiate between bed and lateral erosion. To increase the utility of our findings, we also expanded the analysis to include the years of 2009–2016 prior to augmentation activities. During that period,



the Program collected topographic bare earth LiDAR. From 2016 to present, bathymetric LiDAR has been collected. Topobathymetric LiDAR penetrates the water surface and returns highly accurate estimations of the river bottom. Lack of bathymetry prior to 2016 adds uncertainty to volume change estimates, which is described in more detail below. Throughout this chapter, volume change estimates for 2009–2016 are referred to as Pre-Augmentation. Annual estimates during the augmentation experiment are referred to as Post-Augmentation.

4.3 Methods

4.3.1 Data sources

4.3.1.1 Topographic and bathymetric data

The Program has collected high-resolution LiDAR data across the study area each year since 2009. The data have 2.3 ft spatial resolution and vertical error of less than 3 inches (Dewberry, 2010). Prior to 2016, topographic LiDAR collected elevations only over dry portions of the banks and riverbed. Topographic LiDAR does not collect elevation in wetted areas, which were “hydroflattened” to smooth and approximate the water surface elevation. During dry years such as 2009, (see Table 4.1) water covered a small proportion (25%) of the active channel area, allowing for 75% LiDAR coverage. The primary data source for pre-2016 topography in the wetted portion of the channel was 2009–2016 systematic surveys of channel cross-section elevations conducted for the system-scale channel geomorphology and vegetation monitoring project (Tetra Tech, 2017). Prior to 2009 limited bathymetric survey data is available dating back to 1998.

Starting in 2016, topo-bathymetric LiDAR was deployed which allowed for the collection of both topographic and bathymetric data. Between 2016 and 2021 LiDAR elevation data were collected by Quantum Spatial Inc. (QSI) in either October or November. The data have 2.3 ft spatial resolution and vertical error of less than 3three inches for dry areas and less than or equal to 9 inches for wet areas (QSI, 2016- 2021). For further discussion on LiDAR uncertainty see section 4.3.3.

4.3.1.2 Hydraulic data

Since 2016, annual topo-bathymetric data has been used to update an SRH-2D (Lai, 2008) hydraulic model of the AHR that computes depth, velocity, and shear stress at each two-dimensional (2D) node over a range of in-channel flows (500 to 5,000 cfs). Prior to 2016, two one-dimensional (1D) hydraulic models were created, the first using 2009 LiDAR and survey data, the second using 2012 LiDAR and survey data. Model results from 2009 and 2016–2021 were used in this analysis to clip difference rasters to the active channel and partition lateral erosion from bed aggradation and degradation. To convert 1D model results to 2D water extent polygons, we exported water surface elevation (WSE) data to ArcGIS using HEC-GeoRAS (HEC-RAS, 2008) and created a digital triangulated irregular network (TIN) of the water surface. We then subtracted LiDAR data from the TIN of the modeled WSE, producing a raster of positive depth values where the ground was below the water surface. We then manually removed puddles, abandoned channels, and other low-lying areas that were not hydraulically connected to the river.



1 **Table 4.1.** Data used for volumetric analysis.

	2009 and 2012		2016 - 2021	
LiDAR date, resolution	March 2009, November 2012, 2.3 ft Topographic only		Fall (Oct or Nov), 2.3 ft Topo-bathymetric	
Flow rate during LiDAR collection (cfs)	J2 Return	Overton	J2 Return	Overton
	0–134	200–400	90–2,000	250–2,400
Hydraulic model	HEC-RAS 1D		SRH-2D	

2
3 *4.3.1.3 Hydrologic data*

4 There are two data sources for discharge data between the J2 Return and the KCD. The first is the
5 United States Geological Survey (USGS) stream gage at the Overton Bridge (06768000) located
6 seven miles downstream of the J2 Return and ten miles upstream of the KCD. This gage captures
7 the total flow immediately downstream of the confluence of the J2 Return Channel and the North
8 Channel of the Platte (North Channel). The second source is Central Nebraska Public Power and
9 Irrigation District (CNPPID) records of discharge released from the Tri-County Supply Canal
10 (Supply Canal) into the J2 Return Channel via the J2 Return. Typically, J2 Return releases
11 represent the majority of total flow in the J2 Return Channel except for 200-300 cfs of baseflow.

12 During high flow conditions between 2009 and 2019 there were several occasions when surface
13 flow from the North Channel activated a channel (the breakthrough channel) that runs to the upper
14 end of the J2 Return Channel (see Figure 4.1). The breakthrough channel was bermed in 2019 to
15 prevent flow from entering and endangering a gas pipeline. Prior to being blocked, aerial imagery
16 and changes in topography indicate that the channel periodically conveyed a substantial volume
17 of flow and sediment to the J2 Return Channel.

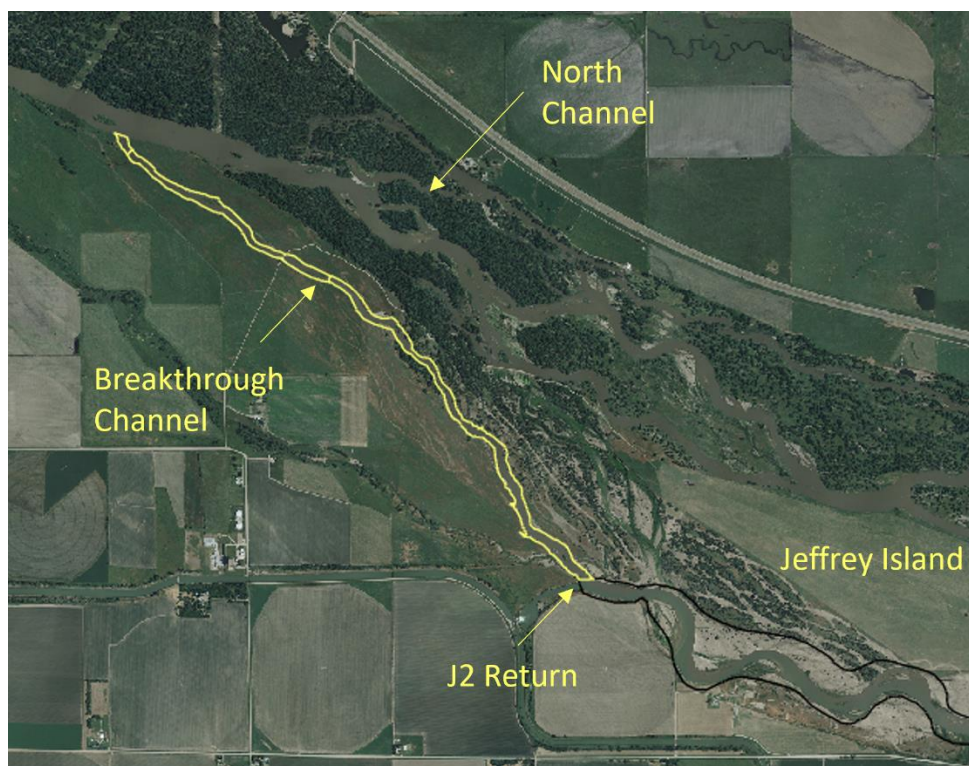


Figure 4.1 Breakthrough channel connecting the North Channel to the J2 Return Channel during high flow conditions prior to 2019.

Figure 4.2 presents 2009–2021 flow at the Overton Bridge (blue) alongside J2 Return releases (orange). J2 Return flows never exceeded 2,025 cfs during this period, whereas the Overton gage shows that there were several months in which mean flow was above 6,000 cfs. The peak daily flow of 15,300 cfs at Overton occurred in June of 2015. This flood had large geomorphic effects downstream of Overton such as high lateral erosion and channel widening (Section 3.6). As a result of the controlled hydrology from the J2 Return (except for occasional breakthrough channel activation), the J2 Return Channel does not experience floods that accelerate sediment transport, erosion, and change. This limits the ability of the channel to advect and convey augmented sediment that is placed within the J2 Return Channel.

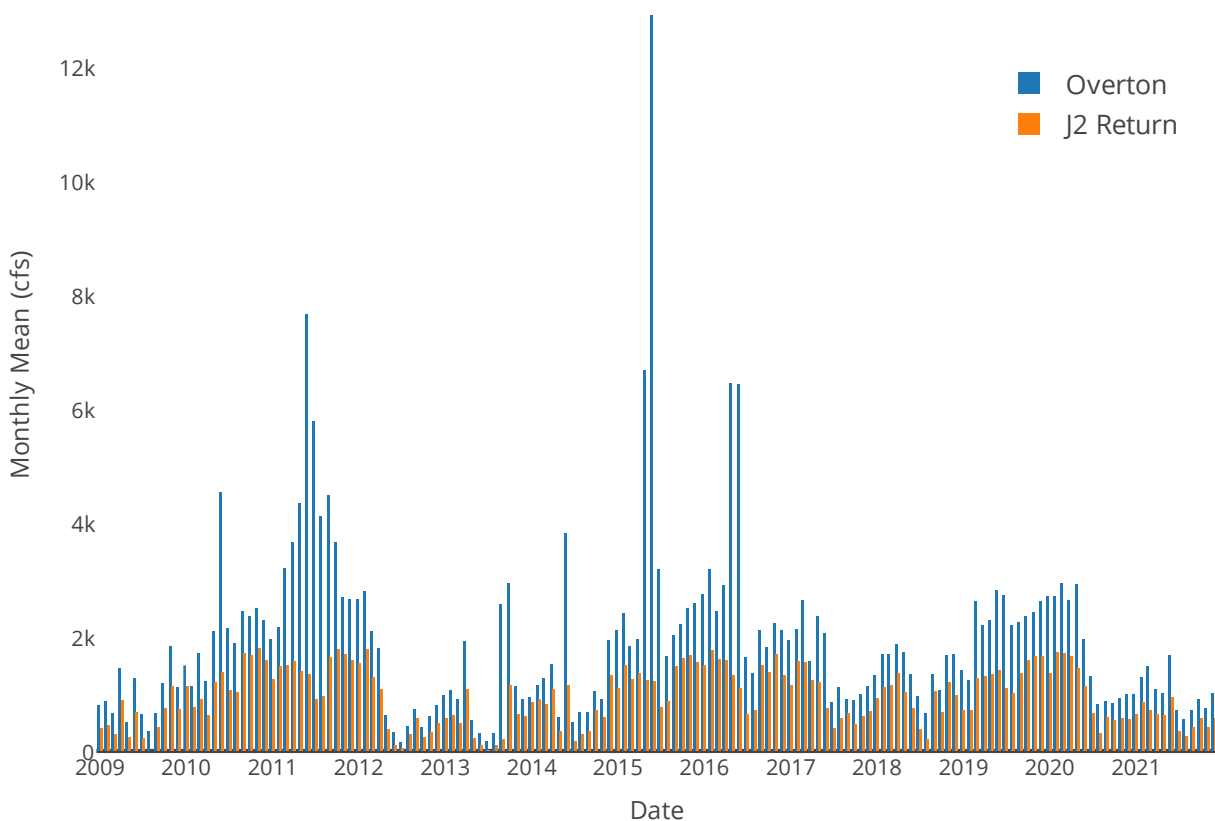


Figure 4.2 Monthly mean discharge from CNPPID to the J2 Return Channel and at the USGS Overton gage from 2009 to 2021.

4.3.1.4 Sediment data

There is very little suspended sediment and no bed load entering the J2 Return Channel from the J2 Return. In the years since the breakthrough channel was plugged (2019),, this has resulted in effectively no sediment entering the upstream end of the channel. As such, the primary source of sediment in that reach (absent breakthrough) has been erosion of bed and bank material.

Initiation of the sediment augmentation experiment in 2017 added a new sediment source through mechanical augmentation of sediment from high terraces immediately downstream of the J2 Return. Table 4.2 shows the amount of sediment that was made available for transport via augmentation in each year. The volume for 2017 is lower than other years because some excavated sediment was used to restore eroded cropland and construct a berm to arrest lateral erosion that was threatening a home along the south bank.

In years when the breakthrough channel was active, large amounts of sediment were also eroded and transported into J2 Return Channel in approximately the same location as the mechanical augmentation. The volume of sediment contributed via the breakthrough channel was calculated using the same method of analyzing difference rasters that was used across the entire study reach (see Section 4.3.2). Prior to annual topo-bathymetric data collection beginning in 2016, volume



change below water surface is calculated as a range of values (Section 4.3.2). Prior to augmentation, the only known source of sediment to the J2 Return Channel was the breakthrough channel which contributed an annual average of 32,800–33,500 yd³ between 2009 and 2016 (Table 4.2, Figure 4.3). Years in which augmentation and breakthrough channel activation both occurred had the highest sediment inputs, with a maximum of 104,000 yd³ in the 2017–2018 year.

Table 4.2 Sediment added to the J2 Return Channel.

	Breakthrough Channel Volume (yd ³)	Augmented Volume (yd ³)	Total (yd ³)
2009 – 2016	262,000–268,300	0	262,000–268,300
2016 – 2017	71,600	23,000	94,600
2017 – 2018	61,100	42,900	104,000
2018 – 2019	19,900	42,300	62,200
2019 – 2020	0	57,700	57,700
2020 – 2021	0	51,300	51,300

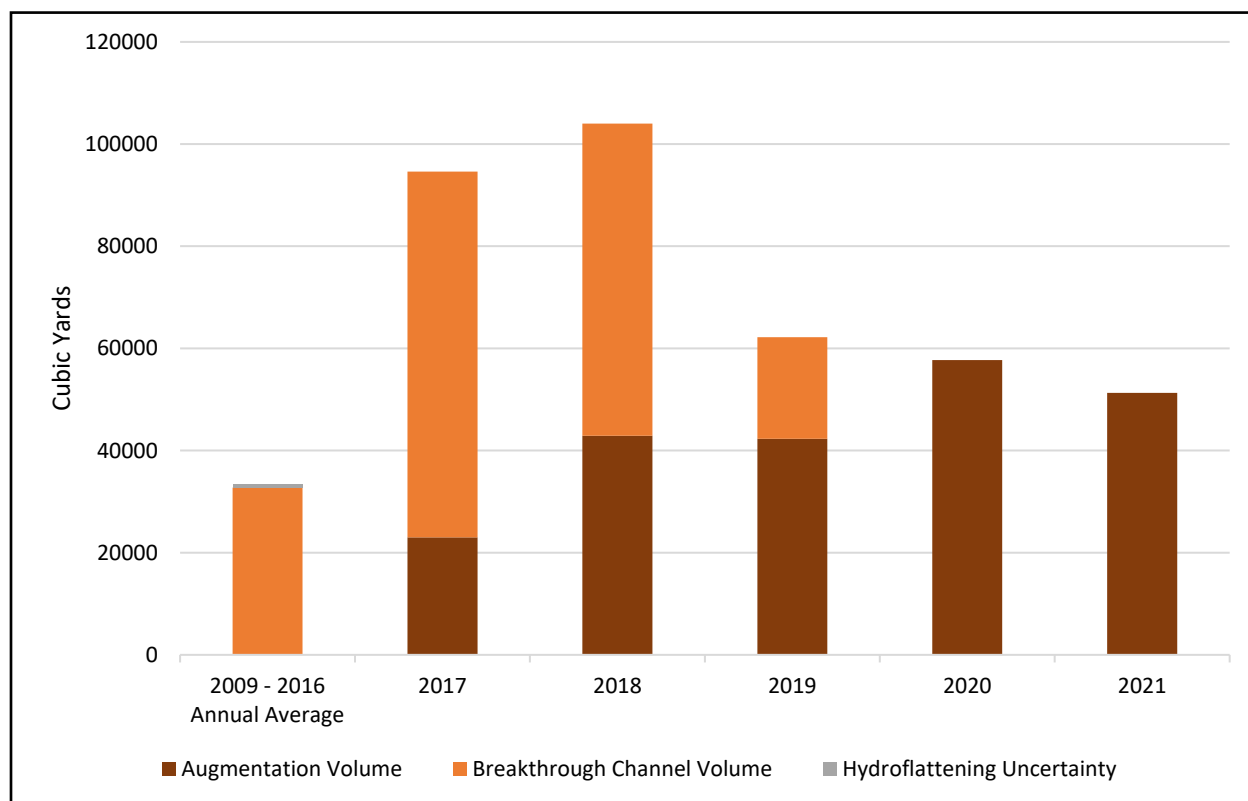


Figure 4.3 Sediment added to the J2 Return Channel downstream of the return through erosion in the breakthrough channel (orange) and sediment augmentation (brown).



4.3.2 Volume change (LiDAR raster differencing)

Annual volume change estimates were developed via LiDAR raster differencing. We created annual difference elevation rasters by subtracting the earlier year from the more recent year. We then clipped the difference rasters to the active channel (Figure 4.4) to remove dry floodplain areas that were not altered by flow. Removing these areas improved our accuracy because we found non-random error in LiDAR data for many floodplain areas due to year-to-year changes in vegetation. The active channel clip area was based on the hydraulic model's active flow conveyance area but manually widened in places to include areas of bank failure that were not wet. The hydraulic model results represented an approximate bankfull discharge of 2,500 cfs for the J2 Return Channel and 5,000 cfs for the reach downstream of the confluence with the North Channel. The active channel changes every year, so delineations are unique for, each analysis year.

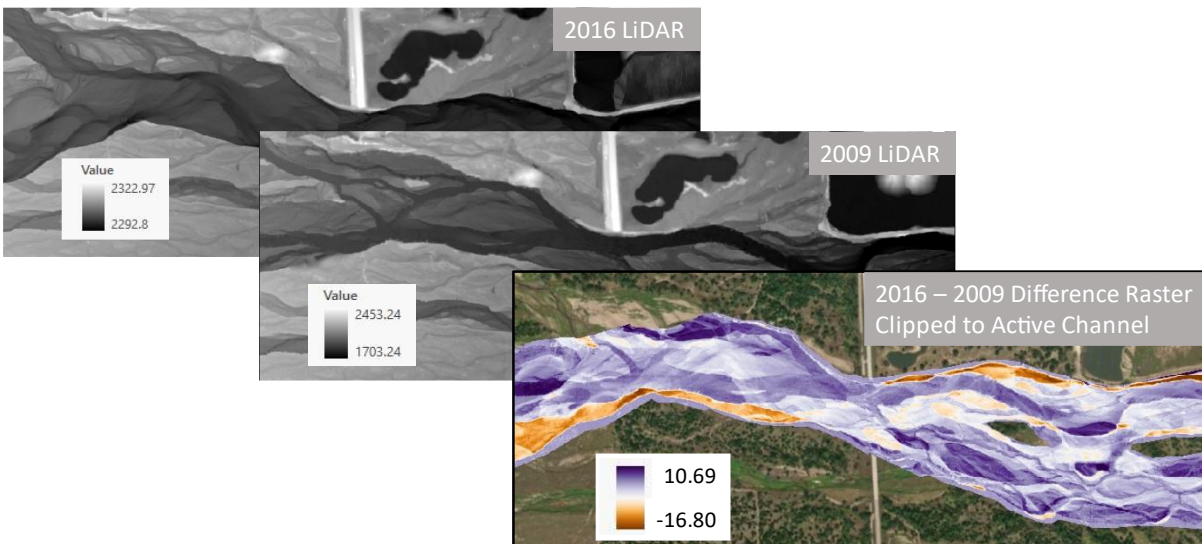


Figure 4.4. Example of raster differencing and clipping to the active channel at the Overton Bridge. 2009 elevations were subtracted from the 2016 elevations, resulting in a raster ranging from 10.69 ft of aggradation (purple) to 16.80 ft of erosion (orange).

In 2009, LiDAR rasters were hydroflattened within the wetted areas so change is presented as a range of possible values based on potential erosion and aggradation below the 2009 water surface. The hydroflattened areas often experienced aggradation as the channel migrated during the intervening years. In the 2016–2009 difference raster, this resulted in a net positive change above the 2009 hydroflattened elevation, meaning that the channel below the 2009 water surface filled in completely with sediment in many places. Based on the 2009 hydraulic model, the average depth of flow on the date of LiDAR collection was one ft. Multiplying this by the hydroflattened area gives a total underwater volume of 156,000 yd³ in the J2 Return Channel reach. We used this estimate to represent maximum potential aggradation not accounted for during raster subtraction due to missing bathymetry data in the 2009 LiDAR.

We defined lateral erosion as areas that experienced bank erosion or failure due to hydraulic activity. Following this erosion, previously dry areas become accessible to flow. To identify these



“newly wet” areas and thus areas of lateral erosion, we converted HEC-RAS and SRH-2D modeled water extents into 3x3 ft WSE raster grids (Figure 4.5A). We then intersected the rasters (2,500 cfs in the J2 Return Channel and 5,000 cfs below the North Channel confluence) and identified cells where water was newly present to create a mask of lateral erosion for each difference raster (Figure 4.5B).

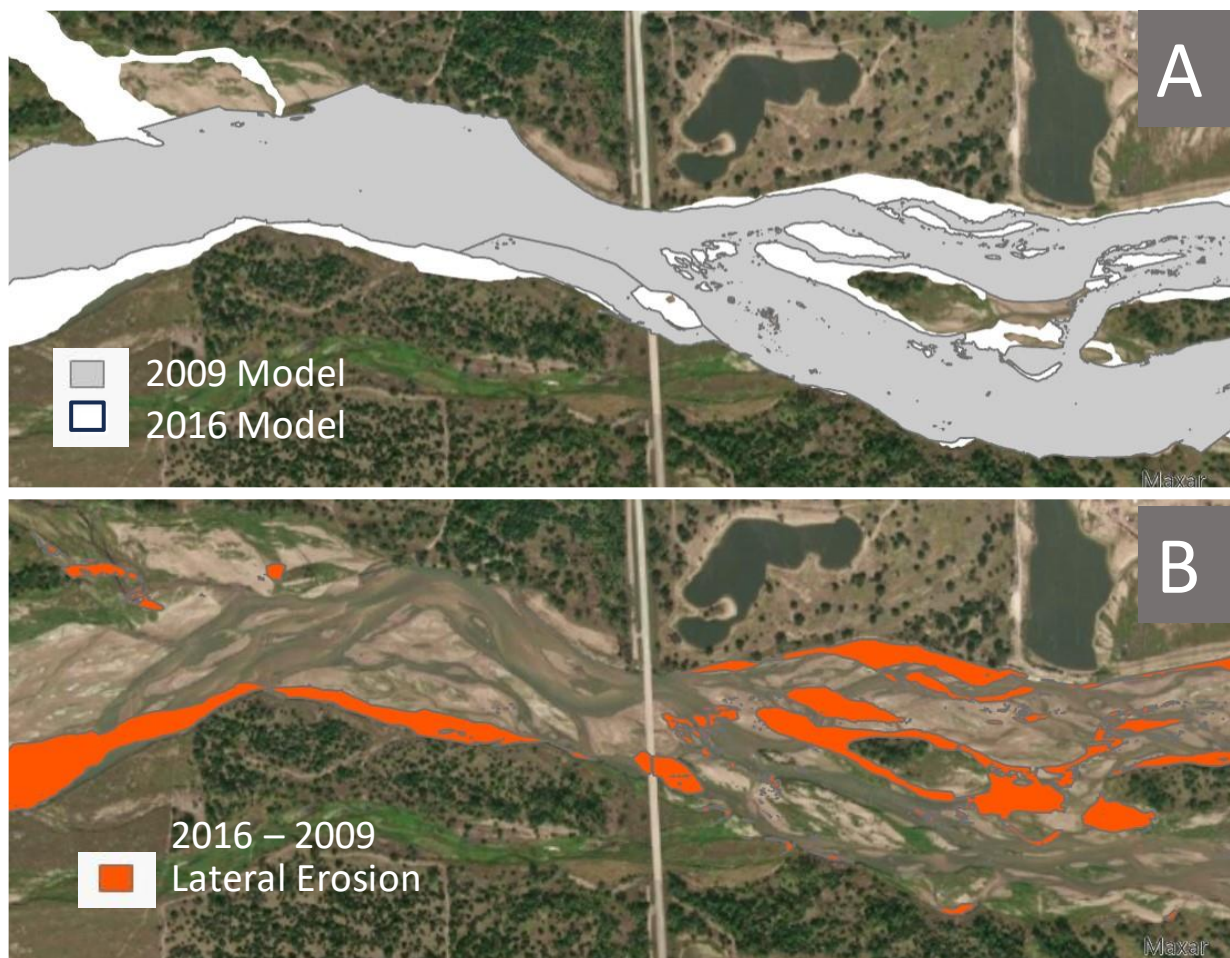


Figure 4.5. Lateral erosion was delineated by differencing hydraulic model results (A) and isolating newly wet areas (B).

Based on results of the System Scale Monitoring Report (PRRIP EDO, 2022b), the average wetted width of the J2 Return Channel is 450 feet. We chose to quantify sediment volume flux from year to year at a resolution of approximately two channel widths (900 feet) along the study reach. To accomplish this, we generated 900-foot-wide rectangles along the channel centerline that encompassed the entire channel. Using these rectangles as regions and values from the difference rasters clipped to the active main channel, we then summarized the data in each region using the ArcGIS Pro Zonal Statistics as Table tool (Figure 4.6). The sum of raster values in each region was multiplied by the area of the difference raster cell (9 ft²) to compute the change in volume for that region. This sum includes all volume change including lateral erosion. We then



used the same process to calculate volume change under the lateral erosion masks. Bed erosion was quantified by subtracting the lateral erosion quantity from the total volume difference for each region.

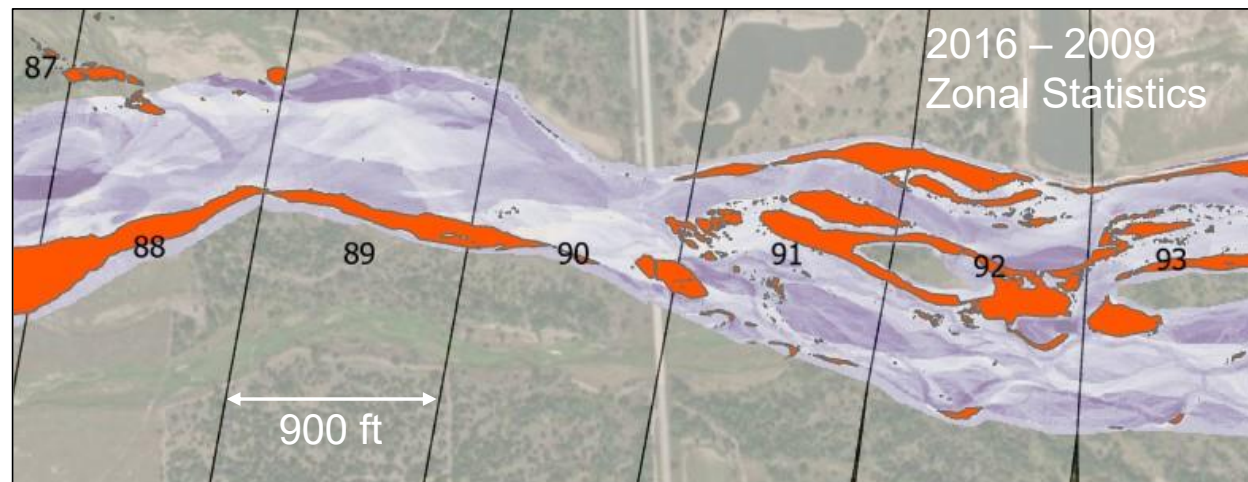


Figure 4.6. Using the zonal statistics tool, elevation differences in each 900-ft wide zone were summed. Zones are bounded in black and numbered 87-93 in this figure. The sums were then converted from ft to ft³ by multiplying the elevation difference by the raster cell area (9 ft²). The process was repeated to look only within the lateral erosion mask, shown in orange, to obtain the volume of lateral erosion in each zone.

4.3.3 Flow normalization of volume change

In most instances, volume change is divided by the number of years over which the change occurred. Another method to examine the volume change is to normalize the results by flow rather than year. This type of normalization allows us to control for the exponential relationship between flow and sediment transport, meaning that we can observe results without needing to account separately for wet and dry years. This procedure can only be used for normalization of volume change downstream of Overton Bridge because we do not have a complete set of flow data for the upstream reach due to ungaged flow from the breakthrough channel.

Normalization by flow was calculated by dividing volume change by the q dividend (Equation 4.1). The q dividend is the square of the flow volume that passed through the channel during the time that the volume change occurred. It is calculated by converting the daily mean flow rate to units of cubic yards per day, then squaring this value. Finally, the squared values are summed, and the resulting quantity is in units of 1/yd³. Sediment transport capacity is often related to a power function of flow, with common exponents ranging from 1.4 to 2.4 (Julien & Simons, 1985). For the purposes of this analysis, we chose an exponent of 2.0 as recommended by our Independent Science Advisory Committee (ISAC, 2023).

Equation 4.1
$$q \text{ dividend} = \sum Q^2$$

4.3.4 Uncertainty in LiDAR differencing

Between 2016 and 2021 LiDAR elevation data were collected by Quantum Spatial Inc. (QSI) in either October or November. The rasters have 3 ft spatial resolution and vertical error of less than



3 inches for dry areas and less than or equal to 9 inches for wet areas (QSI, 2016- 2021). In 2009 LiDAR was collected by Dewberry at the same spatial resolution and with similar dry vertical error. All accuracy values reported by the contractors are presented in Table 4.3. Accuracy was assessed at the time of data collection, and is based on comparison of field RTK GPS ground control check points to the LiDAR DEM. The accuracy values represent the 95% confidence interval, as derived from the population of differences between field-measured and DEM values. Accuracy assessments are designed to meet the guidelines of the Federal Geographic Data Committee National Standard for Spatial Data Accuracy (FGDC, 1998). From 2016–2021 the accuracy assessment data indicate elevation values in wet areas had consistently higher uncertainty than dry areas across all years. As a result of deeper and more turbid water during the period of data collection, wet areas in 2019 had a higher uncertainty value at 9 inches (Table 4.3).

Table 4.3. Vertical accuracy estimates for the LiDAR DEM surfaces from each year for wet and dry areas. Accuracy values represent 95% confidence in the estimate.

Year	Dry Accuracy (in)	Wet Accuracy (in)
2009	3.0	NA
2012	1.6	NA
2016	1.7	3.1
2017	2.2	4.6
2018	1.2	4.2
2019	1.2	9.0
2020	2.2	3.1
2021	1.7	2.1

Several methods exist in literature for quantifying error from difference rasters including the use of fuzzy inference systems (Wheaton et al., 2010; Bangen et al., 2016) for systematic error and the use of probability thresholds to limit noise when quantifying total erosion or total deposition (Lane et. al., 2003). In our assessment of net volume change we were able to disregard normally distributed random errors as these become negligible when summed over a large area (Anderson, 2019). Further, due to our goal of assessing fluctuations in bed volume and the partition between bed and lateral erosion, we determined that probabilistic thresholding would overemphasize the importance of mass bank failure as these large changes would always be above the significance threshold, while subtle bed changes would not. Our priority, therefore, was to eliminate or minimize all sources of systematic error.

Two sources of systematic error were observed in our datasets: those due to flightline-dependent tilts (see Anderson, 2019) and those due to vegetation changes outside the active channel area (e.g. crop fields). To address the first source, QSI performed additional post-processing to correct flight line errors using the 2019 LiDAR flight as a control (QSI, 2020b). The post-processing involved recalibrating 2017 and all future flights to the 2019 dataset by focusing on surfaces that do not change between years (paved roads, building corners, repeat survey markers, etc). This was not completed for the 2009 dataset, in which systematic error due to hydroflattening is



1 already being accounted for by estimating and reporting a range of possible aggradation.
2 Systemic error due to vegetation change was primarily observed outside of the active channel in
3 areas that experience plowing, tree clearing, mowing or haying vs. rest years for grasslands, or
4 other major changes to vegetation height and cover that may be near or within typical accuracy
5 estimates. These typical problem areas are not often located within our area of interest for
6 erosion and deposition (active channel), so by clipping the difference rasters to the active
7 channel, these areas are removed from our calculations. Following this post-processing effort to
8 remove systematic error, and with the given reported accuracies, we believe it is reasonable to
9 quantify change without using thresholds or other methods that may exclude data.

10 **4.4 Results**

11 **4.4.1 Pre- and post-augmentation volume change results**

12 To understand the relative influence of sediment augmentation on volume change and sediment
13 flux within the study area, it is helpful to compare data grouped into pre- and post-augmentation
14 time periods. The earliest Program LiDAR data was collected in 2009 and the first augmentation
15 project occurred in the fall of 2017, prior to LiDAR collection. Therefore, our pre-augmentation
16 period spans 2009–2016 and post-augmentation spans 2016–2021. Given the different lengths of
17 these timespans, results have been annualized or normalized by flow for easier comparison.

18 The net volume change at each station is shown in Figure 4.7, while Figure 4.8 shows the
19 cumulative, or running sum, of volume change beginning at the downstream end of the sediment
20 augmentation area. Figure 4.7A shows that total volume change was primarily negative
21 (degradational) over the full reach for both time periods. Much of this negative change can be
22 attributed to lateral erosion (Figure 4.7B). Sediment augmentation and lateral erosion both
23 produced concentrated signatures in the J2 Return Channel due to mechanical widening and
24 evolving meanders. When lateral erosion is subtracted from total change, the remaining volume
25 can be attributed to changes that occurred in the channel bed (Figure 4.7C). Bed changes were a
26 mix of positive (aggradational) and negative (degradational) across the reach.

27 In the post-augmentation period, areas of aggradation included the upstream end of the reach to
28 Station 70,000 and downstream near the Elm Creek Bridge. In the pre-augmentation period, the
29 reach upstream of the Overton Bridge was primarily negative, but the uncertainty due to the
30 absence of 2009 bathymetry prevents a clear conclusion on the downstream reach. Viewing net
31 change in relation to channel station is helpful for observing variability and identifying specific
32 areas of interest, however, summing change over a longer reach can give more concise
33 conclusions. Table 4.4 3 gives the sum of volume changes upstream and downstream of Overton
34 Bridge. Sums in the upstream reach do not include change in the augmentation project area,
35 instead focusing on non-mechanical change downstream of the projects. Figure 4.8 shows the
36 running sum of change over the full area of interest.

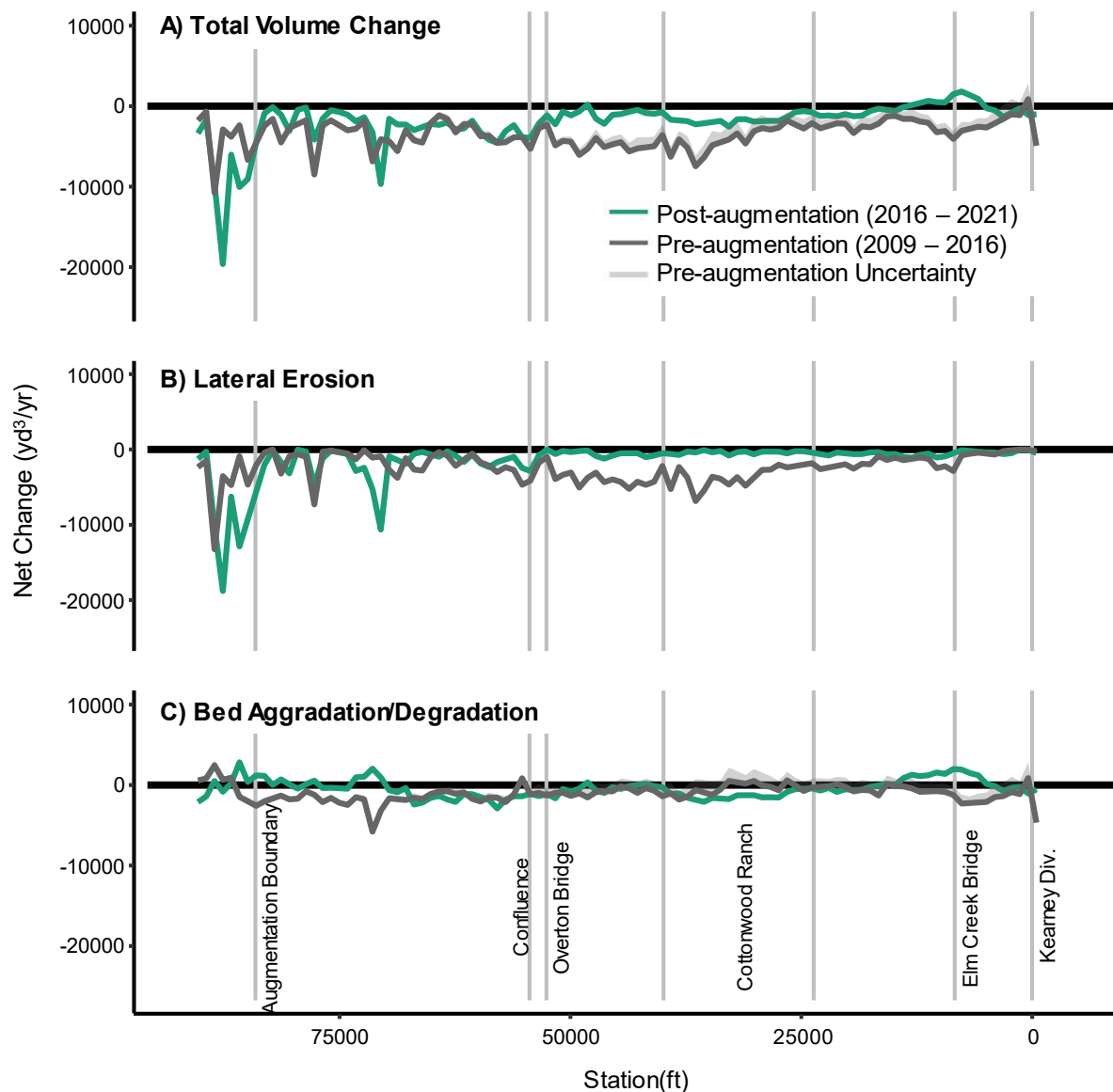


Figure 4.7. Net volume change per year by station. The figure shows the total volume change (A), which is the sum of the lateral erosion (B) and the bed aggradation/degradation (C). Upstream of Overton Bridge lateral erosion was high both pre- and post-augmentation while bed degradation reduced. Downstream of Overton Bridge much less lateral erosion occurred post-augmentation while bed volume change fluctuated around zero during both periods.



Table 4.4. Pre- and post-augmentation volume change broken into two reaches. Negative values indicate net degradation for the reach. Orange cells indicate an increase in degradation from pre- to post-augmentation, while green cells indicate a decrease in degradation.

	Augmentation Boundary to Overton Bridge (yd ³ /yr)		Overton Bridge to KCD (yd ³ /yr)	
	Pre-Augmentation	Post-Augmentation	Pre-Augmentation	Post-Augmentation
Lateral	-63,000	-65,800	-154,400	-29,600
Bed	-59,700 to -42,000	-23,000	-46,100 to 23,700	-21,500
Total	-122,700 to -105,000	-88,800	-200,400 to -130,700	-51,100

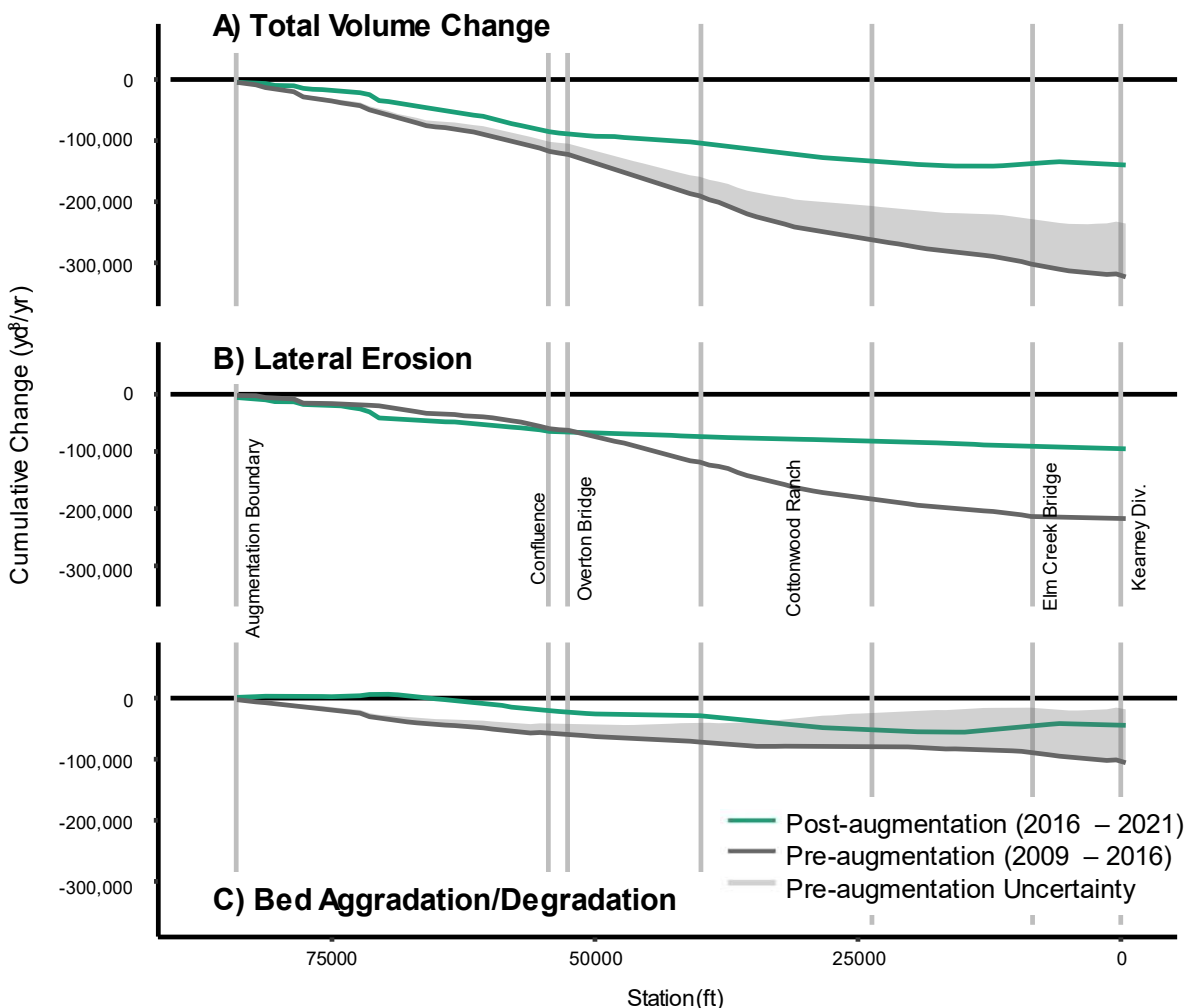


Figure 4.8. Cumulative volume change in the pre- and post-augmentation time periods. Lines represent the running sum of all change starting at the downstream end of augmentation projects. Gray shaded area represents the uncertainty in the pre-augmentation period due to lacking bathymetry data.

While volume change remained negative in the post-augmentation period, Table 4.4 3 and Figures 4.7 and 4.8 show that this change became less negative compared to pre-augmentation. Upstream of the Overton Bridge, the channel bed was degrading at a rate of 0.8 to 1.1 in/yr, averaged over the total area. After augmentation, this rate decreased to 0.4 in/yr, a decrease of 45% to 60% while lateral erosion had a slight increase of 4%. Downstream of the bridge a large reduction in lateral (80%) and total degradation (61%–75%) was observed. At KCD, total volume change and lateral erosion were lower during the post-augmentation period, while the difference in bed degradation is within the uncertainty for the pre-augmentation period.



4.4.2 Flow-normalized volume change results

Given sediment transport increases nonlinearly with flow, it can be helpful to remove flow variability from the analysis to compare volume change under approximately equal flow conditions. For example, given equal flow, we would expect an unstable reach to change more than a stable one. As will be further discussed in Section 4.4.3, the pre-augmentation period experienced greater flow than the post-augmentation period, and Figure 4.9A shows that the pre-augmentation period also experienced greater total volume change. Figure 4.9B shows that when these results are normalized by flow, the difference between pre- and post-augmentation values shrinks to be within the uncertainty bounds over most of the reach¹⁵. The contrast between change normalized by flow (Figure 4.9B) and change not normalized by flow (Figure 4.9A) This indicates that flow is a primary factor in the reduction in downstream volume change in the post-augmentation period. This further suggests that the reach has not become more or less prone to erosion with time. It continues to be degradational on average, with the magnitude of degradation varying with flow.

¹⁵ Note that flow normalized data is only available downstream of Overton Bridge due to incomplete flow data upstream of the bridge.

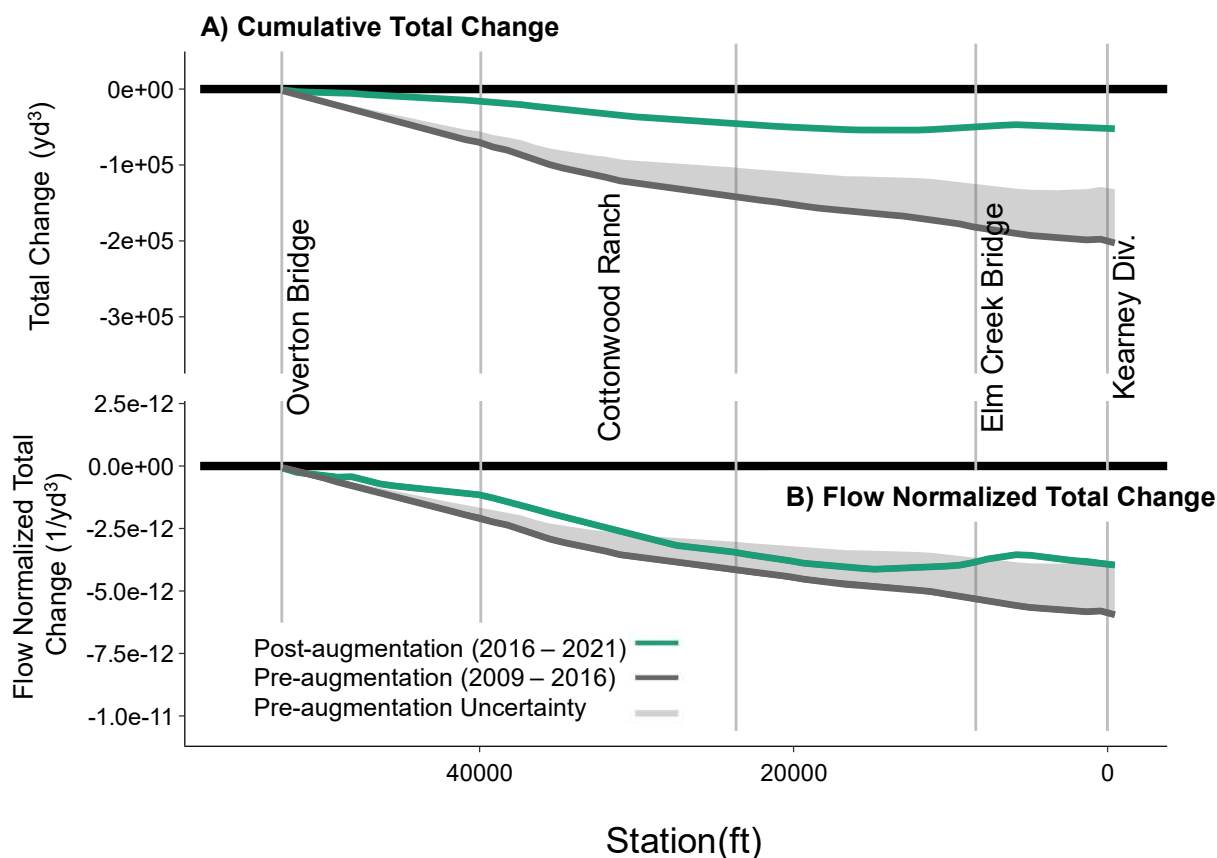


Figure 4.9. Cumulative total volume change downstream of the Overton Bridge. Values in panel B are normalized by flow at the Overton USGS gage, while values in A are not. Normalizing by flow reduces the difference between pre- and post-augmentation volume change.

4.4.3 Effectiveness of sediment augmentation

Our analysis indicates that conditions became less degradational in our study area since the implementation of sediment augmentation. To isolate the part that sediment augmentation played in this improvement, we must consider the other main variable in our system, flow. Downstream from the confluence of the J2 Return Channel and the North Channel, the Overton Bridge USGS gage shows that the pre- and post-augmentation periods were distinct. Figure 4.2 shows that monthly average flow exceeded 6,000 cfs five times in the pre-augmentation period and not once in the post-augmentation period. In addition, the high flow event in June of 2015 brought a maximum daily flow of 15,300cfs, much higher than the maximum daily flow of 9,750cfs during the drier post-augmentation period (Table 4.5).

Table 4.5 Summary of flow during the pre and post-augmentation periods.

	Pre-augmentation		Post-Augmentation	
	J2 Return	Overton Bridge	J2 Return	Overton Bridge



Average Daily Flow (cfs)	960	2,150	970	1,650
Maximum Daily Flow (cfs)	2,030	15,300	1,780	9,750

These differences in flow make it difficult to isolate the effect of sediment augmentation. Fortunately, our full flow record at the Overton gage allows us to approximate volumetric change on the downstream reach independent of flow (Figure 4.9B). Doing so indicates that degradation potential was similar on this reach pre- and post-augmentation. While the post-augmentation change is slightly less degradational in a few locations, the differences are small enough to be within the uncertainty bounds over most of the reach. The high lateral erosion (Table 4.4) and large increases to wetted width (see Chapter 3) in the pre-augmentation period also point towards high flow events being the main driver of change rather than augmentation project sediment. Channel-forming events such as the flood in 2015 caused high lateral erosion, which in turn introduced new sediment to the riverbed. Without high flow events, the post-augmentation period saw only 20% of the pre-augmentation annual lateral erosion downstream of the Overton Bridge.

Upstream of Overton Bridge, flow entering the J2 Return Channel is typically regulated and ranges from 0 to 2,000 cfs. The average release from the Supply Canal was very similar in the pre- and post-augmentation periods (Table 4.5). This indicates that the additional sediment introduced to the system via sediment augmentation projects is likely a key factor in the reduction in bed degradation and total degradation observed in the J2 Return Channel. Figure 4.10 shows the relative volumes of sediment that eroded from the most upstream part of the J2 Return Channel where augmentation projects have occurred (orange). In the post augmentation period, the amount of sediment that eroded, including what was augmented, from the upstream reach increased by 35,500–38,300 yd³/yr. Given that flow was similar in the post-augmentation period, this increase in erosion can be attributed to an increased availability of sediment (23,000 to 57,700 yd³/yr) from sediment augmentation and the breakthrough channel, see Figure 4.3). Relative to this, we see a decrease in bed erosion from downstream of the augmentation area to the Overton Bridge of 16,200 to 33,900 yd³ per year. The similarity between the values of the upstream increase and downstream decrease in erosion indicates that sediment is leaving the augmentation area and reducing bed degradation downstream.

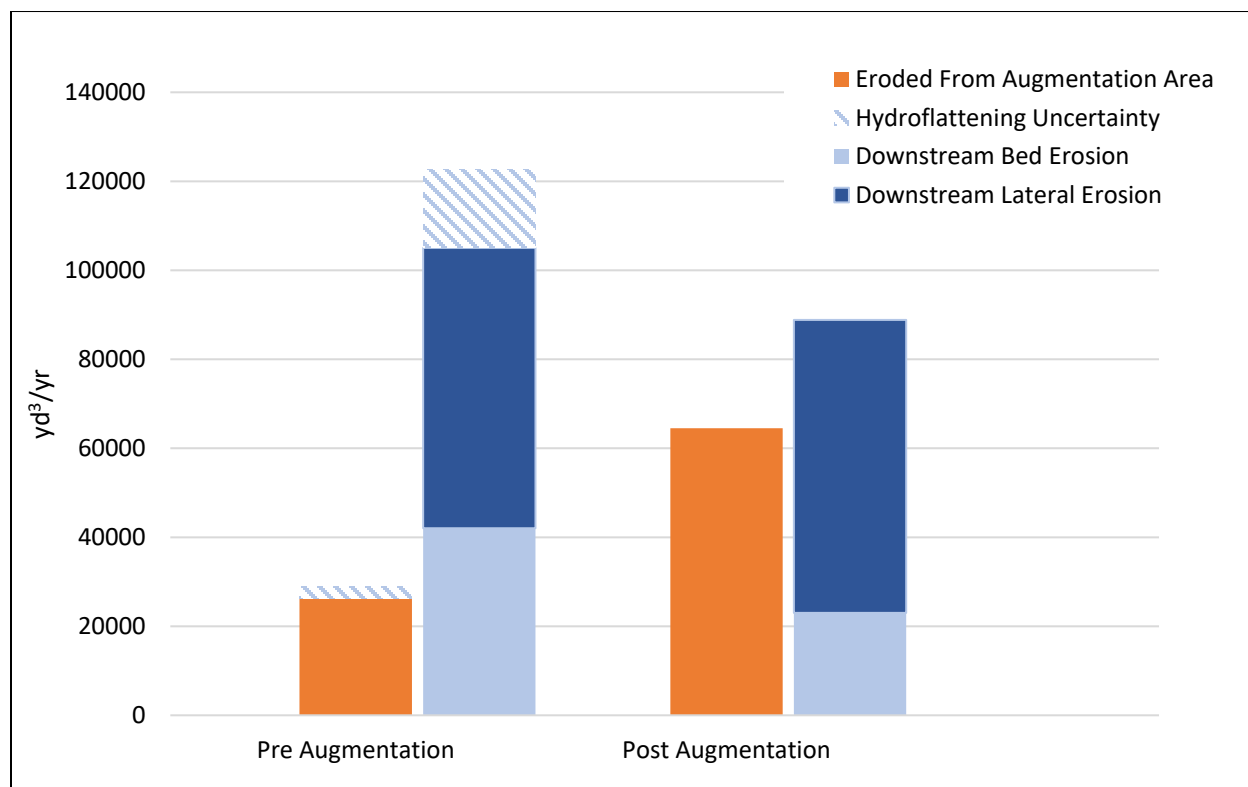


Figure 4.10 Volumes eroded from the J2 Return Channel upstream and within the augmentation project area (orange), and downstream of augmentation projects to the Overton Bridge (blue) in pre- and post-augmentation periods. In the post augmentation period, upstream sediment supply increased and downstream bed erosion decreased. The similarity between the values of increase and decrease indicate that sediment is leaving the augmentation area and reducing bed erosion downstream.

4.4.4 Year-by-Year Volume Change During Augmentation

In the post-augmentation period, annual topo-bathymetric LiDAR data enables a year-by-year examination of volume change. Table 4.6 5 shows there is high variation, but generally less degradation was observed in the most recent two years when the breakthrough channel has been closed. Examining the year-by-year post-augmentation data spatially (Figures 4.11 and 4.12), it is possible to see an expanding zone of positive change just downstream of the augmentation boundary from 2016–2019 (4.11a). This signal is not evident in 2019–2021, perhaps becoming more dispersed as total degradation is reduced in those years.



Table 4.6 Post-augmentation year-by-year volume change divided into two reaches at Overton Bridge. Negative values are in parentheses and indicate net degradation or erosion.

	Downstream augmentation boundary to Overton Bridge			Overton Bridge to KCD		
	Total Volume Change (yd ³)	Lateral Erosion (yd ³)	Bed Agg/Deg (yd ³)	Total Volume Change (yd ³)	Lateral Erosion (yd ³)	Bed Agg/Deg (yd ³)
2017-2016	(117,200)	(76,800)	(40,300)	18,500	(23,300)	41,800
2018-2017	(91,100)	(39,300)	(51,800)	(170,300)	(18,300)	(152,000)
2019-2018	(123,800)	(73,900)	(49,900)	(116,300)	(50,300)	(66,000)
2020-2019	(77,500)	(40,200)	(37,400)	12,100	(26,600)	38,700
2021-2020	(38,900)	(41,600)	2,700	(2,100)	(300)	(1,900)

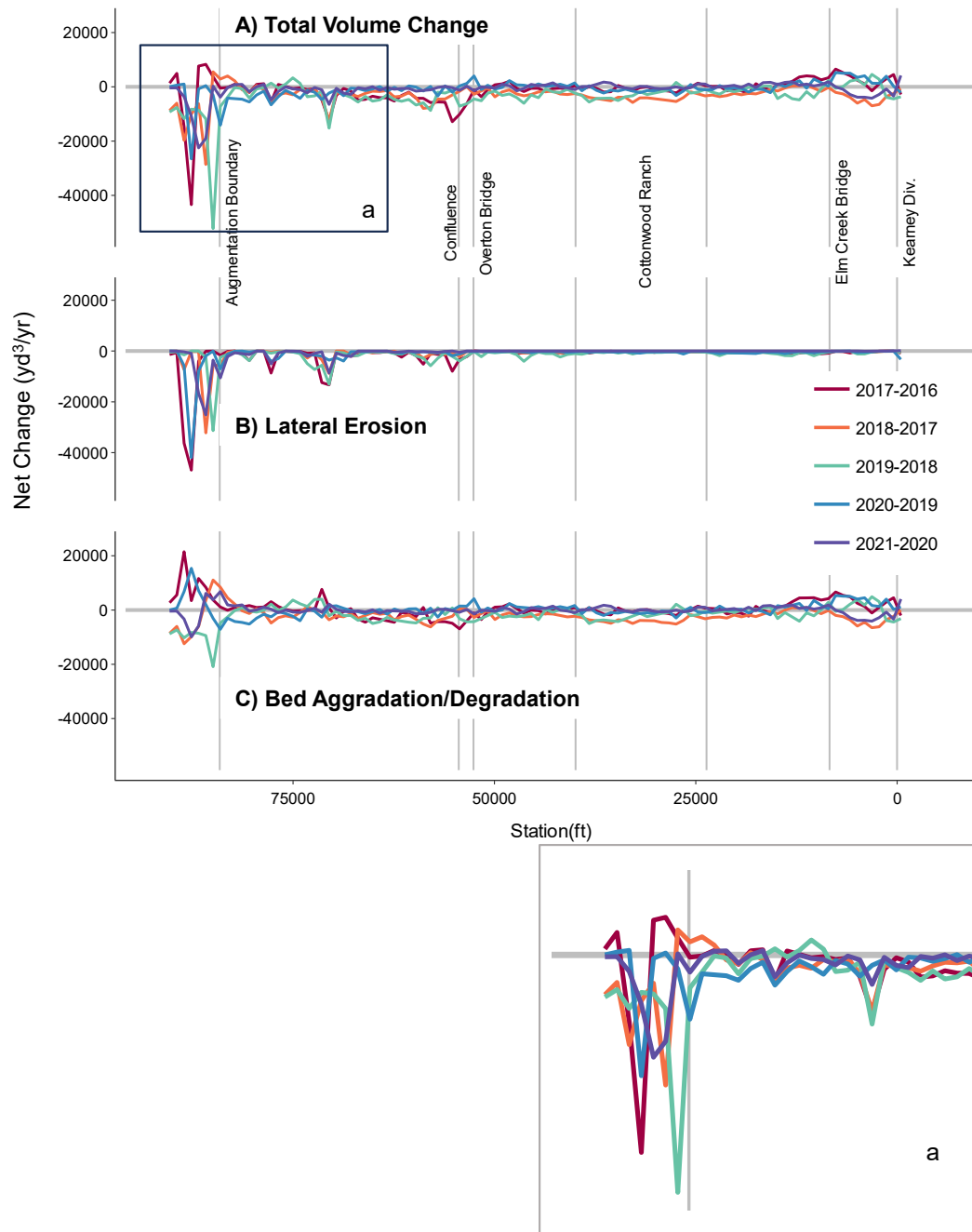


Figure 4.11 Post-augmentation year-by-year net volume change. Inset ‘a’ depicts positive volume change that moves downstream from the augmentation zone in 2016 to 2019. This pattern is disrupted in 2019-2021, perhaps becoming more dispersed as total degradation is reduced in those years.

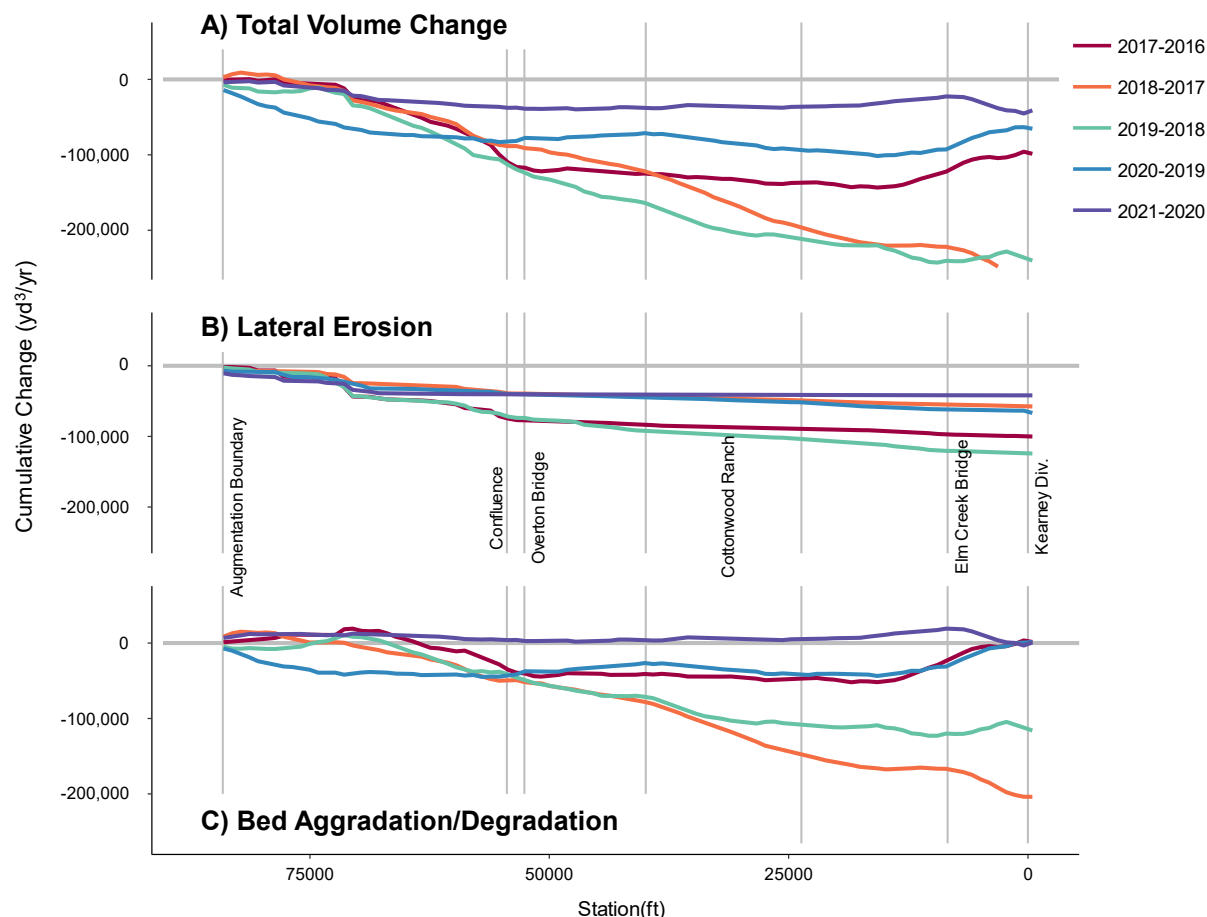


Figure 4.12 Cumulative year-by-year volume change in the post-augmentation period. (A) Lines represent the running sum of all change starting at the downstream end of augmentation projects. The nearly flat lines downstream of Overton Bridge indicate very little lateral erosion occurred (B). Steep slopes indicate high local change, such as the high bed degradation at Cottonwood Ranch from 2017–2019 (C).

Noise due to varying flow and sediment inputs makes the year-by-year data difficult to interpret. General trends seem to be decreasing degradation in the reach upstream of Overton Bridge, though higher flows in 2019 seem to have caused more bed degradation in the 2020–2019 year. Some years (2016 - 2018) have a distinct hump that is likely the signature of augmentation and breakthrough sediment moving downstream (Figure 4.11 inset ‘a’), but in other years no distinct signature is visible and a more dispersed reduction in erosion can be seen. While the reach downstream of Overton Bridge is largely stable, there is year-by-year variation here as well. The steep negative slope in the Cottonwood Ranch area (Figure 4.12) in 2017–2019 shows that this area was degradational during that time, likely due to disking activities in 2018 and higher flow in 2019 (Figure 4.2). After the large-scale lateral erosion that occurred in the flood of 2015, very little additional lateral erosion occurred in the downstream reach during the drier post-augmentation period. This can be observed from the nearly flat slope of lines in Figure 4.12B.



4.5 Discussion

In our full-scale augmentation experiment we evaluated whether 60,000–80,000 tons (40,000–60,000 yd³) of sediment placed immediately downstream of the J2 Return each year could offset the sediment deficit sufficiently to stabilize the J2 Return Channel and prevent incision from progressing downstream. In this chapter we evaluated the effectiveness of augmentation via the morphological approach, using LiDAR data (constrained by hydraulic modeling) to measure actual volumetric change during the experiment. Our findings indicate that the J2 Return Channel remained degradational during the experiment, but bed erosion was reduced, and some areas of aggradation were observed in the first three miles downstream of augmentation. We also found that a large portion of sediment supply in the J2 Return Channel came from lateral erosion of channel banks. Finally, we found that the net volume change downstream of the J2 Return Channel between Overton Bridge and the KCD is dynamic but stable, with no observable signal from augmentation.

In terms of quantitative change, bed degradation in the J2 Return Channel decreased by 45%–60% during the augmentation experiment. We attribute this reduction to augmentation activities because the decrease in erosion (approx. 20,000 to 40,000 yd³/yr) was roughly equal to the augmented material leaving the sediment augmentation project area. The movement of augmented material downstream away from the augmentation area is visible in Fig. 4.11. Given full-scale sediment augmentation arrested approximately half of bed degradation in the J2 Return Channel, the volume, location of augmentation, grain-size distribution, or other design factors may need to be adjusted to address the continued incision in the lower half of the channel. Doubling the annual augmentation volume could hypothetically offset remaining bed degradation, but mechanically augmenting 80,000–120,000 yd³/yr may incur challenges in terms of cost, physical supply, and ability to mobilize the sediment. The Program's current United States Corps of Engineers (USACE) Section 404 permit identifies seven sites from which sediment can be sourced with varying degrees of difficulty. At the current rate of augmentation, these sites have enough sediment for a total of 21 more augmentation projects. Without alteration to the existing permit, doubling the volume of augmented sediment would reduce the number of potential projects by half, with four years of source material from Jeffrey Island and six years of source material from more challenging sites along Plum Creek.

Downstream of Overton Bridge, volume change analysis indicates a dynamic channel with a high degree of spatial and temporal variability during the augmentation period. Spatially, the reach from the Overton Bridge to CWR was stable to slightly aggradational, the CWR reach was slightly degradational, and the reach from CWR to the KCD structure was aggradational during augmentation years. Temporally, the channel bed (excluding lateral erosion) between Overton and KCD was net aggradational or relatively stable in three out of five years, but degradational from 2017–2019. When compared to the pre-augmentation period and normalized for discharge, we observed no major difference in bed erosion during the pre- and post-augmentation periods downstream of Overton Bridge.

The one difference we did observe was substantial lateral erosion that occurred because of the prolonged peak flow event in 2015 which increased mean channel width by more than 200 ft. Channel widths have remained stable since 2015, despite much lower flows in recent years (Chapter 3).



1 Overall, sediment augmentation reduced bed degradation in the J2 Return Channel, but there was
2 no pre- and post-augmentation difference in sediment balance downstream of Overton within the
3 limits of our uncertainty from hydroflattened DEMs. Much of the sediment supply in the J2
4 Return Channel originates from lateral erosion, which recruits stored sediment from the banks.
5 Theoretically, degradation will continue to slowly progress downstream toward the Overton
6 Bridge and will negatively impact habitat at an unknown point in the future. As such, some form
7 of permanent ongoing augmentation in J2 Return Channel is necessary to reduce future risk to
8 downstream habitat, but near- and long-term benefits are difficult to quantify and weigh against
9 the annual cost of augmenting sediment. Accordingly, it may be necessary to evaluate
10 alternatives that allow for some degree of long-term sediment replenishment into the J2 Return
11 Channel without the cost and supply limitations of ongoing mechanical augmentation. This
12 includes alternatives like retrofitting of the Jeffrey Island Sand Dam to pass sediment into the J2
13 Return Channel in a controlled manner. Investigations into passive sediment replenishment and
14 augmentation alternatives will likely begin in late 2023.

15



4.6 References

- Anderson, S. (2019). Uncertainty in quantitative analyses of topographic change: error propagation and the role of thresholding. *Earth Surface Processes and Landforms*, 44, 1015-1033.
- Bangen, S., Hensleigh, J., McHugh, P., & Wheaton, J. (2016). . Error modeling of DEMs from topographic surveys of rivers using fuzzy inference systems. *Water Resources Research*, 52, 1176– 1193.
- Brierley, G., & Fryirs, K. (2005). *Geomorphology and River Management: Applications of the River Styles Framework*. Malden, MA: Blackwell Publishing.
- Dewberry. (2010). *LiDAR Quality Assurance (QA) Final Report Sub-Project 1: Platte River Corridor Nebraska/Kansas LiDAR*.
- Federal Geographic Data Committee (FGDC). (1998). *National Standard for Spatial Data Accuracy*.
- HEC-RAS. (2008). *Hydraulic Reference Manual*. U.S. Army Corps of Engineers, Hydrologic Engineering Center.
- Hensleigh, J. (2013). *Geomorphic Change Detection Using Multi-beam SONAR*. Master's Thesis, Utah State University, Logan, UT.
- Independent Scientific Advisory Committee (ISAC). (2023). *ISAC Report on February 2023 PRRIP Science Plan Reporting Session (SPRS)*. Platte River Recovery Implementation Program (PRRIP).
- Julien, P., & Simons, D. (1985). Sediment Transport Capacity of Overland Flow. *Transactions of the ASAE*, 28(3), 755-762.
- Lai, Y. (2008). *SRH-2D Version 2: Theory and User's Manual*. Bureau of Reclamation Technical Service Center Sedimentation and River Hydraulics Group.
- Lane, S., Westaway, R., & Hicks, M. (2003). Estimation of erosion and deposition volumes in a large, gravel-bed, braided river using synoptic remote sensing. *Earth Surface Processes and Landforms*, 28, 249-271.
- Leopold, L., & Wolman, M. (1957). *River Channel Pattern: Braided, Meandering and Straight*. Washington DC: U.S. Geological Survey Professional Papers.
- Platte River Recovery Implementation Program (PRRIP) Executive Director's Office (EDO). (2022a). *First Increment Extension Science Plan*.
- Platte River Recovery Implementation Program (PRRIP) Executive Director's Office (EDO). (2022b). *System-Scale Geomorphology and Vegetation Monitoring Report 2017-2020*.
- Quantum Spatial Inc. (QSI). (2016). *Platte River, Nebraska – Fall 2016: Topobathymetric LiDAR Technical Data Report*.



- 1 Quantum Spatial Inc. (QSI). (2017). *Platte River, Nebraska – Fall 2017: Topobathymetric*
2 *LiDAR Technical Data Report.*
- 3 Quantum Spatial Inc. (QSI). (2018). *Platte River, Nebraska – Fall 2018, Nebraska:*
4 *Topobathymetric LiDAR Technical Data Report.*
- 5 Quantum Spatial Inc. (QSI). (2019). *Platte River Fall 2019, Nebraska: Topobathymetric LiDAR*
6 *Technical Data Report.*
- 7 Quantum Spatial Inc. (QSI). (2020a). *Platte River Fall 2020, Nebraska: Topobathymetric LiDAR*
8 *Technical Data Report.*
- 9 Quantum Spatial Inc. (QSI). (2020b). *RE: Platte River Recovery Implementation Program,*
10 *Update of baseline data for 2018 and 2017.*
- 11 Quantum Spatial Inc. (QSI). (2021). *Platte River Fall 2021, Nebraska: Topobathymetric LiDAR*
12 *Technical Data Report.*
- 13 Rosgen, D. (1994). A Classification of Natural Rivers. *Catena*, 22, 169-199.
- 14 Tetra Tech. (2017). *Final 2016 Platte River Final Data Analysis Report.*
- 15 The Flatwater Group, Inc. (2010). *Platte River from the Lexington to Odessa Bridges Sediment*
16 *Augmentation Experiment Alternatives Screening Study Summary Report.*
- 17 Vericat, D., Wheaton, J., & Brasington, J. (2017). Revisiting the Morphological Approach:
18 Opportunities and Challenges with Repeat High-Resolution Topography. In D. Tsutsumi,
19 & J. Laronne, *Gravel-Bed Rivers* (pp. 121-158). Chichester, UK: John Wiley & Sons,
20 Ltd.
- 21 Wheaton, J., Brasington, J., Darby, S., & Sear, D. (2010). Accounting for uncertainty in DEMs
22 from repeat topographic surveys: improved sediment budgets. *Earth Surface Processes*
23 *and Landforms*, 35, 136-156.
- 24